TECHNISCHE UNIVERSITÄT MÜNCHEN

Fakultät für Medizin

III. Medizinische Klinik für Hämatologie

und internistische Onkologie,

Klinikum rechts der Isar

Inhibition of MCL-1 blocks the development of KRAS-driven adenocarcinoma of the lung

Enkhtsetseg Munkhbaatar

Vollständiger Abdruck der von der Fakultät für Medizin der Technischen Universität München zur Erlangung des akademischen Grades eines

Doctor of Philosophy (Ph.D.)

genehmigten Dissertation.

Vorsitzender: Univ.-Prof. Dr. Roland M. Schmid

Betreuer: Priv.-Doz. Dr. Philipp J. Jost

Prüfer der Dissertation:

1. Univ.-Prof. Dr. Mathias Heikenwälder

2. apl. Prof. Dr. Jens Th. Siveke

Die Dissertation wurde am 11.12.2014 bei der Fakultät für Medizin der Technischen Universität München eingereicht und durch die Fakultät für Medizin am 04.03.2015 angenommen.

Table of Contents

1. INTRODUCTION 4
1.1 Lung cancer....4
1.1.1 Lung cancer incidence....4
1.1.2 Lung cancer classification and staging....4
1.1.3 Diagnosis and treatment outlines of lung cancer....6
1.1.4 The spectrum of genetic aberration in lung cancer....7
1.1.4.1 Frequently affected signaling pathways in lung cancer....7
1.1.4.2 Aberrantly activated transcription factors identified in lung cancer....9
1.1.4.3 Aberrations in receptor tyrosine kinases in lung cancer specimen....9
1.1.4.4 The role of apoptotic regulators in lung cancer....11
1.1.4.5 Deregulated expression of angiogenic factors and their correlation to vascular structures in lung cancer....11
1.1.4.6 The contribution of tumor suppressors to lung cancer progression....12
1.2 The *RAS* oncogene and its function....13
1.2.1 Receptor-associated adaptor proteins in RAS signaling....13
1.2.2 RAS effector pathways....14
1.2.3 *RAS* mutations in human cancer....17
1.3 Molecular characteristics of the pro-survival BCL-2 family member MCL-1....17
1.3.1 Molecular properties of MCL-1....17
1.3.2 The biological functions of MCL-1....18
1.3.3 Regulatory mechanisms that control MCL-1....21
1.3.4 The requirement of MCL-1 in normal development....24
1.3.5 Cancer development and maintenance by MCL-1....25
1.4 Mouse models of lung cancer....26
1.5 Specific aims of this project....29

2. MATERIALS AND METHODS....31
2.1 Cell culture....31
2.2 Transfection and transduction with BIM_S variants....31
2.3 Transfection and transduction with *Kras* constructs....31
2.4 Inducible expression of BIM_S variants in human NSCLC cell lines....32
2.5 ABT-737 treatment....32
2.6 Apoptosis array....32
2.7 Gene expression array....33
2.8 Immunoblotting....33
2.9 Mouse strains....33
2.10 Tumor induction....33
2.11 Tissue harvesting....34
2.12 Tumor burden analysis....34
2.13 Evaluation of lung tumors....34
2.14 Infection of *LacZ* mice and examination of adenoviral CRE functionality....35
2.15 Hematoxylin and Eosin (H&E) stain....36
2.16 Alcian Blue- Periodic Acid Schiff staining (AB-PAS)....36
2.17 Immunohistochemistry (IHC)....37
2.18 *In situ* hybridization (ISH)....37
2.19 Quantification of staining (H&E, IHC and ISH)....38
2.20 ABT-263 treatment....38
2.21 Cisplatin treatment....38
2.22 Absorption based X-ray micro-CT....39
2.23 Statistical analysis....39

3. RESULTS....40
3.1 Anti-apoptotic function of $Kras^{G12D}$ in murine embryonic fibroblasts....40

3.2 Lung cancer cell lines are resistant to inhibition of BCL-2, BCL-X_L and BCL-W 41
3.3 Survival of lung cancer cell lines is dependent on MCL-1 expression 44
3.4 Generation of a *Kras*^{G12D}-driven lung cancer mouse model and confirmation of adenoviral CRE functionality 46
3.5 Deletion of *Mcl-1* and structural integrity of the lung 48
3.6 Characterization of *Mcl-1* deletion in mutant KRAS driven tumorigenesis 50
3.7 *Mcl-1* deletion reduces tumor burden 50
3.8 Deletion of *Mcl-1* triggers formation of large anaplastic tumors 54
3.9 *Mcl-1* deletion results in an elevated activation of STAT3 56
3.10 Treatment response to chemotherapy in lung cancer harboring deletions of *Mcl-1* 58
3.10.1 Pharmacologic inhibition of BCL-2, BCL-X_L and BCL-W does not confer additional treatment response 60
3.10.2 Characterization of *Mcl-1* deletion on the effect of cisplatin treatment 62
4. DISCUSSION 65
STUDY IMPLICATIONS AND FURTHER QUESTIONS 77
5. ABBREVIATIONS 79
ACKNOWLEDGEMENTS 82
REFERENCES 83

1. INTRODUCTION

1.1 Lung cancer

1.1.1 Lung cancer incidence

Lung cancer is the most commonly diagnosed cancer worldwide, with an estimated 1.8 million new cases (12.9% of total) in 2012. In men, the highest incidence rates are observed in Central and Eastern Europe (53.5 per 100,000) and Eastern Asia (50.4 per 100,000). In women, the highest incidence rates are observed in Northern America (33.8 per 100,000) and Northern Europe (23.7 per 100,000). Notably, lung cancer is the leading cause of cancer death worldwide with an estimated 1.59 million deaths per year (19.4% of total). The overall ratio of death to incidence is 0.87 suggesting that many patients die from their disease (Globalcan 2012, International Agency for Research on Cancer, World Health Organization). The most important cause of lung cancer is smoking and the risk of developing lung cancer is 20 to 30 fold increased in smokers. However, only a fraction of smokers develop lung cancer, suggesting that there might be genetic predispositions to lung cancer development (Minna et al., 2002). The majority of lung cancer cases are diagnosed at advanced stages and lung cancer patients suffer from low 5-year overall survival rates (Heist and Engelman, 2012).

1.1.2 Lung cancer classification and staging

Lung cancer has been classified into two major classes: small cell lung cancer (SCLC) accounting for approximately 20% of cases and non-small cell lung cancer (NSCLC) accounting for approximately 80% of lung cancer cases (Schiller, 2001). NSCLC includes common histological subtypes such as adenocarcinoma, squamous cell carcinoma and large cell carcinoma amongst others. Historically, the distinction between SCLC and NSCLC was important because of distinct clinical aspects such as extent and localization of metastasis and the response to anti-neoplastic treatments. However, recently the importance of the differentiation between the subtypes within NSCLC has been emphasized by the observation that adenocarcinoma and squamous cell carcinoma harbor very different genetic mutations (Travis, 2011).

Classification of lung tumors is mainly based on the microscopic appearance of hematoxylin-eosion (H&E) stained tumor sections. In addition to light microscopic evaluation of H&E sections an adenocarcinoma marker thyroid transcription factor-1

(TTF-1), a squamous marker p40 or p63, and/or mucin stains are recommended to classify the sections further (Travis et al., 2013b).

Squamous cell carcinoma mostly arises in segmental bronchi and extends to lobar and larger bronchi. The morphologic features of squamous cell cancer are intercellular bridging, squamous pearl formation and keratinization. The tumor cells have esophilic keratinized cytoplasm (Travis, 2011).

Adenocarcinoma is the most common type of lung cancer and according to the International Association for the Study of Lung Cancer/American Thoracic Society/European Respiratory Society (IASLC/ATS/ERS), it is further sub-classified into minimal invasive, invasive and variants of invasive adenocarcinoma subtypes. Minimal invasive adenocarcinoma primarily contains a lepidic growth pattern showing small (5mm or less) invasive components. Lepidic predominant adenocarcinoma, a type of invasive adenocarcinoma, contains a lepidic growth pattern of type II pneumocytes or Clara cells and has a greater than 5 mm invasive component. Other types of invasive adenocarcinoma are acinar adenocarcinoma with round to oval malignant glands, papillary adenocarcinoma containing cuboidal to columnar tumor cells, micropapillary adenocarcinoma composed of small papillary cluster of glandular cells and solid adenocarcinoma with mucin consisting tumor cells with abundant cytoplasm and vesicular nuclei with several nucleoli. The variants of adenocarcinoma (invasive mucinous, colloid, fetal and enteric adenocarcinoma) show lepidic, acinar, papillary or micropapillary growth composed of columnar cells with abundant apical mucin and small nuclei (Travis, 2011).

Large cell carcinomas are mostly located in the peripheral lung with an appearance of large necrotic tumors. The tumor shows histological features such as sheets and nests of large polygonal cells containing vesicular nuclei and prominent nucleoli. The diagnosis of this tumor is largely based on the exclusion of other tumor types (Travis, 2011).

SCLC is found typically in peribronchial locations with infiltration of the bronchial submucosa and peribronchial tissue. SCLC is characterized by histologic features such as small and round to fusi-form shaped cells with scant cytoplasm and granular nuclear chromatin. Necrosis is a common phenomenon and mitotic rates are high with an average of 80 mitoses per 2 mm^2 (Travis, 2010; Travis, 2011).

In addition to classifying the tumor type, the staging of the extent of disease at the time of diagnosis is the most important factor for predicting prognosis and treatment choice. Currently the most accepted lung cancer staging system is the 7^{th} TNM staging of malignant tumor published by the Union for International Cancer Control (UICC), which includes a revision of the TNM system announced by

International Association for the Study of Lung Cancer (IASLC). In this staging system, which is based on the anatomical extent of the disease, the T descriptor defines the size of the tumor, N refers to extent of metastasis to regional lymph nodes and M to distant metastasis (Mirsadraee et al., 2012). Based on these TNM descriptors, stage groups are defined. The stage groups range from stage Ia to stage IV, with stage IV as the most advanced stage of the disease (Detterbeck et al., 2009). The TNM staging has been used primarily for NSCLC whilst a two-staged classification, (very) limited- and extensive-stage disease system, is applied for SCLC (Mirsadraee et al., 2012).

1.1.3 Diagnosis and treatment outlines of lung cancer

Fundamental diagnostic procedures are based on chest X-rays, chest computed tomography (CT) scans, and biopsies. Diagnosis is further confirmed and sub-classified based on results of histological and/or cytological analysis of biopsies (National Cancer Institute: PDQ® Non-Small Cell Lung Cancer Treatment. Bethesda, MD: National Cancer Institute). The differential diagnosis and subsequent treatment decision is based on the microscopic evaluation of histologic material to differentiate between NSCLC and SCLC, as well as between sub-types such as adenocarcinoma and squamous cell carcinoma.

SCLC is highly aggressive and generally not treated with surgical resection due to its high tendency for metastasis. Radiation and (combination)-chemotherapy are the main therapeutic options. The treatment regimen is dependent on the nature of the disease and the extent of metastatic spread. Limited stage disease is often treated with combined modality treatment (combination of etoposide and cisplatin with radiation therapy). The duration of treatment usually extends to 4 to 6 cycles of chemotherapy. The dose and timing of radiation therapy is still controversial, however, usually patients receive a dose of 2 Gy once daily up to a total of 50 Gy (Bogart et al., 2004). The standard treatment option for extensive-stage SCLC is etoposide in combination with platinum (cisplatin or carboplatin). Despite treatment, survival of both limited and extensive-staged SCLC patients is low, with median survival of 16-24 months and 6-12 months, respectively (National Cancer Institute: PDQ® Small Cell Lung Cancer Treatment. Bethesda, MD: National Cancer Institute).

Treatment options for NSCLC patients are based specifically on the stage of the disease. Briefly, surgical resection and radiation and/or adjuvant chemotherapy represent the options at early stages of the disease (Schiller, 2001). Radiation can be combined with platinum (cisplatin or carboplatin) compound based chemotherapy

to offer improved responses to therapy (National Cancer Institute: PDQ® Non-small Cell Lung Cancer Treatment. Bethesda, MD: National Cancer Institute). In patients with advanced staged disease, platinum combination with cytotoxic drugs such as vinorelbine, paclitaxel, docetaxel, gemcitabine, or irinotecan and targeted therapies such as EGFR inhibitors and ALK inhibitors, according to the presence of genetic mutations, are treatment choices (Evans, 2001; Heist and Engelman, 2012). NSCLCs are relatively insensitive to chemotherapy compared to SCLC (National Cancer Institute: PDQ® Non-small Cell Lung Cancer Treatment. Bethesda, MD: National Cancer Institute). Furthermore, cure in NSCLC patients is rare and seen only in a small fraction of the patients, which is primarily based on the fact that most patients are diagnosed at advanced stages (Heist and Engelman, 2012; Travis, 2011).

1.1.4 The spectrum of genetic aberration in lung cancer

In an enormous effort to understand the genetic mechanisms driving lung cancer, multiple molecular alterations have been identified. Genetic alterations occur at the chromosomal, DNA (nucleotide), and epigenetic level, resulting in activation and/or amplification of oncogenes and deletion and/or inactivation of tumor suppressor genes. Importantly, the two major types of lung cancer, SCLC and NSCLC, show a distinct pattern of genetic alteration (Zochbauer-Muller et al., 2002). This is exemplified by the genetic mutation frequency for *p53* and Retinoblastoma (*RB)* in approximately 90% of SCLC (Dosaka-Akita et al., 2000; Sameshima et al., 1992) whereas only 50% and 30% of NSCLC harbor the mutated *p53* and *RB,* respectively (Ahrendt et al., 2003; Reissmann et al., 1993). A detailed description of the affected genes and signaling pathways is shown below.

1.1.4.1 Frequently affected signaling pathways in lung cancer

The rat sarcoma viral oncogene homologue (RAS) family of proto-oncogenes encodes 4 distinct small guanosine triphosphotases (GTPases): HRAS, NRAS, KRAS4A and KRAS4B. The RAS proteins transduce signals from receptor tyrosine kinases (RTK) at the cell surface (Pylayeva-Gupta et al., 2011). Activating point mutations of *KRAS* occur in approximately 30% of NSCLC, particularly in adenocarcinoma (Heist and Engelman, 2012; Rodenhuis et al., 1988; Slebos et al., 1990; The Cancer Genome Atlas Research Network, 2014). The activating mutations are localized in codons 12, 13, and 61, with codon 12 being the most often mutated. The mutations result in constitutively active KRAS signaling driving cell proliferation

and survival (Rodenhuis et al., 1988). The mutations in codon 12 causing the substitution of glycine to valine or arginine, is correlated with poorer prognosis compared with other amino acid substitutions. This suggests that specific amino acid substitutions mediate a specific transformation activity of KRAS (Keohavong et al., 1996). *KRAS* mutations are found to be mutually exclusive with epidermal growth factor receptor (*EGFR)* mutations in lung adenocarcinoma (The Cancer Genome Atlas Research Network, 2014). In addition to point mutations of *KRAS,* the respective genomic region is amplified in a portion of lung adenocarcinoma resulting also in an elevated signal transduction to downstream signaling pathways (Weir et al., 2007). More details about the functional consequences of mutated *RAS* signaling and its role in lung cancer are discussed in chapter 1.2.

V-raf murine sarcoma viral oncogene homologue B (BRAF), a downstream effector of RAS, is a serine/threonine kinase involved in RAS-MAPK signaling which regulates the transcription of genes responsible for cell proliferation and survival (Paik et al., 2011). Mutations of *BRAF* have been identified in 3% of NSCLC, primarily in adenocarcinoma (3-10%). The most common *BRAF* mutation is V600E within the kinase domain, which is followed by the mutations G469A and D594G (Brose et al., 2002; Paik et al., 2011; The Cancer Genome Atlas Research Network, 2014). These mutations cause elevated kinase activity of BRAF and result in the stimulation of the downstream pathway (Davies et al., 2002).

Phosphoinositide 3-Kinase (PI3K) activates the PI3K-AKT-mTOR signaling pathway, a RAS effector pathway, that mediates cell proliferation and survival (Marte and Downward, 1997). PI3K is a heterodimer consisting of a regulatory and a catalytic subunit and mutations in *PI3KCA,* which encodes the catalytic unit, have been identified in 4% of lung cancer (Samuels et al., 2004). The mutational incidence, however, was lower in adenocarcinoma (1-7%) than in squamous cell lung carcinoma (6.5-16%) (Kawano et al., 2006; The Cancer Genome Atlas Research Network, 2012, 2014). Mutations in *PIK3CA* can be found in both smokers and nonsmokers and can co-occur with *EGFR* mutations (Kawano et al., 2006).

Members of the *NOTCH* family can act as tumor suppressors or promoters depending on the cellular context. For example, *NOTCH3* is overexpressed due to the translocation of chromosome 19 in NSCLC (Dang et al., 2000). The activated form of NOTCH3, NOTCH3IC is found in approximately 40% of all tested NSCLC cell lines and inhibition of NOTCH3 activation blocks cell proliferation and induces apoptosis (Konishi et al., 2007). These somatic mutations result in the constitutive

activation of the respective signaling pathways, mediating mitogenic signaling irrespective of up-stream stimulation by their specific ligand.

1.1.4.2 Aberrantly activated transcription factors identified in lung cancer

The *MYC* family proto-oncogenes, *c-MYC, L-MYC* and *N-MYC,* encode transcription factors that regulate cellular growth, metabolism, DNA replication, cell cycle progression, cell adhesion, differentiation, and apoptosis (Pelengaris et al., 2002; Tansey, 2014). Furthermore, chromosomal segments near or containing the *MYC* gene are amplified in lung adeno- and squamous cell carcinoma (The Cancer Genome Atlas Research Network, 2012, 2014; Weir et al., 2007) and *L-MYC* is frequently overexpressed in SCLC samples (Tansey, 2014). As expected for a highly active pro-proliferative transcription factor, and as shown in many other cancer subtypes other than lung cancer, amplification of *MYC* was found to be associated with a poor prognosis (Iwakawa et al., 2011). The importance of MYC for tumorigenicity was further confirmed experimentally by inhibition of MYC using the expression of a dominant-negative MYC mutant to eradicate lung cancers and prolong survival of tumor-bearing mice (Soucek et al., 2013).

SOX2 is an important transcription factor in the regulation of pluripotent stem cells. SOX2 promotes differentiation and proliferation of basal tracheal cells (Bass et al., 2009). Amplification of chromosome 3q26.33, which contains *SOX2,* is found in squamous cell carcinoma and ectopic expression of *SOX2* cooperates with fibroblast growth factor receptor 2 (*FGFR2*) in the transformation of immortalized tracheobronchial epithelial cells (Bass et al., 2009). *SOX2* amplification is also found in approximately 27% of SCLC (Rudin et al., 2012). In addition, amplification and overexpression of *p63* are found in 16% of squamous cell carcinoma (The Cancer Genome Atlas Research Network, 2012). SOX2 and p63 interact and co-regulate genes expression, which are critical for maintaining the immature precursor population in the squamous epithelial population and for survival of squamous cell carcinoma cells that harbor *SOX2* amplifications (Watanabe et al., 2014). Furthermore, p63 is a useful and largely specific marker for the detection of squamous cell carcinoma, with a positive detection in 88% of histologically proven squamous cell carcinoma (Jorda et al., 2009).

1.1.4.3 Aberrations in receptor tyrosine kinases in lung cancer specimen

Activation of receptor tyrosine kinases triggers signaling cascades involved in cellular growth, cellular differentiation and survival, and aberrant activation commonly results in malignant transformation.

Activating mutations of the tyrosine kinase domain of the *EGFR,* also known as *ERBB1,* result in constitutively active EGFR leading to the hyperactivation of downstream pro-survival signaling (Sordella et al., 2004). The most common mutations are frame-shift deletions of exon 19 and point mutations at codon 858 in exon 21 (Lynch et al., 2004). *EGFR* is mutated in 14% of lung adenocarcinoma and significantly amplified in both adenocarcinoma and squamous cell carcinoma of lung (The Cancer Genome Atlas Research Network, 2012, 2014). Furthermore, *EGFR* is overexpressed in 13% of NSCLC (Reissmann et al., 1999). Another member of the EGFR subfamily, *ERBB2*, also known as *HER2/Neu*, is mutated mainly in adenocarcinoma. In 1.7-10% of adenocarcinomas, *ERBB2* mutations have been identified, which mainly locate to the kinase domain (Stephens et al., 2004; The Cancer Genome Atlas Research Network, 2014). Gain-of-function mutations of *ERBB2* induce survival and proliferation together driving cellular transformation (Wang et al., 2006). Moreover, genetic amplifications of *ERBB2* are found in approximately 1% of adenocarcinoma further supporting the importance of this gene for a small subset of adenocarcinoma of the lung (Stephens et al., 2004; The Cancer Genome Atlas Research Network, 2014).

MNNG-HOS transforming gene (*MET)* (Cooper et al., 1984) encodes the receptor tyrosine kinase of the hepatocyte growth factor (HGF). Activation of MET by the binding of its ligand induces the activation of the downstream RAS-MAPK and PI3K pathway together promoting cellular survival and proliferation (Birchmeier et al., 2003). *MET* has been identified to be mutated in NSCLC and deregulated MET-HGF signaling induces tumorigenesis (Kong-Beltran et al., 2006). Amplification and activating mutations of *MET,* which increase protein stability, occur in 7% of all adenocarcinomas (Kong-Beltran et al., 2006; The Cancer Genome Atlas Research Network, 2014).

The anaplastic lymphoma kinase (*ALK*) gene encodes a receptor tyrosine kinase, which is also aberrantly activated in lung cancer. The availability of a clinically tested and approved small molecule inhibitor of ALK identifies genetic aberrations of this gene as particular important. Genetically, NSCLC are characterized by an inversion within chromosome 2p, which results in a fusion gene between *EML4* and *ALK*, which together results in the formation of a constitutively active fusion protein (Soda et al., 2007). ALK signaling leads to the activation of RAS-MEK-ERK, JAK3-STAT3, and the PI3K-AKT pathways (Heist and Engelman, 2012). The fusion oncogene is primarily associated with adenocarcinoma and was identified in 4% of young nonsmoking patients (Takeuchi et al., 2008; Wong et al., 2009). Patients diagnosed with primary adenocarcinoma of the lung are tested for

the presence of this fusion oncogene at our hospital to identify patients that might profit from the use of ALK inhibitors (e.g. crizotinib) for treatment.

ROS1 is a receptor tyrosine kinase of the insulin receptor family and *ROS1* fusions were identified as potential driver mutations in a NSCLC cell line (HCC78; *SLC34A2-ROS1*) and a NSCLC patient sample (*CD74-ROS1*) (Rikova et al., 2007). These fusions lead to constitutive kinase activity of ROS1. Approximately 2% of NSCLC harbor *ROS1* rearrangements and *ROS1*-positive NSCLCs arise in young never-smokers with adenocarcinoma, similarly to patients with *ALK*-rearranged NSCLCs (Bergethon et al., 2012; The Cancer Genome Atlas Research Network, 2014). The activating mutations and/or overexpressions of receptor tyrosine kinases enable cancer cells to acquire the ability to self provide growth signaling by ligand-independent activation thereby driving malignant transformation and sustained survival.

1.1.4.4 The role of apoptotic regulators in lung cancer

The genetic amplification of pro-survival members of the B-cell lymphoma 2 (*BCL-2*) family results in acquired resistance to apoptosis. The pro-survival BCL-2 proteins inhibit apoptosis, also termed programmed cell death, by maintaining mitochondrial integrity. The pro-survival members of *BCL-2* family, such as *BCL-2L1*, also termed *BCL-*X_L, and myeloid cell leukemia-1 (*MCL-1*), are frequently genetically amplified in lung cancer. Lung cancer cell lines harboring these amplifications are dependent on the continued expression of these genes for cellular survival (Beroukhim et al., 2010; Tonon et al., 2005). A detailed description about the frequency of genetic amplifications of the chromosomal locus harboring *MCL-1* and its functional consequences are shown in chapter 1.3.

Early correlative studies on BCL-2 family proteins have suggested that approximately 76% of SCLC, 25% of squamous cell carcinoma and 12% of adenocarcinoma of the lung express BCL-2, however a clear clinical correlation from these studies cannot be drawn (Kaiser et al., 1996; Pezzella et al., 1993).

1.1.4.5 Deregulated expression of angiogenic factors and their correlation to vascular structures in lung cancer

Angiogenesis is important for the progression of cancers originating from almost any epithelial or mesenchymal tissue. The balance between pro- and anti-angiogenic molecules dictates whether angiogenesis can occur (also termed the 'angiogenic switch') (Bergers and Benjamin, 2003). Tumors secrete pro-angiogenic growth factors such as the vascular endothelial growth factor, VEGF (Prager et al., 2011).

VEGF is a pro-angiogenic factor that is involved in all steps of angiogenesis: vascular permeability, endothelial cell proliferation, endothelial cell migration or invasion into the surrounding tissue and capillary-like tube formation (Prager et al., 2011). VEGF is expressed in 45-50% of NSCLC and is associated with an increased intra-tumoral microvascular density and poor prognosis (Masuya et al., 2001; O'Byrne et al., 2000). In addition, interleukin-8 (IL-8) expression, a member of the CXC chemokine family, is observed in approximately 50% of NSCLC and correlated with hyper-vascularity (Masuya et al., 2001). Another angiogenic factor, platelet-derived endothelial cell growth factor (PD-ECGF), is expressed in 25%-30% of NSCLC and linked to high microvessel density (Koukourakis et al., 1997; O'Byrne et al., 2000). Notably, PD-ECGF is expressed at lower levels in SCLC compared to NSCLC (Yamashita et al., 1999). Together, the elevated expression levels observed in angiogenic factors might contribute to the progression of lung cancers by supporting tumor growth by delivering nutrients and oxygen to tumor cells.

1.1.4.6 The contribution of tumor suppressors to lung cancer progression

Tumor suppressor genes, such as *p53 and RB*, are frequently inactivated to evade growth suppression (Hanahan and Weinberg, 2011). p53 induces cell cycle arrest and apoptosis in response to cellular stress. It functions as a sequence-specific transcription factor, activating the expression of a wide range of genes such as *p21* to control G1/S transition, or *GADD45* in G2/M DNA damage checkpoint, or *BAX, PUMA* or *NOXA* to induce apoptosis (Ihrie et al., 2003; Meuwissen and Berns, 2005; Yakovlev et al., 2004). Inactivation of p53 occurs through missense mutations and/or deletion in 50% of NSCLC and in 80-90% of SCLC (Ahrendt et al., 2003; Sameshima et al., 1992; The Cancer Genome Atlas Research Network, 2014). In unstressed cells, expression of p53 is kept low by MDM2 which is a p53 specific E3 ubiquitin ligase (Moll and Petrenko, 2003). *MDM2* is found to be significantly amplified in lung adenocarcinoma (The Cancer Genome Atlas Research Network, 2014).

Deregulation of the cyclin-dependent kinase (CDK)-retinoblastoma protein (RB) pathway, which is critical for controlling the G1/S cell cycle transition, is often found in human malignancies. Deregulation can be induced by inactivation of the CDK inhibitor *p16^{Ink4a}*, by overexpression of the *cyclin D1* gene, or by direct mutational inactivation of the *RB* gene (DeGregori, 2006). p16^{INK4A} binds to CDK4 to inhibit its interaction with cyclin D1. Cyclin D1 associated CDK4 phosphorylates RB to release cells from cell cycle arrest (Malumbres et al., 2003). The main component of the pathway, *RB* is often found mutated in SCLC (90%) and 30% of NSCLC

(Dosaka-Akita et al., 2000; Reissmann et al., 1993). $p16^{INK4A}$ and $p14^{ARF}$ are encoded by *CDKN2A*, and the second protein $p14^{ARF}$ prevents degradation of p53 by interacting with MDM2 (Fong et al., 2003). *CDKN2A* is inactivated by point mutations and deletions as well as by epigenetic silencing by hypermethylation in lung adenocarcinoma and 78% of squamous cell carcinoma (The Cancer Genome Atlas Research Network, 2012, 2014).

Another example of a loss-of-function mutations in a tumor suppressor gene is the phosphatase and tensin homolog (*PTEN),* which encodes a lipid phosphatase that negatively regulates the PI3K-AKT pathway resulting in cell cycle arrest and apoptosis. Loss of *PTEN* leads to constitutive PI3K-AKT signaling (Johnson et al., 2012). *PTEN* is mutated in both adenocarcinoma and squamous cell carcinoma and the chromosomal region containing *PTEN* is often deleted (The Cancer Genome Atlas Research Network, 2012, 2014)

Finally, neurofibromin-1 (*NF-1*), a negative regulator of the RAS pathway, is inactivated by somatic mutations and by deletion in 11% of lung adenocarcinoma, especially in samples lacking an activated oncogene, as well as in squamous cell carcinoma (The Cancer Genome Atlas Research Network, 2012, 2014). The inactivation of tumor suppressor genes enables cancer cells to evade negative regulation of cell proliferation thereby driving neoplastic growth.

1.2 The *RAS* oncogene and its function

1.2.1 Receptor-associated adaptor proteins in RAS signaling

As described in section 1.1.4.1, activating mutations of *KRAS* are often found in lung cancer, specifically in lung adenocarcinoma. In this section, RAS signaling will be briefly discussed to elucidate how constitutively active KRAS contributes to malignant transformation. Ligand binding to receptor tyrosine kinases, such as EGFR and platelet derived growth factor receptor (PDGFR), results in the dimerization, phosphorylation and subsequent activation of the receptor. The adaptor protein growth-factor receptor-bound protein-2 (GRB2) links the phosphorylated receptor tyrosine kinases to Son of sevenless (SOS) (Buday and Downward, 1993). SOS is one of many guanine nucleotide-exchange factors (GEFs) that together with guanine nucleotide releasing proteins (GRFs) positively regulate RAS activity (Downward et al., 1990). SOS and RAS-GRF catalyze the release of GDP from RAS and the exchange for GTP to activate RAS (Bowtell et al., 1992; Shou et al., 1992).

RAS GTPase-activating proteins (GAPs) negatively regulate RAS activity by accelerating its intrinsic GTPase activity resulting in formation of the GDP-bound

inactive RAS (Scheffzek et al., 1997). GAP (120 kDa) and NF-1 stimulates the GTPase activity of RAS (Martin et al., 1990).

1.2.2 RAS effector pathways

Activation by GTP binding induces a conformational change in the RAS protein, which favors interactions with downstream adaptor proteins. Multiple downstream effector pathways are activated by RAS, of which the Mitogen-activated protein (MAP) kinase and PI3K-AKT are the best characterized.

MAP kinase cascade. MAP kinases are a family of serine/threonine kinases that transduce signals from cellular membranes to the nucleus. A MAP kinase cascade consists of 3 protein kinase reactions. A MAP kinase kinase kinase (MAPKKK) phosphorylates a MAP kinase kinase (MAPKK). The phosphorylated MAPKK can then phosphorylate a MAP kinase. The activated MAP kinase further phosphorylates other cytoplasmic proteins and translocates to the nucleus to regulate transcription factor activities (Hagemann and Blank, 2001).

The Rapidly accelerated fibrosarcoma (RAF) family, MAPKKKs with serine/threonine kinase specificity, interacts preferentially with GTP-bound RAS and is subsequently activated (Moodie et al., 1993; Zhang et al., 1993). RAF proteins phosphorylate MEK, a family of MAPKKs (Alessi et al., 1994). Activated phospho-MEK1/2 positively regulates ERK1/2 (MAPK), serine/threonine kinases, also by phosphorylation (Seger et al., 1992). In turn, ERKs directly phosphorylate a set of transcription factors including E26 transcription factors (ETS-1), activation-protein-1 (AP-1) and c-MYC (Chang et al., 2003). These transcription factors then promote cellular survival and proliferation. In addition, ETS-1 and AP-1 activate transcription of cyclin D1, which is important for cell cycle progression (Albanese et al., 1995; Hitomi and Stacey, 1999). Furthermore, *c-MYC* is a well-known proto-oncogene that regulates cell proliferation and survival (Chang et al., 2003). Moreover, ERK1/2 phosphorylate the pro-apoptotic BH3-only protein BIM_{EL} to trigger its degradation, thereby repressing cell death (Luciano et al., 2003).

MAPKKK and MAPKK also modulate the c-Jun N-terminal kinase (JNK) cascade, also known as stress-activated protein kinase (SAPK), and p38 MAPK. Activation of JNK induces a wide range of cellular responses through phosphorylation of target proteins unique to stress response and also targets shared with the MAPKs ELK1 and AP1 (Kyriakis and Avruch, 1996; Whitmarsh et al., 1995). p38 MAPK can be activated by a variety of extracellular signals including osmotic

stress, cytokines, radiation and tumor necrosis factor (TNF) (Coulthard et al., 2009). Phosphorylated p38 MAPK activates a wide range of targets that include transcription factors, protein kinases, cytosolic and nuclear proteins inducing inflammatory responses, cell differentiation, cell-cycle arrest, apoptosis, and cytokine production (Coulthard et al., 2009).

PI3K-AKT pathway. The catalytic subunit of phosphoinositide 3-kinase (PI3K) is a RAS effector as it directly interacts with GTP-bound RAS (Rodriguez-Viciana et al., 1994). PI3K is a lipid kinase that phosphorylates phosphatidylinositol-4,5-biphosphate (PIP2) and generates phosphatidylinositol-3,4,5- triphosphate (PIP3). The phospholipid product binds to the protein kinase B (also known as AKT) through the AKT pleckstrin homology (PH) domain and facilitates dimerization, plasma membrane localization, and activation of AKT (Bader et al., 2005; Franke et al., 1997). Activation of AKT protects cells from cell death (Khwaja et al., 1997; Marte and Downward, 1997) through, at least partially, phosphorylation and inhibition of the pro-apoptotic BCL-2 protein, BAD (Datta et al., 1997; del Peso et al., 1997) and downregulation of BAK1 (Rosen et al., 1998). Furthermore, cell proliferation is promoted by AKT, through inhibition of Forkhead box (FOX) family, which positively regulates the cyclin-dependent kinase inhibitors $p27^{kip1}$ and $p21^{cip1}$ (Bader et al., 2005). AKT also phosphorylates the cyclin-dependent kinase inhibitor $p21^{WAF1/CIP1}$ to promote cell cycle progression (Zhou et al., 2001). Furthermore, AKT mediates transcriptional activity of nuclear factor kappa B (NF-κB) by directly and indirectly stimulating the inhibitor of NF-κB kinase IKK. NF-κB is a pleiotropic transcription factor promoting cellular survival, proliferation, angiogenesis and cell invasion (Bader et al., 2005).

Additional RAS effectors. Activated RAS interacts with and activates RAL guanine exchange factors (RALGEFs). These exchange factors are responsible for the activation of RAS-like (RAL) GTPases (Wolthuis et al., 1998). The RAL GTPases, RALA and RALB, promote tumorigenesis through regulation of proliferation and survival (Chien and White, 2003). Moreover, RAL is involved in regulation of vesicle trafficking by direct interaction with Sec5, an integral component of the exocyst complex, a multisubunit complex required for targeting of secretory vesicles (Moskalenko et al., 2002). Downstream targets of the RAS/RAL GTPase cascade are the phospholipase D (PLD) proteins. PLDs regulate cell cycle progression, and overexpression of either PLD1 or PLD2 overcomes cell cycle arrest induced by high

level of RAF signals, possibly through reversing increases in the cell cycle inhibitor, $p21^{Cip1}$ (Joseph et al., 2002).

T-cell lymphoma invasion and metastasis-1 (TIAM1), a RAC-specific GEF, associates with GTP-bound RAS through a RAS-binding domain. TIAM1 mediates RAS activation of RAC (Lambert et al., 2002). Once activated, RAC1 stimulates actin filament accumulation at the plasma membrane, forming membrane ruffles. In addition to cytoskeletal organization, RAC1 is also required for cellular transformation by RAS. Activated Val-12 RAC1-expressing Rat1 fibroblasts exhibit all the hallmarks of malignant transformation (Qiu et al., 1995).

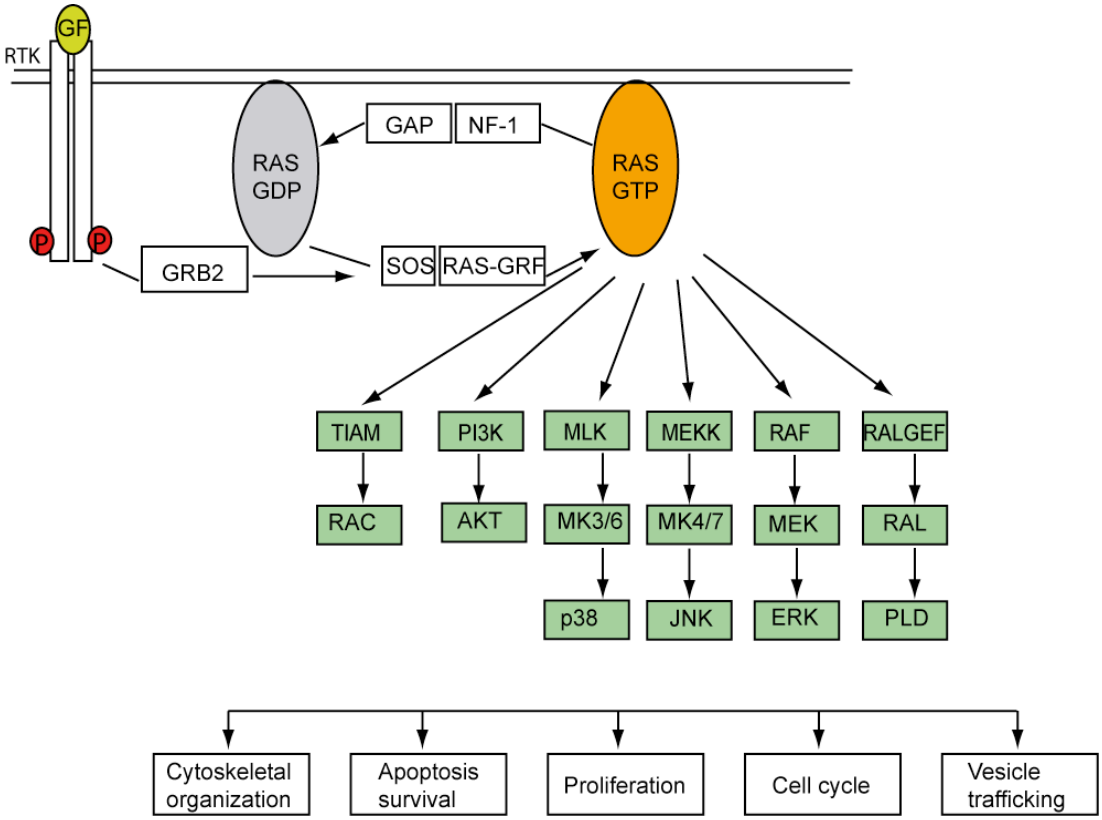

Figure 1. Molecular mechanisms of RAS signaling and the respective downstream signaling pathways. Activated GTP-bound RAS signals to multiple and diverse downstream effector signaling pathways including RAF, p38, JNK, PI3K, RALGEF, and TIAM. These pathways regulate cellular survival, proliferation, cytoskeletal organization, and vesicle trafficking. RTK-receptor tyrosine kinase, GF- growth factor.

In summary, many genetic lesions result in the aberrant activation of the RAS signaling pathway. Shown in Figure 1 is a simplified version of the effector pathways described above (Figure 1). Importantly, the signal transduction induced by activated RAS is complex and a great deal of cross talk between the individual effector pathways is present. Once activated, RAS induces numerous signaling pathways to stimulate cell proliferation, survival and differentiation. The critical contribution of

mutated KRAS to lung cancer progression lead us to utilize this oncogenic model system to study the effects of apoptotic re-activation in lung cancer development.

1.2.3 *RAS* mutations in human cancer

RAS mutations arise in approximately 30% of human cancer with certain *RAS* mutations occurring predominantly in specific types of cancers (Schubbert et al., 2007). *KRAS* is mutated primarily in colonic (Bos et al., 1987), lung (as described in section 1.1.4), pancreatic (Almoguera et al., 1988), biliary tract, and endometrial cancer (Rodenhuis and Slebos, 1990; Rodenhuis et al., 1988). *NRAS* is mutated mainly in hematopoietic malignancies, such as acute myeloid leukemia (Bos et al., 1985; Janssen et al., 1985), and skin malignancies (Padua et al., 1985). *HRAS* mutations are frequently observed in skin (Pylayeva-Gupta et al., 2011) and bladder cancers (Fujita et al., 1984). This pattern of cancer specific *RAS* mutations possibly reflects different expression levels of the *RAS* genes and/or distinct functions of these genes in certain tissues (Leon et al., 1987). Missense point mutations of codon 12 of *RAS* are responsible for the oncogenic conversion of N- and HRAS, resulting in their constitutively active GTP-bound states (Tabin and Weinberg, 1985; Trahey and McCormick, 1987). In addition to mutations of codon 12, mutations of codon 13 are also found in acute myeloid leukemia patients causing activation of RAS (Bos et al., 1985). Finally, point mutations of codon 61 were shown to cause the transforming activity of NRAS and HRAS, isolated from neuroblastoma and from lung carcinoma cell lines, respectively (Taparowsky et al., 1983; Yuasa et al., 1983).

1.3 Molecular characteristics of the pro-survival BCL-2 family member MCL-1

1.3.1 Molecular properties of MCL-1

Myeloid cell leukemia-1 *(MCL-1*) is a pro-survival member of BCL-2 family, initially identified as an early-induction gene in human myeloid cell leukemia cell line (ML-1) during phorbol ester induced differentiation. *MCL-1* encodes a 37.4 kDa protein (350 amino acids) which contains sequences that are rich in proline, glutamic acid, serine, and threonine residues (PEST). The carboxyl terminal portion of MCL-1 (139 amino acids) shows significant sequence similarity (59%) and sequence identity (35%) to the corresponding region of BCL-2 (Kozopas et al., 1993). MCL-1 shares conserved regions, BCL-2 homology (BH) domains, with other BCL-2 proteins. The gene contains 2 introns and 3 exons. The BH1 domain is encoded by exon 2 while the BH2 domains spans exon 2 and exon 3. The BH3 domain, which mediates interactions with other BCL-2 family members (Chittenden et al., 1995), is located in

exon 1. In addition, exon 1 encodes the PEST sequences that target the protein for proteolysis (Akgul et al., 2000b). *MCL-1* mRNA and the protein both have short half-lives in the range of a few minutes (Akgul et al., 2000a; Moulding et al., 2001). MCL-1 localizes to the mitochondrial membranes (Akgul et al., 2000a; Perciavalle et al., 2012; Yang et al., 1995), and within the cytosol (Jamil et al., 2005) and nucleus (Fujise et al., 2000).

1.3.2 The biological functions of MCL-1

MCL-1 belongs to the BCL-2 protein family, which regulates the stress induced apoptotic pathway. The intrinsic apoptotic pathway is defined to a large degree by the interaction within the three subgroups of the BCL-2 family (pro-apoptotic BH3-only proteins, pro-survival BCL-2 proteins, and pro-apoptotic BCL-2 effectors). The interaction takes place in the cytosol and at the mitochondria (Youle and Strasser, 2008). Cellular stresses activate the pro-death BH3-only proteins. The most important members of this pro-apoptotic BH3-only protein group include BCL-2-interacting mediator of cell death (BIM or BCL-2L11), p53 upregulated modulator of apoptosis (PUMA), Phorbol-12-myristate-13-acetate-induced protein 1 (PMAIP1 or NOXA), BCL-2-associated death promoter (BAD) and BH3-interacting-domain death agonist (BID). These pro-apoptotic members directly or indirectly block the action of the pro-survival BCL-2 members such as BCL-2, B-cell lymphoma-extra large (BCL-X_L or BLC-2L1), BCL-2-like 2 (BCL-2L2 or BCL-W), BCL-2-like 10 (BCL-2L10 or BCL-B), MCL-1 and BCL-2 related protein A1 (A1 or BFL-1). The interaction between both groups largely defines whether apoptosis is induced or not. The effectors of cell death at the mitochondria are BCL-2-associated X protein (BAX), BCL-2 antagonist/killer (BAK), and possibly BCL-2-related ovarian killer protein (BOK) (Adams and Cory, 2007; Czabotar et al., 2014).

The pro-survival members and the pro-apoptotic effectors share four BH domain (Hinds et al., 2003; Kvansakul et al., 2008; Muchmore et al., 1996; Petros et al., 2001; Suzuki et al., 2000) and exhibit similar structures: a central hydrophobic alpha-helix (α5) surrounded by amphipathic helices. This fold forms an elongated hydrophobic cleft, delineated by α-helices 2,3,4 and 6, that constitutes the binding site for other BCL-2 family members (Muchmore et al., 1996). As the name suggests, the BH3-only proteins, the initiators of apoptosis, contain only a BH3 domain which is essential for binding to pro-survival members of the family, and for their killing activity (Huang and Strasser, 2000).

The intrinsic apoptotic pathway. Diverse cytotoxic stresses such as cytokine deprivation, chemotherapeutics, oncogenic stress, and intracellular damage (Cory et al., 2003) stimulate apoptosis regulated by the BCL-2 protein family (the intrinsic pathway). These stresses activate BH3-only proteins and induce apoptosis by two distinct proposed mechanisms (Kuwana et al., 2005): indirect (Letai et al., 2002; Willis et al., 2005; Willis et al., 2007) or direct activation of the pro-apoptotic effectors BAK and BAX (Gavathiotis et al., 2008; Letai et al., 2002).

The indirect model for induction of BAX and BAK activation, or neutralization of pro-survival BCL-2 proteins, has been well characterized. In this model, induced BH3-only proteins bind to pro-survivals thereby preventing their ability to sequester BAX and BAK (Fletcher et al., 2008; Oltvai et al., 1993; Willis et al., 2005). All pro-survivals bind to BAX, whereas only MCL-1 and BCL-X_L can sequester BAK (Wang et al., 1998; Willis et al., 2005). Increased binding of BH3-only proteins to pro-survivals restrains them from inhibiting BAX and BAK activation (Chen et al., 2005). BH3-only proteins bind selectively to pro-survival proteins. For example, BAD is selective for BCL-2, BCL-X_L and BCL-W, while NOXA neutralizes only MCL-1 and A1 (Chen et al., 2005). BIM, PUMA and tBID are able to inhibit all pro-survival proteins (Figure 2) (Certo et al., 2006; Chen et al., 2005; Kuwana et al., 2005).

In the alternative model, which is not mutually exclusive to the indirect activation model, BH3-only proteins directly activate BAX and BAK. Pro-survival proteins neutralize BH3-only protein in order to prevent them from activating BAX and BAK. Activator BH3-only proteins, tBID and BIM activate BAX directly (Kuwana et al., 2005; Letai et al., 2002), whereas sensitizer BH3-only proteins such as BAD, neutralize pro-survival proteins to prevent them from sequestering BAX and BAK (Letai et al., 2002). Biological contexts, such as stimuli and cell types, may dictate which pathway dominates (Czabotar et al., 2014).

After activation, BAX and BAK begin to form oligomers that permeabilize the mitochondrial outer membrane (Dewson et al., 2008; Dewson et al., 2012). This leads to the release of cytochrome C (Kluck et al., 1997), activation of caspase 9 and apoptotic protease activating factor-1 (APAF1). Activated caspase 9 processes and activates effector caspases 3, 6 and 7, the final effectors of cell death (Li et al., 1997). BID links the intrinsic pathway to the death receptor-mediated apoptotic pathway of apoptosis (the extrinsic pathway) (Li et al., 1998; Luo et al., 1998). BID structurally resembles the multi-BH domain members with its buried BH3-domain. Cleavage of BID by caspase 8 generates truncated BID (tBID) exposing its BH3 thereby rendering it highly active (Li et al., 1998; Luo et al., 1998) (Figure 2).

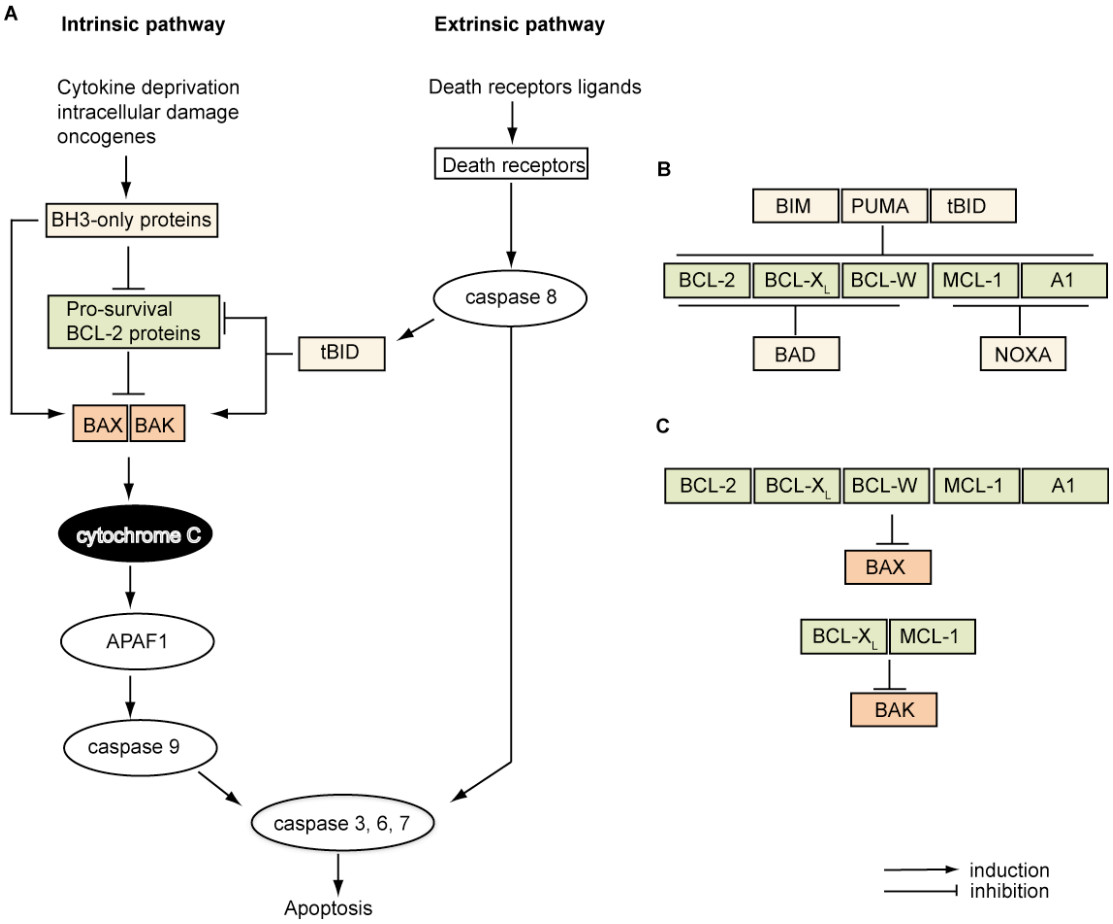

Figure 2. The BCL-2 family regulates the intrinsic and the extrinsic apoptotic signaling pathway. (A) Intrinsic and extrinsic apoptotic signaling pathways. A diverse range of stimuli, including oncogenic stress and intracellular damage, initiate the intrinsic pathway (also known as stress pathway) of apoptosis. The stimuli activate BH3-only proteins resulting in the inhibition of the pro-survival BCL-2 family members. Consequently, activation of BAX and BAK is induced causing the permeabilization of the mitochondrial outer membrane and the release of cytochrome c from the mitochondria. Alternatively, BH3-only proteins can directly activate BAX and BAK to cause pore formation. The cytochrome C release induces caspase 9 activation in a complex with APAF1 (also termed apoptosome) resulting in the processing and activation of the effector caspases 3, 6 and 7. The extrinsic (death receptor-mediated) pathway is induced by binding of death receptors ligands such as FASL, TRAIL or TNF to their respective receptor. This results in caspase 8 activation (Youle and Strasser, 2008). The activated caspase 8 cleaves BID generating truncated BID (tBID), which engages the intrinsic and the extrinsic pathway. Both pathways converge at the level of activated caspase 3, which eventually causes apoptosis. (B,C) Selectivity of the BCL-2 proteins in their interaction (see the text).

Mitochondrial homeostasis. MCL-1 was long considered a purely anti-apoptotic protein by virtue of its binding and inhibition of BAX or BAK. However, recent data suggest that distinct variants of MCL-1 reside at the outer mitochondrial membrane, as well as the inner mitochondrial membrane and matrix. This finding was suggesting an alternative function of MCL-1. Indeed, MCL-1 localized at the outer membrane (40 kDa and 38 kDa) antagonizes pro-apoptotic BCL-2 proteins and inhibits cell

death. However, MCL-1 localized at the inner mitochondrial membrane and matrix (36 kDa) is required for maintaining the normal structure of the inner membrane, mitochondrial fusion, and adenosine triphosphate (ATP) production and thereby promotes mitochondrial homeostasis, and the respiratory chain and bioenergetic function (Perciavalle et al., 2012). Matrix-localized MCL-1 exhibits an attenuated ability to inhibit apoptosis as it does not bind to BH3-only pro-apoptotic proteins (Huang and Yang-Yen, 2010). Proteolytic cleavage of the N-terminus of MCL is responsible for the generation of the matrix isoform of MCL-1 (De Biasio et al., 2007; Perciavalle et al., 2012). MCL-1 is cleaved by the mitochondrial processing peptidase (MPP) after import into the mitochondrial matrix (Huang and Yang-Yen, 2010).

Cell cycle regulation. In addition to regulating cell survival and mitochondrial function, some data suggest that MCL-1 might to be involved in cell cycle regulation. Cycling cells are more susceptible to cell death compared to non-dividing cells which are more resistant to killing (Zinkel et al., 2006). The function of MCL-1 in cell cycle regulation was proposed to regulate cell cycle at S and G_2/M stages. Unique among the BCL-2 proteins, MCL-1 specifically interacts with proliferating cell nuclear antigen (PCNA) in the nucleus. Overexpression of MCL-1 inhibits S-phase of cell cycle through its interaction with PCNA (Fujise et al., 2000). Furthermore Jamil and colleagues have shown that a short nuclear form of MCL-1 (snMCL-1) regulates cell cycle through its inhibitory effect on CDK1. snMCL-1 binding to CDK1 abolished the ability of CDK-1 to interact with its partners (cyclin B1), thereby resulting in cell cycle inhibition. snMCL-1 association with CDK1 predominantly at G2/M was observed in several cell lines indicating it is not a cell type specific phenomenon (Jamil et al., 2005). Additional data confirming the cell cycle regulatory role of MCL-1 will be helpful to place these observations into context and differentiate the anti-apoptotic from a purely cell cycle-regulatory function.

1.3.3 Regulatory mechanisms that control MCL-1

Transcriptional regulation. Upregulation of *MCL-1* expression is induced by multiple cytokines and growth factors. Interleukin-3 (IL-3) induces *MCL-1* expression by the PI3K-AKT pathway (Wang et al., 1999), whereas signaling via the PI3K-AKT pathway is involved in IL-5-mediated *MCL-1* expression (Huang et al., 2000). Granulocyte-macrophage colony-stimulating factor (GM-CSF) was shown to promote survival of cells by inducing *MCL-1* expression (Chao et al., 1998) and growth factors, such as EGF and VEGF, protect cells from staurosporine- and starvation-

induced apoptosis by upregulating *MCL-1* expression (Le Gouill et al., 2004; Leu et al., 2000).

In addition, members of the signal transducer and activators of transcription (STAT) family also positively regulate *MCL-1* expression. The promoter region of *MCL-1* contains transcription factor binding sites including STAT responsive elements (Akgul et al., 2000b). STAT3, in response to IL-6 (Puthier et al., 1999), and VEGF (Lee et al., 2005), and STAT5, in response to BCR-ABL signaling, induce *MCL-1* expression (Aichberger et al., 2005). Furthermore, hypoxia-inducible factor-1 apha (HIF-1α) mediates *MCL-1* upregulation in order to protect cells under hypoxic condition (Liu et al., 2006). A few conditions have been identified that downregulate *MCL-1* expression such as survival factor withdrawal (Chao et al., 1998), and induction of apoptosis by staurosporine (Iglesias-Serret et al., 2003). *MCL-1* expression can be repressed by the transcription factor E2F-1 binding directly to the *MCL-1* promoter (Croxton et al., 2002). Together this data show that MCL-1 is a target for many different inflammatory and pro-survival signaling pathways, however post-translational regulation seems to be more important in the biological context than transcriptional control (see below).

Post-transcriptional regulation. Alternative splicing of *MCL-1* mRNA gives rise to different splicing isoforms; full length (*MCL-1L)*, short variant (*MCL-1S)* and extra short *(MCL-1ES) MCL-1*. MCL-1S results from the splicing out of exon 2, which induces a frame shift downstream of the BH3 domain and loss of the BH1, BH2, and transmembrane (TM) domains (C-terminus truncated). MCL-1S structurally resembles BH3-only proteins and specifically interacts with MCL-1L, but not with the pro-apoptotic members of BCL-2 family. Overexpression of MCL-1S induces apoptosis and in healthy cells MCL-1S is expressed at low levels (Bae et al., 2000; Bingle et al., 2000). MCL-1ES, which results from splicing within the first coding exon, does not interact with pro-apoptotic BCL-2 members. However, like MCL-1S, MCL-1ES induces apoptosis by interacting with MCL-1L (Kim et al., 2009), independently of BAX and BAK. MCL-1L facilitates the localization of MCL-1ES to the mitochondria, where MCL-1ES oligomerizes and permeabilizes mitochondrial outer membranes, leading to cytochrome C release (Kim and Bae, 2013).

Translational regulation. Several microRNAs regulate MCL-1 at the translational level. Mir-29b negatively regulates *MCL-1* expression by binding to its target sequence. Expression of mir-29b was found to be reduced in malignant cells and overexpression of mir-29b decreased MCL-1 protein level (Mott et al., 2007).

Furthermore, mir-133b and mir-101 target *MCL-1*. Expression of both these microRNAs were shown to be downregulated, and inversely associated with overexpression of *MCL-1* mRNA in NSCLC tissue when compared to adjacent healthy tissue (Crawford et al., 2009; Luo et al., 2012). *MCL-1* expression is also negatively regulated by an RNA binding protein, CUGBP2 (Subramaniam et al., 2008). Overexpression of these regulators induces downregulation of MCL-1 and induces apoptosis.

Post-translational regulation. Multiple mechanisms have been shown to regulate MCL-1 at the post-translational level. Phosphorylation of the PEST region of MCL-1 in response to diverse stimuli regulates its function and stability (Thomas et al., 2010). Turnover of MCL-1 is slowed down via phosphorylation by ERK at the threonine 163 (Thr^{163}) residue that lies within the ERK site in the PEST region (Domina et al., 2004). Consistently, ERK-1 mediated phosphorylation of MCL-1 at Thr^{92} and Thr^{163} also stabilize the protein (Ding et al., 2008). However, phosphorylation of Serine 64 (Ser^{64}) by CDK1, 2 and JNK-1 does not affect the stability of the protein and is associated with increased anti-apoptotic activity of MCL-1 (Kobayashi et al., 2007). Kodama et al., have shown that simultaneous phosphorylation of Ser^{121} and Thr^{163} by JNK-1 stabilizes MCL-1 and protects cells against TNFα-induced apoptosis (Kodama et al., 2009). In contrast, an independent study has shown that phosphorylation of the same residues by the JNK pathway (JNK/p38), in response to oxidative stress, negatively regulates MCL-1, resulting in decreased anti-apoptotic activity (Inoshita et al., 2002). Glycogen synthase kinase-3 (GSK-3) phosphorylates MCL-1 at Ser^{155}, Ser^{159}, and Thr^{163} sequentially and leads to degradation of MCL-1 through associating it with ubiquitin E3-ligase b-TrCP (Ding et al., 2007a). Moreover, MCL-1 is phosphorylated by GSK-3 at Ser^{159} in response to IL-3 withdrawal (Maurer et al., 2006) and this phosphorylation, upon UV-irradiation, requires prior phosphorylation by JNK (priming phosphorylation) (Morel et al., 2009). Consequently, MCL-1 is ubiquinated by b-TrCP and degraded by proteasome (Ding et al., 2007b).

Proteasome-mediated and caspase-dependent degradation of MCL-1 have been noted. E3 ubiquitin ligases are responsible for the polyubiquitination of MCL-1 thereby mediating its proteasomal degradation. MCL-1 Ubiquitin Ligase E3 (MULE) specifically interacts with MCL-1 through its BH3 domain and ubiquitinates MCL-1 at 5 lysine residues (Zhong et al., 2005). Moreover, b-TrCP is another E3-ligase that targets MCL-1 for ubiquitination after phosphorylation by GSK-3 (Ding et al., 2007a). Conversely, at least 2 deubiquitinases have been identified that act on MCL-1.

USP9X and KU70 directly interact with MCL-1 and stabilize it by removing lysine-48 linked polyubiquitin chains (Schwickart et al., 2010; Wang et al., 2014b).

Furthermore, MCL-1 has been proposed to be downregulated through cleavage at Asp^{127} and Asp^{157} by caspase 3 during apoptosis, which generates pro-apoptotic MCL-1 by removal of the N-terminus (Weng et al., 2005). However, further validation of this data is required since Clohessy and colleagues contradicted this model (Clohessy et al., 2004). In addition to caspase 3, Granzyme B (GrB) cleavage of MCL-1 also impairs its ability to inhibit apoptosis (Han et al., 2004).

Taken together, MCL-1 is tightly regulated at multiple levels by diverse mechanisms indicating the complexity of pro-survival regulation in healthy and transformed cells. As MCL-1 is a protein with a short half-life, inhibition of transcription and/or translation can immediately affect MCL-1 levels in the cells that critically depend on the sustained presence of MCL-1.

1.3.4 The requirement of MCL-1 in normal development

MCL-1 is unique among pro-survival BCL-2 molecules as it is the only one, together with BCL-X_L, that is required for the normal development of the developing embryo. MCL-1 is essential for early embryonic development as deletion of *Mcl-1* results in peri-implantation embryonic lethality (Rinkenberger et al., 2000). This is interesting since *Bcl-x_L*-deficient embryos survive substantially longer until approximately E12.5 (Motoyama et al., 1995). MCL-1 is required for maintenance of T- and B-cells, neutrophil, and hematopoietic stem cells because removal of *Mcl-1* induced rapid loss of these lineages *in vivo* (Opferman et al., 2003). Loss of *Mcl-1* also results in neutropenia (Steimer et al., 2009) and loss of early bone marrow progenitor populations including hematopoietic stem cells (Opferman et al., 2005).

MCL-1 was also shown to be essential for survival of non-hematopoietic cells including neurons, cardiomyocytes and hepatocytes. This is exemplified by the fact that MCL-1 is required for cortical neurogenesis and the survival of neurons after DNA damage (Arbour et al., 2008). Moreover, pups bearing *Mcl-1* deletion specifically in the heart die within the first 10 days after birth and exhibit myocardial degeneration. In adult mice removal of *Mcl-1* in the heart leads to rapid cardiomyopathy by causing disorganized sarcomeres and swollen mitochondria in myocytes and impairment of autophagy and also leads to rapid lethality. Genetic removal of *Bax* and *Bak* could largely rescue this lethality suggesting an apoptotic mechanism of cell death (Thomas et al., 2013; Wang et al., 2013). Hepatocyte specific deletion of *Mcl-1* leads to liver cell damage due to spontaneous induction of

apoptosis and *Mcl-1* deleted livers are smaller and susceptible to hepatocellular damage (Vick et al., 2009).

1.3.5 Cancer development and maintenance by MCL-1

Defects in apoptosis promote tumorigenesis by allowing an extended life span of cells thereby effectively increasing the chances of acquiring additional mutations. On the other hand, the blockade of apoptosis protects cancer cells from death driven by oncogenic alterations and deprivation of nutrition effectively driving carcinogenesis. *MCL-1* is frequently amplified in multiple cancers including lung, breast and gastrointestinal cancer, which is suggestive for an anti-apoptotic role in these cancers (Beroukhim et al., 2010). Elevated levels of MCL-1 are associated with a resistance to chemotherapy, relapse of disease and poor prognosis (Kaufmann et al., 1998; Pepper et al., 2008; Stam et al., 2010). In addition, MCL-1 is also overexpressed in solid tumors such as melanoma (Wong et al., 2008) and hepatocellular carcinoma (Sieghart et al., 2006). Until now, there are only limited data available on the role of MCL-1 in cancer development and sustained cancer cell survival within the context of the whole organism. Data from Glaser and colleagues show that the genetic deletion of *Mcl-1* using the inducible CRE-mediated deletion of the *Mcl-1* gene results in rapid induction of cell death of leukemic blast cells in a mouse model of acute myeloid leukemia (Glaser et al., 2012). However, the role of MCL-1 in epithelial cancers has not been functionally analyzed so far.

Specifically in lung cancers, MCL-1 is overexpressed in approximately 60% of primary specimens of NSCLC (Borner et al., 1999) and chemotherapy naive NSCLC samples (Wesarg et al., 2007). Furthermore, MCL-1 is also abundantly expressed in NSCLC tumors in comparison to adjacent normal tissues and cell lines (Song et al., 2005). Overexpression of MCL-1 induces resistance to therapeutic agents such as ABT-737 (Song et al., 2005; Wesarg et al., 2007). Histologically, *MCL-1* overexpression is detected in 8-12.5% and approximately 6% of tested lung adeno- and squamous cell carcinoma, respectively (Catalogue of somatic mutations in cancer, accessed in October, 2014). Downregulation of MCL-1 by antisense oligonucleotide induces apoptosis in NSCLC cell lines indicating its importance for survival of these cells (Borner et al., 1999; Zhang et al., 2011).

Because of its overexpression and/or amplification in a variety of cancers (Beroukhim et al., 2010), and association with resistance to chemotherapy and poor prognosis (Wei et al., 2006; Wuilleme-Toumi et al., 2005), there has been an increasing interest in developing MCL-1 specific inhibitors. Although several

moderately potent MCL-1 inhibitors have been described (Abulwerdi et al., 2014; Friberg et al., 2013), current MCL-1 specific inhibitors have not shown satisfactory efficacy. The difficulty in targeting MCL-1 is possibly due to the structural rigidity of the BH3 binding groove of MCL-1, which is more rigid than BCL-X_L and BCL-2 (Czabotar et al., 2007; Czabotar et al., 2014). A pan inhibitor of BCL-2 protein inhibitor, obatoclax, antagonizes MCL-1 (Nguyen et al., 2007), however, its binding affinity for MCL-1 is as low as that of the BH3 mimetic ABT-737 (which is considered to bind to BCL-2, BCL-X_L and BCL-W, but not efficiently to MCL-1 and A1 (Oltersdorf et al., 2005)) (Billard, 2013). Furthermore, obatoclax is not as specific to BCL-2 proteins and not as potent as ABT-737. Therefore obatoclax kinetics of apoptosis induction is low (Vogler et al., 2009). Additionally, ligands that are specific for MCL-1 have been developed. Lee and colleagues developed a BH3-like ligand derived from the BIM protein, BIM_s2A. BIM_s2A targets MCL-1 specifically without degrading it (Lee et al., 2008) and the effect of MCL-1 inactivation by BIM_s2A on human NSCLC cell lines will be described in section 3.3.

1.4 Mouse models of lung cancer

Lung cancer can be induced in mice by a variety of carcinogenesis protocols (Farago et al., 2012). Several approaches have been used to generate mouse models of lung cancer such as genetically engineered, spontaneous mutant models, and carcinogen induced models.

The susceptibility to spontaneous development of lung tumor varies largely in distinct in-bred mouse strains. The most sensitive mouse strains to spontaneous development of lung tumor include A/J and SWR, and intermediate sensitive strains include BALB/c and O20. Furthermore, CBA and C3H, and DBA and C57BL/6 are relatively resistant and the most resistant strains, respectively. The sensitive strains are also susceptible to chemical induction of lung tumors (Shimkin and Stoner, 1975). Susceptibility for spontaneous lung tumorgenesis in the sensitive strains can be attributed to a polymorphism in intron 2 of *Kras,* which may influence gene expression and thereby increase the risk of developing lung cancer (You et al., 1992; You et al., 1993). With analysis of recombinant inbred strains derived from interbreeding the susceptible A/J and resistant C57BL/6 strains, three pulmonary adenoma susceptibility (*Pas*) loci have been suggested (Malkinson et al., 1985). *Pas-1* was later identified with the analysis of progeny derived from the cross between A/J and CH3/He and located at the distal end of chromosome 6 (Gariboldi et al., 1993). Subsequently, *Kras* was linked to the *Pas-1* locus (Lin et al., 1998).

Additional *Pas* loci have been mapped within the mouse genome, such as the *Par2* locus on chromosome 18 in BALB/cByJ (Festing et al., 1998; Obata et al., 1996) and the *Pas* loci on chromosomes 7, 9, and 19 (Devereux and Kaplan, 1998; Festing et al., 1998; Festing et al., 1994; Malkinson, 1999; Obata et al., 1996).

A wide range of chemical carcinogens with distinct potencies can induce pulmonary adenoma and adenocarcinoma (Malkinson, 1989; Shimkin and Stoner, 1975). Potent carcinogens are urethane, components in tobacco such as polycyclic aromatic hydrocarbons and nitrosamines, and aflotoxin. These carcinogens initiate and/or promote tumorigenesis (Tuveson and Jacks, 1999). However, only very few mouse models for chemically induced squamous cell carcinoma have been developed (Wakamatsu et al., 2007). Intratracheal instillation of methyl carbamate (Nettesheim and Hammons, 1971) and topical application of N-nitroso-tris-chloroethylureas (Rehm et al., 1991) have been shown to induce squamous cell carcinoma in mice. Skin painting with N-nitroso-tris-chloroethylureas induced squamous cell carcinoma in lung of the susceptible strains such as SWR/J, NIH Swiss, A/J, BALB/cJ, and FVB/J (Wang et al., 2004).

In parallel, many genetically engineered mouse models of lung cancer have been generated that closely resemble human lung cancer in many aspects and facilitate the study of specific genes in implicated in tumor initiation and maintenance.

Mouse models for NSCLC, primarily adenocarcinoma, have been generated by the introduction of a number of mutations found in human NSCLC. A large number of studies have been conducted using conditional knock-in mice that carry a mutation in *Kras (lox-STOP-lox-Kras^{G12D}* mice*)*. Expression of CRE recombinase induces *Kras^{G12D}* or *Kras^{V12}* expression from the endogenous locus by inducing the removal of the loxP site flanked (floxed) STOP element (Jackson et al., 2001; Meuwissen et al., 2001). Adenoviral mediated delivery of CRE enabled the model to closely mimic the development of the human tumor by causing sporadic activation of the *Kras* oncogene in individual cells that remain surrounded by normal cells. After activation of *Kras^{G12D}* expression, mice develop lesions ranging from atypical adenomatous hyperplasia to adenocarcinoma but no detectable metastasis (Jackson et al., 2001). Furthermore, it was shown that only a fraction of *Kras^{V12}* expressing bronchiolo-alveolar cells transformed leading to the formation of adenoma and adenocarcinoma suggesting heterogeneity either in alveolar cells, or in the microenvironment controlled by the surrounding cells (Guerra et al., 2003; Kwon and Berns, 2013). *Lox-STOP-lox-Kras^{G12D}* (*lsl-Kras^{G12D}*) mice have been crossed with other strains in order to generate combined strains such as *lsl-Kras$^{G12D/+}$ p53$^{fl/fl}$* or *lsl-p53$^{R270H/fl}$* or *lsl-p53$^{R172H/fl}$* (Jackson et al., 2005), *lsl-Kras$^{G12D/+}$Lkb1$^{fl/fl}$* (Ji et al., 2007),

lsl-Kras$^{G12D/+}$*Pten*$^{fl/fl}$ *CCSP-CRE* (Li et al., 2008), and *lsl-Kras*$^{G12D/+}$ *Rb*$^{fl/fl}$ or *p130*$^{fl/fl}$ (Ho et al., 2009). The mouse model used in this thesis is based on the inducible induction of mutant *Kras* be CRE-mediated deletion of the STOP cassette blocking expression in combination with loxP-flanked alleles for *Mcl-1* (further details below). Genetically engineered mouse models of lung cancer are summarized in Table 1.

Table 1. Lung cancer mouse models

Initiating / additional mutation	Genetic alteration	Tumor induction	Phenotype	Relevance to human lung cancer
Kras activation	*lsl-Kras*$^{G12D/+}$	Endogenous expression of *Kras*^{G12D} upon infection of lung with AdenoCRE.	Atypical adenomatous hyperplasia to adenocarcinoma (adenocarcinoma spectrum). Metastasis not reported.	*KRAS* mutated in ~20%- 30% of lung adenocarcinomas. (Jackson et al., 2001)
	lsl-Kras^{G12Vgeo} *RERTn*^{ERT}	4OHT mediated expression of CRE-ERT	Adenoma and adenocarcinoma. Only fraction of *Kras*^{V12} expressing cells proliferate.	(Guerra et al., 2003)
Kras activation *p53* inactivation	*lsl-Kras*$^{G12D/+}$ *p53*$^{fl/fl}$ *or* *lsl-p53*$^{R270H/fl}$ *or* *lsl-p53*$^{R172H/fl}$	Viral CRE mediated expression of *Kras*^{G12D} and *p53* mutants: deletion of both *p53* alleles; one deleted and one mutant (R270H) or (R172H).	Adenocarcinoma spectrum. Accelerated progression of *Kras*^{G12D} induced tumor to higher grade. metastasis to thoracic lymph nodes and kidney.	*p53* mutated in ~10%-35% of human lung adenocarcinoma. (Jackson et al., 2005)
Kras activation *Lkb1 (Stk11)* inactivation	*lsl-Kras*$^{G12D/+}$ *Lkb1*$^{fl/fl}$ or *Lkb1*$^{fl/-}$	Viral CRE mediated expression of *Kras*^{G12D} and inactivation of *Lkb1*	Short latency, adeno-, squamous cell and large cell carcinoma. Metastasis to lymph nodes and skeleton.	*LKB1* mutated in 8%- 26% of human lung adenocarcinoma and squamous cell carcinoma. (Ji et al., 2007)
Kras activation *Pten* inactivation	*lsl-Kras*$^{G12D/+}$ *Pten*$^{fl/fl}$ *CCSP-CRE*	CRE mediated Expression of *Kras*^{G12D} and inactivation of *Pten*	Adenocarcinoma spectrum; accelerated tumorigenesis. Metastasis.	*PTEN* mutated in 3% of human lung carcinoma. (Li et al., 2008)
Kras activation *Rb* or *p130* inactivation	*lsl-Kras*$^{G12D/+}$ *Rb*$^{fl/fl}$ or *p130*$^{fl/fl}$	Viral CRE mediated expression of *Kras*^{G12D} and inactivation of *Rb* or *p130*	Adenocarcinoma spectrum. Increased tumor burden, decreased survival, and higher grade tumor in comparison to *Kras*^{G12D} alone.	*RB* mutated in 3% of human lung adenocarcinoma. (Ho et al., 2009)
Kras activation	*Kras*^{LA2}	Spontaneous lung tumor development	Adenocarcinoma spectrum. Metastasis to thoracic lymph node, kidney. Prone to thymic lymphoma, skin papilloma.	*KRAS* mutated in ~20%- 30% of lung adenocarcinomas. (Johnson et al., 2001)

Egfr activation	*Tet-O-Egfr*^{L858R} or *TetO-Egfr*^{Del19} *CCSP-rtTA*	CCSP-rtTA doxycycline inducible	Adenocarcinoma spectrum. Deletion of exon 19 induced multifocal invasive adenocarcinoma; L858R tumors have shorter latency and are diffuse.	*EGFR* mutated in 23% of lung adeno-carcinoma. L858R mutations in 35%-45% of all *EGFR* mutations, and exon 19 deletions for 45%-50% of all *EGFR* mutations (Politi et al., 2006; Regales et al., 2007)
Pi3kca (PI3K p110-α subunit) activation	*Tet-O-Pi3kca*^{H1047R} *CCSP-rtTA*	CCSP-rtTA doxycycline inducible	Adenocarcinoma spectrum. Bronchioalveolar features	*PIK3CA* mutated in 2% of human lung carcinoma (Engelman et al., 2008)
Eml4-Alk chimeric oncogene	*Tet-O-Eml4-Alk* *CCSP-rtTA*	CCSP-rtTA doxycycline inducible	Short latency and adenocarcinomas with predominantly bronchioloalveolar carcinoma features	*ALK* somatic rearrangements identified in 6% of human lung adeno-carcinoma (Chen et al., 2010)
p53 and *Rb* inactivation	*p53*$^{fl/fl}$ *Rb*$^{fl/fl}$	Viral CRE mediated inactivation of *p53* and *Rb*	Aggressive SCLC histology, metastasis to extrapulmonary sites.	*p53* and *RB* mutated in >90% of human SCLC (Meuwissen et al., 2003)
p53, *Rb* and *p130* inactivation	*p53*$^{fl/fl}$ *Rb*$^{fl/fl}$ *p130*$^{fl/fl}$	Viral CRE mediated inactivation of *p53*, *Rb, and p130*	Accelerated tumorigenesis with unchanged histology compared to *p53*$^{fl/fl}$ *Rb*$^{fl/fl}$	There are cases of *p130* loss in human SCLC, and lower *p130* are associated with poor prognosis.(Schaffer et al., 2010)

Data adapted from (Farago et al., 2012; Kwon and Berns, 2013).

1.5 Specific aims of this project

The aim of my thesis was to determine the consequence of genetic inactivation of MCL-1 in KRAS-driven adenocarcinoma of the lung. This was based on the hypothesis that functional inhibition of pro-survival MCL-1 will be capable of overcoming the apoptotic resistance of KRAS-mutated lung adenocarcinoma. I based my hypothesis on the notion that the induction of apoptosis might reduce the cellular survival of NSCLC cancer cells and thereby decreases the tumor burden of diseased mice. My study is therefore driven by the translational approach to define the basis for targeting MCL-1 pharmacologically in patients with adenocarcinoma of the lung in the future.

My **first aim** was to characterize the expression of MCL-1 and the dependency on MCL-1 in human non-small cell lung cancer cell lines with or without mutations in *KRAS*. Mutations in *KRAS* cause the deregulation of multiple

downstream effector pathways and subsequently result in constitutively active oncogenic signal transduction. I therefore tested whether induction of apoptosis was capable of overcoming the sustained survival despite the presence of multiple activated mitogenic signaling pathways, which render KRAS-mutated adenocarcinoma a clinically challenging disease (de Castro Carpeño and Belda-Iniesta, 2013).

My **second aim** was to substantiate my findings obtained from my cell culture studies within the context of the whole organism. I have therefore established a murine model of KRAS-induced lung adenocarcinoma to study tumorigenesis *in vivo*. Next to mutations in *p53*, mutant *KRAS* constitutes the most commonly affected genetic lesion in lung adenocarcinoma in human patients (approximately 30% of all cases) and the model was therefore chosen as the clinically most relevant mouse model system (The Cancer Genome Atlas Research Network, 2014). Previous data have suggested a critical contribution of MCL-1 to sustained cancer cell survival especially in adenocarcinoma of the lung as represented by the fact that genetic amplifications of the genomic locus of *MCL-1* are frequently observed in human pulmonary adenocarcinoma (Beroukhim et al., 2010). Previous studies have also shown that, at least *in vitro*, downregulation of MCL-1 by genetic approaches induced substantial apoptosis in established lung cancer cell lines (Zhang et al., 2011). However, the functional relevance of MCL-1 in lung cancer development was so far not defined *in vivo.*

My **third aim** was to test whether conventional therapeutic options such as chemotherapy or BH3-mimetics were able to kill tumor cells more efficiently if *Mcl-1* was deleted. I therefore checked if reducing MCL-1 expression might increase the response of established lung tumors to pharmacologic inhibition of pro-survival BCL-2 family proteins other than MCL-1 *in vivo*. In addition, I monitored success of cisplatin treatment with or without additional *Mcl-1* deletion. Diseased mice were subjected to state-of-the-art biomedical imaging using positron emission imaging combined with computed tomography imaging after cisplatin treatment to monitor treatment response.

My **fourth aim** was to understand the molecular mechanisms that control the survival of cancer cells upon genetic deletion of *Mcl-1*. In addition, I wanted to characterize the lung cancer lesions that arise despite *Mcl-1* deletion to understand potential escape mechanisms. I therefore tested the molecular response of lung cancer lesions to the genetic deletion of *Mcl-1 in vivo* using a multitude of immunohistochemical staining protocols.

2. MATERIALS AND METHODS

2.1 Cell culture

Unless otherwise indicated, all cell culture media and reagents were purchased from Gibco, Life Science. Human NSCLC cell lines H358 (bronchioalveolar carcinoma derived), H1975 (adenocarcinoma derived) and H2170 (squamous cell carcinoma derived) were obtained from ATCC and cultured in RPMI medium 1640 with following supplements: 10% fetal bovine serum (FBS), 2mM L-Glutamine, 10 mM HEPES, 1mM sodium pyruvate, 0.15% sodium bicarbonate (Sigma-Aldrich), 25 mM glucose (Sigma-Aldrich) and 1% penicillin/streptomycin. Human Embryonic Kidney 293T cells (HEK293T) were cultured in DMEM with 10% FBS and 1% penicillin/streptomycin.

Wild type (WT) and *Mcl-1* knock-out (*Mcl-1*^{ko}) murine embryonic fibroblasts (MEF) (from Walter and Eliza Hall Institute of Medical Research) were cultured in DMEM supplemented with 10% FBS, 50 μM 2-mercopethanol and 1% penicillin/streptomycin. All cells were cultured at 37°C in an atmosphere containing 5% CO_2.

2.2 Transfection and transduction with BIM_s variants

The doxycycline-responsive lentiviral vector pFTRE3G_pGK3G_GFP containing BIM_s variants are previously described (Chen et al., 2005; Kelly et al., 2014; Lee et al., 2008). Lentiviral particles were produced by transfecting HEK293T cells, using *Metafectene*® Pro (Biontex, cat# T040) according to the manufacturer's protocol, with the lentiviral packaging constructs psPAX and pMD2MG (7.5 μg of each) and 15 μg of target DNA – lentiviral inducible BIM_s variants. Twenty-four and forty-eight hours after transfection, the supernatants were collected and filtered with 0.45 μm filters. Target cells (H358, H1975 and H2170) were incubated with the viral supernatant supplemented with polybrene (4 μg/ml) for 30 min at 37°C and then spun (2200 rpm) for 1 hour at room temperature (RT), and then for 1.5 hours at 32°C. After the spin infection, the target cells were incubated with the supernatant for 48 hours and subsequently the supernatant was changed to fresh medium.

2.3 Transfection and transduction with *Kras* constructs

HEK293T cells were transiently transfected with either 14.4 μg pBabe puro encoding WT *Kras* or *Kras*^{G12D} (kindly provided by Oleksi Petronko (Ischenko et al., 2013)) alongside the retroviral packaging plasmids, gag (4.8 μg) and env (2.4 μg), using *Metafectene*® Pro (Biontex, cat# T040) according to the manufacturer's protocol.

Twenty-four and forty-eight hours after transfection, the supernatants containing virus were collected and passed through 0.45 μm filters. To infect target cells, WT and *Mcl-1*^{ko} MEF, the retroviral supernatants supplemented with 4 μg/ml polybrene were incubated with 1*10^5 cells per construct for 30 min at 37°C and spun for 1 hour at 2200 rpm at 32°C. Afterwards, the supernatant was removed and the cells were seeded in 6 well plates with fresh medium. Three days after the infection, selection was started with 1 μg/ml puromycin and the cells maintained under the selection.

2.4 Inducible expression of BIM$_S$ variants in human NSCLC cell lines

The lentivirally transduced cells (mentioned in 2.2) were seeded in a 96 well plate (8*10^3 per well) and next day treated with 1μg/ml doxycycline to induce the expression of BIM$_S$ variants. Twenty-four and forty eight-hours after the induction, viable cells were determined with propidium iodide (PI) staining (3μg/ml) and FACS analysis. PI-negative and green fluorescent protein (GFP)-positive cells were considered to be live cells. Cell viability was expressed relative to untreated NSCLC cell lines, assigned as 100%.

2.5 ABT-737 treatment

Human NSCLC cells, H358, H1975 and H2170, were seeded as described in 2.4 prior to the addition of ABT-737 (Active Biochem, cat# A-1002; (Oltersdorf et al., 2005)). The cells were incubated with ABT-737 dissolved in dimethyl sulfoxide (DMSO) to final concentrations of 0.01, 0.1, 1 and 10 μM for 48 hours.

WT and *Mcl-1*^{ko} MEF transduced with the retroviral constructs expressing WT *Kras* or *Kras*^{G12D} were seeded in 96 well plates at 5*10^3 cells/well and incubated with ABT-737 at final concentrations of 0.05-1 μM for 48 hours. Cell viability was checked with the CellTiter-Glo® assay (Promega, cat# G7175) according to the manufacturer's protocol and presented relative to vehicle (DMSO) treated cells.

2.6 Apoptosis array

WT MEF were transduced with pBabe puro *Kras*^{G12D} or empty vector pBabe puro as in section 2.3 and subsequently RNA was isolated using the NucleoSpin® RNA kit (Macherey-Nagel, cat# 740955.50). cDNA was synthesized from 1 μg RNA by using SuperScpript® II Reverse Transcriptase (Invitogen, cat# 18064-014) according to the manufacturer's protocol. The expression of *Bcl-2* family genes in *Kras*^{G12D} or vector control transduced WT MEF were determined by performing a RT² Profiler™ PCR Array (Qiagen, cat# PAMM-012ZA) with a real-time cycler (Roche LightCycler 480) according to the protocol provided. Analysis was performed with fit-points by the

cycler and Web-based software, available at http://www.SABioscience.com/ pcrarraydataanalysis.php. The change of gene expression relative to empty vector control was calculated.

2.7 Gene expression array

Robust Multi-array Average (RMA) normalized gene expression array data was provided by AG Saur (II. Medizinische Klinik, MRI, TUM) in a collabration. Gene expression from two independently prepared *lsl-Kras*$^{G12D/+}$ MEF treated with AdenoCRE relative to control treated *lsl-Kras*$^{G12D/+}$ MEF were calculated.

2.8 Immunoblotting

One day before cell lysate preparation, cells were seeded (1*10^6 per 10 cm dish). Cells were lysed using RIPA buffer (Cell signaling cat# 9806) containing protease inhibitors (complete protease inhibitor cocktail, Roche) and protein concentrations were determined by BCA assay (Thermo Scientific cat# 23225). Total protein extracts (20 μg/lane) were denatured in Laemmli loading buffer containing 5% β-mercaptoethanol and followed by separation by SDS-PAGE and transfer onto nitrocellulose membranes. Antibodies used were MCL-1 (1:1000, Bundoora Mab lab, clone# 19C4-15), BCL-2 (anti-human, 1:1000, WEHI, clone# Bcl-2-100; anti-mouse, 1:1000, BD Bioscience, clone# 3F11), BCL-X_L (1:1000, BD Bioscience, cat# 610212), BIM (1:1000, Enzo Life science, cat# ADI-AAP-33-E), cleaved caspase 3 (1:1000, Cell signaling, cat# 9662), KRAS (1:1000, Calbiochem, clone# 234-4.2) and β-ACTIN (HPR-conjugated, 1:40,000, Cell signaling, clone# 12F5).

2.9 Mouse strains

Previously established *lox-STOP-lox-Kras*^{G12D} (*lsl-Kras*^{G12D}) (Jackson et al., 2001) and *Mcl-1* floxed (Opferman et al., 2003) mice were used to generate *lsl-Kras*^{G12D} *Mcl-1*^{floxed} mice.

2.10 Tumor induction

Six to eight week old *lsl-Kras*$^{G12D/+}$ *Mcl-1*$^{+/+}$, *lsl-Kras*$^{G12D+}$ *Mcl-1*$^{fl/+}$, *lsl-Kras*$^{G12D+}$ *Mcl-1*$^{fl/fl,}$ and *Mcl-1*$^{fl/+}$ mice were infected with 5*10^6 plaque forming units (PFU) of AdenoCRE (provided by Dr. Martina Anton, Institut für Experimentelle Onkologie und Therapieforschung, MRI, TUM). AdenoCRE:$CaCL_2$ co-precipates were prepared as described previously (Fasbender et al., 1998) and administered by two 62.5 μl intranasal instillations (as described in(Jackson et al., 2001)) at 4 min apart. The mice were anesthetized according to their weight with a mixture of Medetomidine

(0.5 mg/kg), Midazolam (5 mg/kg) and Fentanyl (0.05 mg/kg) (MMF) (mixed together at the pharmacy of the hospital).

2.11 Tissue harvesting

The AdenoCRE infected mice were sacrificed at 19 weeks post-infection. The lungs were inflated with 42°C warm 0.6% agarose in phosphate buffered saline (PBS) or with air (for CT scan) and harvested. The lungs were fixed in 4% paraformaldehyde (PFA) overnight at room RT and subsequently placed in 70% ethanol and sent for dehydration and paraffin infiltration. The tissues were then paraffin embedded.

2.12 Tumor burden analysis

A quantitative analysis was performed to analyze the tumor burden in the lungs at 19 weeks post-infection. All formalin fixed paraffin embedded (FFPE) lungs were sectioned into 3 step-sections at 100 μm intervals. Each step-section consisted of 8 sections that were 2 μm (for hematoxylin and eosin (H&E) and immunohistochemistry (IHC)) or 5 μm (for *in situ* hybridization (ISH)) thick. The third section of each step-sections were H&E stained and further used for tumor burden analysis. The sections were scanned with a SCN400 slide scanner (Leica microsystems) and the area (μm^2) of individual tumors (lesions) and total lung area (μm^2) on the sections were determined by manually defining the lesion a lung area using the free hand mode of the Tissue IA image analysis software (Slidepath, Leica microsystems). The total numbers of the lesions on each section were counted. The ratio of tumor area to lung area was defined as the sum all lesion areas divided by total lung area on the sections. Three H&E stained sections per animal were analyzed (Figure 3).

2.13 Evaluation of lung tumors

Histological grading of tumor was performed at 19 weeks post-infection with AdenoCRE infection by PD. Dr. Specht, Institut für Allgemeine Pathologie und Pathologische Anatomie, MRI, TUM. Definitions of the lesions were made according to a previously published recommendation (Nikitin et al., 2004). Briefly, hyperplasia was defined as increased number of cuboidal, columnar, ciliated or mucous cells without atypia. Atypical adenomatous hyperplasia (AAH) was defined as focal or diffuse lesions involving alveoli or terminal bronchioles and constaining relatively uniform atypical cells with nuclear hyperchromasia. Adenomas are well-defined areas consisting of cuboidal to columnar cells lining the alveoli, showing either a papillary, solid or mixed growth pattern. Adenocarcinomas show a substantial

heterogeneity of growth patterns with a diameter of more than 5 mm. Nuclear and cellular atypia and loss of architecture are considered additional criteria for malignancy.

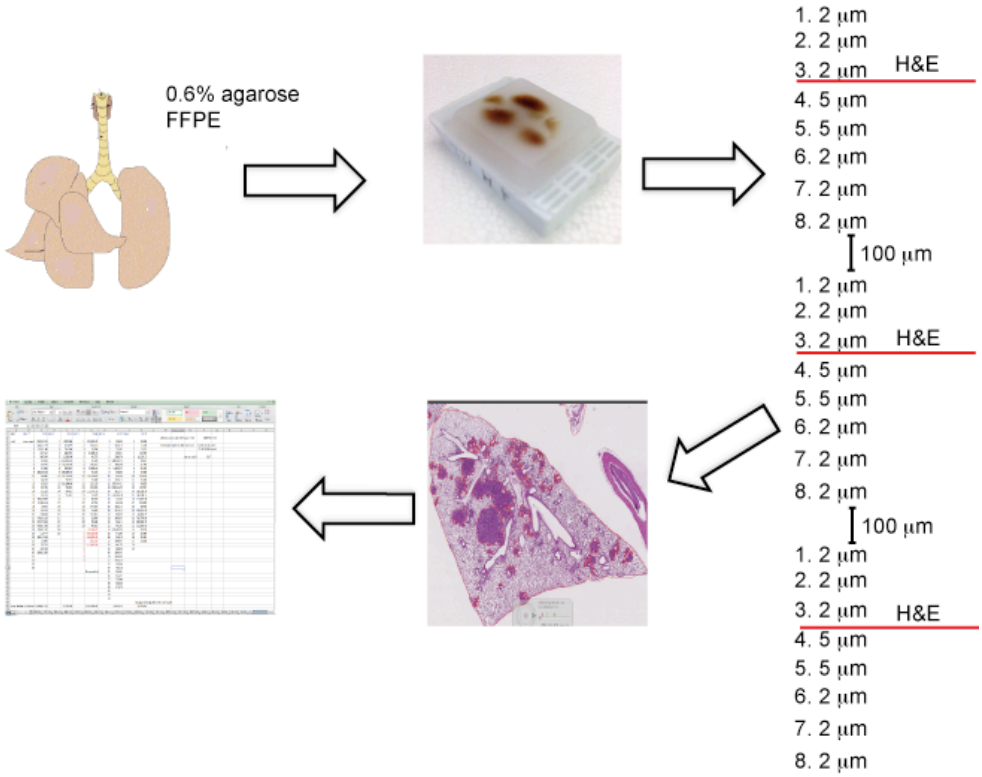

Figure 3. Schematic illustrations of workflow and the tissue sectioning for tumor burden analysis. FFPE lungs were step-sectioned at 100µm intervals into 3 individual step-sections. Every third section of each step-section was H&E stained and scanned with a SCN400 slide scanner (Leica microsystems) for quantification and analysis of tumor burden with Tissue IA image analysis software (Slidepath, Leica microsystems).

2.14 Infection of *LacZ* mice and examination of adenoviral CRE functionality

Six to eight week old *ROSA26 lsl-LacZ* mice (Soriano, 1999), kindly provided by AG Siveke (II. Medizinische Klinik, MRI, TUM), were infected with $5*10^8$ PFU of AdenoCRE as described in 2.12. Seventy-two hours after the infection, the mice were sacrificed. The lungs were inflated with 4% PFA and harvested. Afterwards, the lungs were fixed in 4% PFA for 1 hour, subsequently in 15% sucrose for 5 hours and then in 30% sucrose overnight. These fixation steps were performed at 4°C and followed by embedding the tissue with Tissue-Tek® O.C.T.™ Compound (Sakura, cat# 4583). To test for *LacZ* expression induced by CRE activity, X-Gal staining was performed as follows: 10 µm thick frozen tissue sections were dried at RT for 2 hours and then fixed in 4% PFA for 10 min. Afterwards, the section slides were washed in PBS 3 times for 5 min each and then incubated in X-gal staining solution at 37°C for

48 hours. The X-gal staining solution consisted of PBS containing Potassium hexacyanoferrate (III) (Sigma, cat# P8131) (5mM), Potassium Ferrocyanide (Fluka BioChem, cat# 60279) (5mM), Magnesium Chloride (2mM) and X-gal (1mg/ml) dissolved in dimethylformamid. After the staining for 48 hours, the slides were rinsed in PBS 3 times for 5 min each and counterstained with nuclear fast red solution (Vector, cat#H3403) for 10 min. The slides were washed in dH_20 for a few seconds and dehydrated through graded ethanol 80%, 96% and 99% for 10-15 seconds each. Subsequently, the slides were incubated in Histoclear 2 times for 5 min each and mounted with Pertex (Leica Biosystems). *LacZ* expressing cells were stained blue.

2.15 Hematoxylin and Eosin (H&E) stain

Two μm FFPE tissue sections were stained with hematoxylin, of which an oxidation product, hemalum, stains cellular nuclei blue, and eosin stains basophilic structures such as external and internal proteins pink. The tissue sections were incubated at 60 °C for 20 min to improve deparaffinization. The sections were then incubated in an organic solvent (Roticlear®, ROTH) 3 times for 2 min each with frequent agitation to deparaffinize. Subsequently, the slides were incubated in 100% ethanol 3 times for 1 min each and washed with dH_2O shortly in order to rehydrate the tissue. Next, the slides were incubated in Harris's hematoxylin (VWR International) for 5 min. The slides were immediately transferred into fresh dH_2O and rinsed several times with fresh dH_2O until the washing water was clear. To remove excessive dye, prevent precipitation, and to emphasize stained structures the slides were shortly submerged in acid ethanol (0.5% hydrochloric acid (HCl) in ethanol) and immediately washed with tap water. The contrast between nuclei and cytoplasm was enhanced by rinsing the slides shortly with ammonia in dH_20 (40 drops of ammonia in 500 ml ddH_20, pH 9-10). This step changes soluble red phase hemalum to the insoluble blue phase by altering pH. The slides were washed with dH_20 and transferred into 70% ethanol shortly. Afterwards, the slides were incubated in eosin for 2 min with frequent agitation. After the staining, the sections were incubated in 100% ethanol 3 times 2 min each to dehydrate and then in Roticlear® 3 times shortly. The slides were mounted with mounting medium Pertex^{TM} (MEDITE) and covered with coverslips and allowed to dry.

2.16 Alcian Blue- Periodic Acid Schiff staining (AB-PAS)

Using 2 μm sections, AB-PAS staining was performed with a stain kit (Leica biosystems, cat# 38016SS5) according to the protocol provided with the kit. The alcian blue stains acidic mucin blue while the PAS stains the neutral mucins bright

magenta. Tissues or cells that contain both neutral and acidic mucins may exhibit dark blue to purple.

2.17 Immunohistochemistry (IHC)

Immunohistochemical stainings were performed on an automated staining system, Bond Max (Leica microsystems) by AG Heikenwälder (Institut für Virologie, MRI, TUM). The following antibodies were used: Ki67 (1:200, NeoMarkers/LabVision Corporation, cat# RM-9106-S0, antigen retrieval: 1mM EDTA buffer), cleaved caspase 3 (Asp175) (1:300, Celll signaling, cat# 9661, antigen retrieval: 1mM EDTA buffer), phospho-STAT3 (Tyr705) (1:100, Cell signaling, cat# 9145, antigen retrieval: 1mM EDTA buffer), c-MYC (1:100, abcam, cat# ab32072, antigen retrieval: 1mM EDTA buffer), CD3 (1:300, NeoMarkers/LabVision Corporation, cat# RM-9107-S0, antigen retrieval: 1mM EDTA buffer), B220 (1:3000, BD Bioscience, cat# 55084, antigen retrieval: 1mM EDTA buffer), F4/80 (1:120, BMA Biomedicals AG, cat# T-2006, antigen retrieval: 1mM EDTA buffer) and myeloperoxidase (MPO) (1:200, Labvision Thermoscientific Neomarkers, cat# RB-373-A0, antigen retrieval: 1mM EDTA buffer). Anti- CC10 (1:100, antigen retrieval: citrate buffer) and SP-C (1:500, antigen retrieval: citrate buffer) antibodies were kindly provided by Petia Jeliazkova (II. Medizische Klinink, MRI, TUM). For TTF-1 staining, 2 μm FFPE tissue sections were stained with anti-TTF-1 antibody using Vector® M.O.M.™ Immunodetection Kit (Vector laboratories, cat# PK2200) according to the manufacturer's protocol. The sections were incubated in anti-TTF-1 antibody (Dako, cat# M3575) in M.O.M.™ diluent with ratio of 1: 200 for 1 hour at RT.

2.18 *In situ* hybridization (ISH)

In order to check *Mcl-1* expression in the lesions RNA *in situ* hydridization based RNAscope® 2.0 FFPE assay was used according to the manual (Advanced Cell Diagnostics, Inc, Rev 20120921), as described previously (Wang et al., 2012). Briefly, 5 μm thick FFPE tissue sections were baked in a tissue drying oven at 60 °C for 1 hour prior to the assay and tissue sections were deparaffinized with xylene and rehydrated with series of ethanol lines. Subsequently, the tissue sections were incubated with proteases to permeabilize cells after blocking endogenous peroxidases. Afterwards, positive (*mmUBC*, cat# 310771), negative (*dapB*, cat# 310043), and target probes (*mmMcl-1*, cat# 317241) were incubated with the tissue for 2 hours, and the incubation was followed by amplification steps to amplify the probe signals. The signals were detected by a chromogenic reaction and subsequently the tissue section was counterstained with Gill's hematoxylin. The

probe incubation and amplification steps (partially) were performed at 40^{o}C degrees. Quantification of the signals was performed manually (section 2.19).

2.19 Quantification of staining (H&E, IHC and ISH)

Unless otherwise indicated, for quantification of stainings and image acquisition, slides were scanned using a SCN400 slide scanner (Leica microsystems) by AG Heikenwälder (Institut für Virologie, MRI, TUM), and analyzed using Tissue IA image analysis software (Slidepath, Leica microsystems). Quantifications of ISH were carried out manually. Number of positive signal for *Mcl-1* RNA was counted in individual 2000 μm^2 tumor areas (approximately 20 cells each).

2.20 ABT-263 treatment

Tumor bearing mice were treated with ABT-263 (Active Biocehm, cat# A-1001) by oral gavage (*p.o.)* with a dose of 100 mg/kg daily for 14 consecutive days starting at 29 weeks after AdenoCRE infection. ABT-263 was formulated in 60% Phosal 50 PG (a kind gift from Phospholipoid GmBH), 30% PEG-400 (Sigma, cat# 06885) and 10% ethanol as described in (Corcoran et al., 2013). The treatment period was followed by an observational period of 2 weeks. Tumor response to ABT-263 treatment was monitored by small animal micro-CT (FMT-XCT) three times (once before, once after the treatment and once after the observational period). The CT scan, at 65 kV, 0.1mA current with 100 μm resolution, reconstruction and segmentation of tumors whose boundaries were clearly defined with the scans, were performed by Xiaopeng Ma (Institut für Biologische und Medizinische Bildgebung, Helmholtz Zentrum München). Tumors responses to the treatment were presented as tumor volume relative to initial volume, which was assigned as 100%.

2.21 Cisplatin treatment

Mice with already established lung tumors were treated with a single dose of cisplatin (7mg/kg) intraperitoneally (*i.p.*) 24 weeks after AdenoCRE infection as previously described (Oliver et al., 2010). Dynamics of the tumor response were determined with 2-deoxy-2-[^{18}F] fluoro-D-glucose (^{18}F-FDG) positron emission tomography-computed tomography (PET/CT) before and after treatment (day 2 and day 4). ^{18}F-FDG PET/CT were performed as described by (Li et al., 2012) and the analysis was carried out by Zhoulei Li in a collaboration with AG Keller (III. Medizinische Klinik, MRI, TUM). Tumor response was shown as ^{18}F-FDG uptake by tumors in comparison to the uptake before the treatment which was assigned as 100%.

2.22 Absorption based X-ray micro-CT

Air inflated formalin fixed lungs (section 2.11) were kept in 70% ethanol until staining with the contrast agent 1% iodine (I_2) dissolved in absolute ethanol (I2E) as previously described (Metscher, 2009). The lungs were measured for approximately 12 hours/lung with absorption-based X-ray micro-CT (versaXRM-500 from Zeiss Xradia) with the following parameters: voltage 40 kV, power 3W and resolution 11-13 μm. During the measurement, the lungs were fixed in an ethanol filled tube. The measurements and reconstruction was conducted in a collaboration by Pidassa Bidola (IMETUM / Chair of Biomedical Physics (E17), TUM).

2.23 Statistical analysis

Statistical analyses were conducted using unpaired two-tailed *t*-test or Mann Whitney test (where there were too different sample sizes) with Graph Prism 5.0.

3. RESULTS

3.1 Anti-apoptotic function of *Kras*^{G12D} in murine embryonic fibroblasts

Mutations in *KRAS* are frequently observed in human NSCLC. To study the anti-apoptotic effects of mutant KRAS and the contribution of MCL-1 to the survival of lung cancer cells, I utilized SV40-immortalized murine embryonic fibroblasts (MEF) proficient or deficient for *Mcl-1*. Pharmacologic inhibition of BCL-2 family members using the BH3 mimetic ABT-737, which binds to BCL-2, BCL-X_L and BCL-W, allowed differentiating between the functional relevance of MCL-1 in direct comparison to other pro-survival BCL-2 family members. WT and *Mcl-1*$^{-/-}$ MEF were transduced with retroviral constructs containing vectors expressing either WT *Kras* or the oncogenic mutant *Kras*^{G12D}. Expression of either *Kras* variant did not cause apparent changes in the expression of the BCL-2 family proteins BCL-2 and BCL-X_L, whereas BIM was substantially reduced in *Mcl-1*$^{-/-}$ MEF compared to control (Figure 4A). WT and *Mcl-1*$^{-/-}$ MEF expressing *Kras* WT or *Kras*^{G12D} were then cultured in ABT-737 range from 50 nM to 1 μM for 48 hours and viability of the cells was detected using CellTiter-Glo® assay. WT MEF were relatively resistant to ABT-737 independent of whether *Kras* or control (empty vector) was expressed (Figure 4B). In contrast, *Mcl-1*-deficient MEF were highly sensitive to ABT-737 compared to WT MEF irrespective of KRAS expression. Expression of WT *Kras* in *Mcl-1*$^{-/-}$ MEF did not significantly increase survival compared to *Mcl-1*$^{-/-}$ MEF expressing only the empty vector control. However, oncogenic *Kras*^{G12D} in *Mcl-1*$^{-/-}$ MEF increased the resistance to cell death induced by ABT-737, particularly at lower doses of ABT-737 (Figure 4C). These data indicate that KRAS^{G12D} protects cells from cell death induced by the inhibition of pro-survival BCL-2 proteins most notably in the context of MCL-1 deficient MEF.

In order to better understand the mechanisms promoting the anti-apoptotic effect of *Kras*^{G12D} expression, I sought to investigate the influence of *Kras*^{G12D} expression on *Bcl-2* family proteins in WT MEF. For this purpose, a quantitative real-time polymerase chain reaction (qPCR)-based gene expression array focusing on the 90 most important apoptotic regulators was utilized (Qiagen) to test for differences in gene expression upon mutant KRAS signaling. *Kras*^{G12D} increased the expression of pro-survival genes of the *Bcl-2* family, particularly of *Bcl-2a1a* (*A1*) and *Bcl-2l10* (*Bcl-B*), which were upregulated substantially (Figure 4D). In addition, *Mcl-1, Bcl-2l2 (Bcl-W)* and *Bcl-2l1* (*Bcl-x*$_L$) expression were also elevated (Figure 4D). Expression of *Bcl-2l11* (*Bim*) and *Bad*, pro-apoptotic BH3-only members of the

BCL-2 family, were reduced upon *Kras*^{G12D} expression (Figure 4D), together suggesting an anti-apoptotic effects of mutated KRAS.

To confirm this data, I utilized a whole genome gene expression array based on the affymetrix platform performed in MEF. We utilized MEF from lox-STOP-lox*Kras*^{G12D} (lsl-*Kras*^{G12D}) mice and infected two independent MEF cell lines with adenovirus expressing CRE recombinase (AdenoCRE). Consistent with the qPCR-based data, I found that the gene expression array from *lsl-Kras*$^{G12D/+}$ MEF after adenoviral CRE infection also showed elevated expression of *A1, Bcl-x*$_L$ and *Mcl-1* (cooperation with AG Saur, II. Medizinische Klinik, MRI, TUM) (Figure 4D and E). Although *Bcl-2* expression was not consistent between the assay systems, it was upregulated in two independent MEF cell lines from lsl-*Kras*$^{G12D/+}$ mice after infection with AdenoCRE (Figure 4E). Despite consistent upregulation of pro-survival *Bcl-2* members *A1, Mcl-1* and *Bcl-x*$_L$ in line with an anti-apoptotic effect of mutant KRAS, expression of pro-apoptotic members was variable in response to *Kras*^{G12D} expression in both assays. Ectopic expression of *Kras*^{G12D} in WT MEF resulted in a reduced expression of pro-apoptotic *Bim*, *Bad* and *Bak* and elevated expression of *Bax* and *Bok* expression (Figure 4D). However, in transgenic *lsl-Kras*$^{G12D/+}$ MEF, *Bim* expression was slightly upregulated, and expression of other pro-apoptotic members of *Bcl-2* family were not consistent between independent *Kras*$^{G12D/+}$ MEF (Figure 4E).

Taken together, MCL-1 potently protects MEF from cell death. Upon genetic deletion of *Mcl-1*, mutant KRAS is capable of significantly blocking cell death in MEF, which is consistent with an anti-apoptotic function of oncogenic KRAS. Oncogenic KRAS up-regulates the expression of pro-survival *Bcl-2* family members such as *Mcl-1, Bcl-x*$_L$ and *A1*.

3.2 Lung cancer cell lines are resistant to inhibition of BCL-2, BCL-X$_L$ and BCL-W

Pro-survival BCL-2 members are highly expressed in primary human lung cancer samples (Beroukhim et al., 2010; Song et al., 2005). Therefore, I examined NSCLC cell lines for expression of BCL-2 pro-survival proteins. The cell lines studied were the human KRAS-mutated NSCLC cell line H358 (bronchioalveolar carcinoma), the KRAS WT H1975 (adenocarcinoma), and the KRAS WT H2170 (squamous cell carcinoma) cell lines. Expression patterns of the BCL-2 proteins varied among these cell lines and MCL-1 was highly expressed in H358 and in H2170 cells but not in H1975 cells.

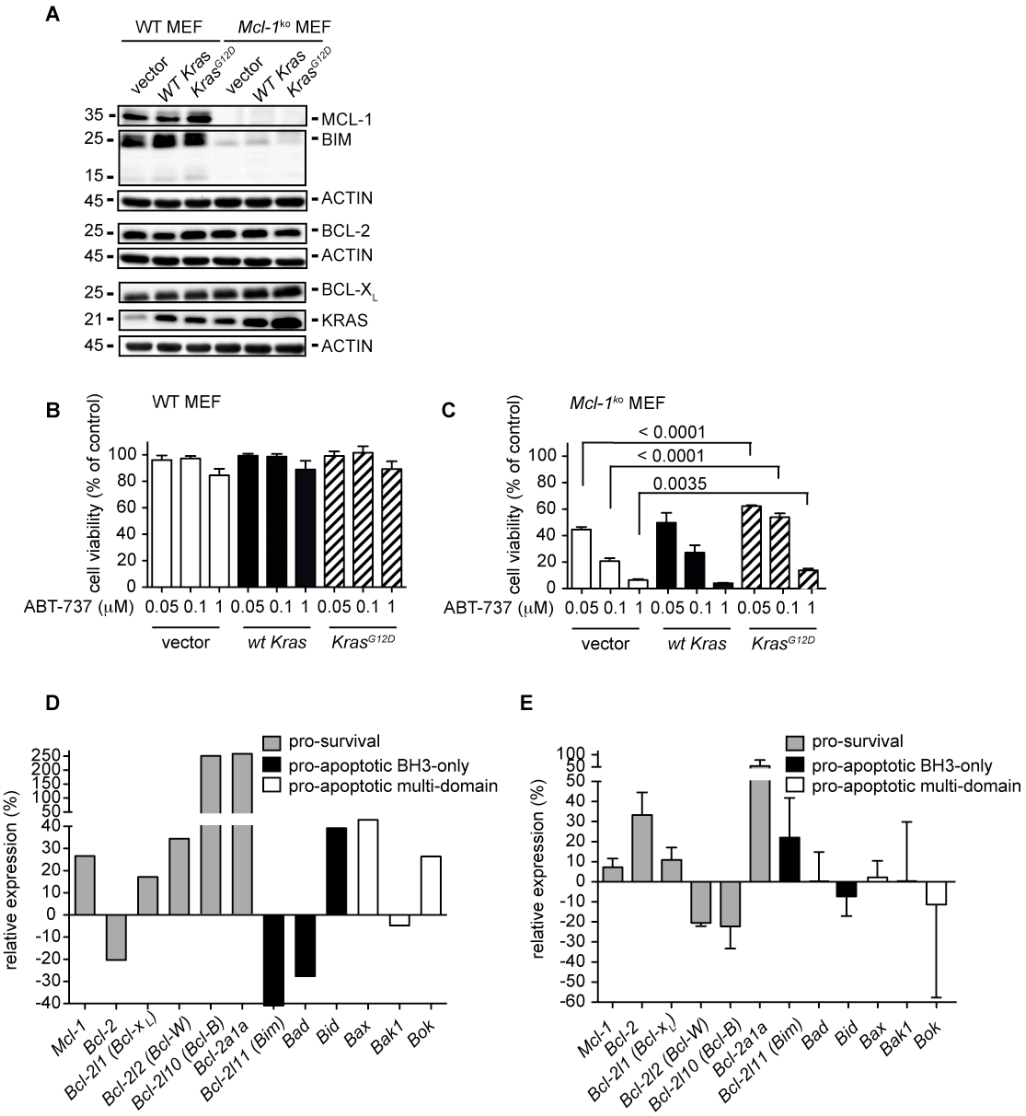

Figure 4. Oncogenic *Kras* upregulates expression of pro-survival *Bcl-2* genes and protects from cell death. (A) Immunoblotting to detect MCL-1, BCL-2, BCL-X_L, BIM, and KRAS protein in extracts from WT and *Mcl-1*$^{-/-}$ MEF stably expressing retroviral constructs carrying WT *Kras* and *Kras*^{G12D}. (B) WT MEF and (C) *Mcl-1*$^{-/-}$ MEF stably expressing retroviral constructs carrying WT *Kras* and *Kras*^{G12D} were treated with ABT-737 (0.05 to 1 μM) for 48 hours and cell viability was determined by CellTiter-Glo® luminescent cell viability assay. Results were normalized to vehicle treated controls. Each line was assayed in replicate in 3 independent experiments and data are presented as the mean±SEM. Unpaired two-tailed *t*-test was used for statistical analysis. (D) Expression of *Bcl-2* family member genes in WT MEF stably expressing *Kras*^{G12D} relative to the control (empty vector) were examined by the qPCR-based RT^2 Profiler PCR array (Qiagen) and analyzed by manufacturer's online based software. Gene expression of control was assigned as 0. (E) Expression of *Bcl-2* genes after activation of expression of endogenous *Kras*^{G12D} in *lsl-Kras*$^{G12D/+}$ MEF by AdenoCRE treatment relative to untreated control *lsl-Kras*$^{G12D/+}$ MEF. Relative expressions were presented as the mean±SEM of 2 independent Robust Multi-array Average (RMA) normalized gene expression array on 2 independently prepared *lsl-Kras*$^{G12D/+}$ MEF lines. Gene expression of control was assigned as 0.

An elevated expression was also detected for BCL-2 in H1975 and H2170. Furthermore, BCL-X_L and BIM expression were relatively constant in the three cell lines (Figure 5A). I therefore sought to investigate the functional relevance of MCL-1

and other pro-survival BCL-2 family members. The indicated cell lines (H358, H1975 and H2170) were incubated with ABT-737, at 0.01 μM to 10 μM, for 48 hours and cell viability was assayed with the CellTiter-Glo® assay (Figure 5B). All the cell lines showed significant resistance to ABT-737 irrespective of their protein expression profile. However, the low MCL-1, and high BCL-2 and BLC-X_L expressing cell line H1975 tended to be slightly more sensitive to high dose ABT-737 (10 μM) in comparison to the other cell lines. Of note, the ABT-737 doses utilized to observe any toxic effect in these cell lines *in vitro* are clearly too high to represent a viable treatment option *in vivo*. The resistance to inhibition of BCL-2, BCL-X_L and BCL-W imply that these proteins are not critically important survival factors for the tested cell lines irrespective of their KRAS status. Furthermore, MCL-1 is probably responsible for the resistance to undergo apoptosis.

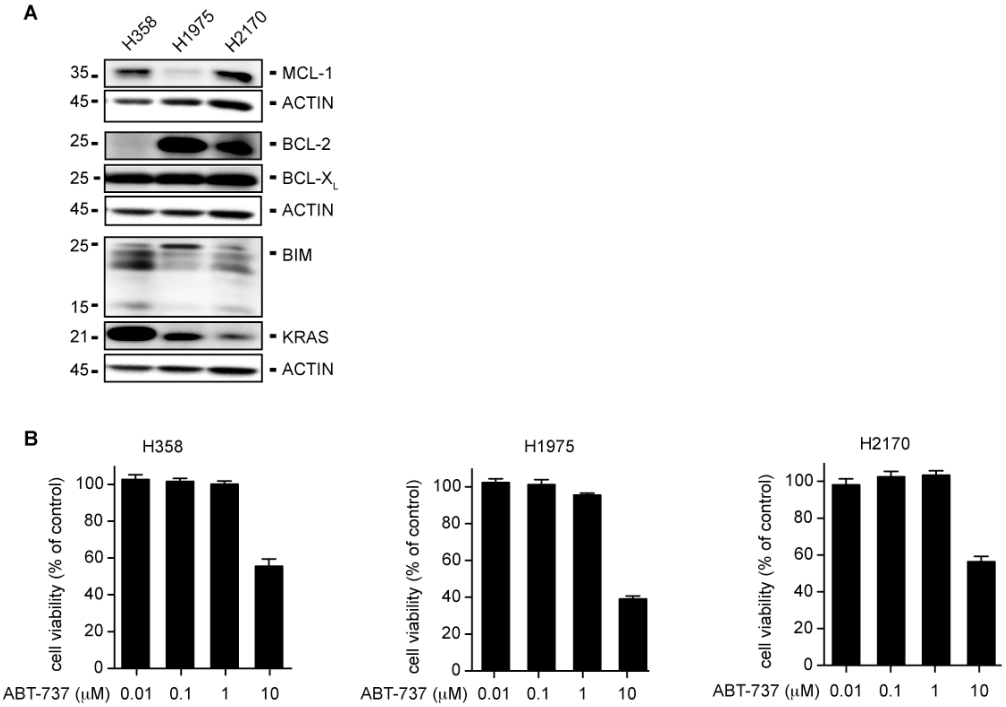

Figure 5. Human lung cancer cells are largely resistant to BCL-2, BCL-X_L and BCL-W inhibition. (A) Immunoblotting to detect BCL-2 family members (MCL-1, BCL-2, BCL-X_L and BIM) and KRAS in extracts from human NSCLC cell lines: a bronchioalveolar carcinoma cell line H358; an adenocarcinoma cell line H1975; a squamous cell line H2170. β-ACTIN served as a loading control. (B) Viability of the indicated cell lines was determined 48 hours after the addition of ABT-737 to the medium with final concentration 0.01 to 10 μM by CellTiter-Glo® luminescent cell viability assay. Results were normalized to vehicle treated controls. Each line was assayed in replicate in 3 independent experiments and data are presented as mean± SEM.

3.3 Survival of lung cancer cell lines is dependent on MCL-1 expression

In order to verify that MCL-1 expression was the key factor conferring resistance to ABT-737 in the NSCLC cell lines I sought to confirm the functional relevance of MCL-1 by specifically blocking its activity without affecting alternative BCL-2 family members. Due to the lack of specific and potent inhibitors of MCL-1, mutated BIM_S variants that harbor mutations in their BH3 domain defining the specificity of their binding to individual pro-survival BCL-2 family members were utilized. NSCLC cell lines were transduced with doxycycline-responsive lentiviral vectors encoding for BH3-only BIM_S variants generated previously (Chen et al., 2005; Kelly et al., 2014; Lee et al., 2008). The BIM_s variants were engineered to block either MCL-1 only (BIM_S2A) or, alternatively, only block BCL-2, BCL-X_L and BCL-W (BIM_SBAD) (similar to the BH3-only protein BAD), or not block any pro-survival BCL-2 protein at all (BIM_S4E), or block all pro-survival BCL-2 family proteins (BIM_SWT) (Figure 6A). After lentiviral transduction, the cells were sorted for GFP expression. Culturing the cells in the presence of doxycycline for 24 and 48 hours induced expression of the BIM_S variants. Cell viability was checked by flow cytometry and viable cells were defined as GFP-positive/PI-negative (Figure 6B). The expression of the BIM_S variants was verified by western blotting (Figure 6C). In the NSCLC cell lines expressing high levels of MCL-1 (H358 and H2170) BIM_S2A killed significantly better than BIM_SBAD. In these cell lines, the killing efficacy of BIM_S2A (blocking only MCL-1) was similar to that of BIM_SWT suggesting that MCL-1 was the most important anti-apoptotic protein. Expression of BIM_SBAD killed H358 and H2170 only marginally and comparable to the level of cell death observed in BIM_S4E, which is a functionally dead BIM mutant not binding to any pro-survival BCL-2 family protein. In contrast, H1975 cells, expressing low levels of MCL-1, responded to the induced expression of BIM_SBAD better than to the expression of BIM_S2A implying that MCL-1 inhibition only partially killed these cells and that the maximal killing efficacy was obtained when all pro-survival BCL-2 family members were blocked (Figure 6B and C).

The results were further confirmed by assaying for protein expression 24 hours after the induction of BIM_S variant expression (Figure 6C). Cleaved caspase 3, a marker for the induction of apoptosis, was detected upon expression of BIM_SWT but not BIM_S4E in all cell lines. Increased cleavage of caspase 3 upon BIM_S2A expression in H358 and H2170 compared to BIM_SBAD was consistent with the data from the survival assay that showed increased cell death upon BIM_S2A expression. In the MCL-1-low cell line, H1975, BIM_SBAD and BIM_S2A induced comparable cleavage of caspase 3.

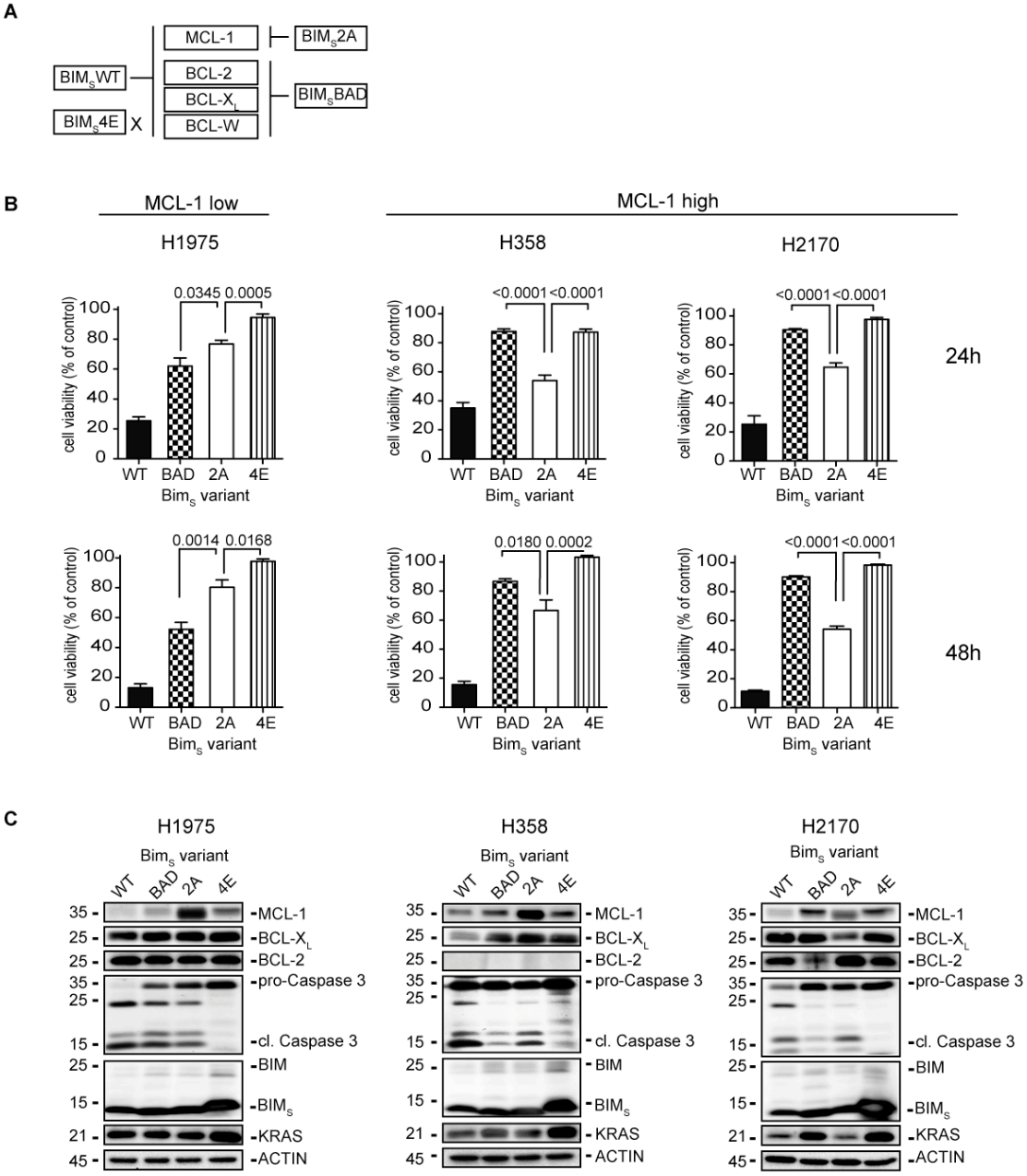

Figure 6. Survival of human lung cancer cells depends on MCL-1 expression. (A) Schematic diagram of the binding specificities of BIM_S variants to the BCL-2 pro-survival proteins. (B) Viability of the indicated cell lines stably infected with lentiviral constructs carrying vectors for doxycycline-inducible expression of BIM_S variants was determined 24 and 48 hours after the addition of doxycycline to the medium (1 μg/ml) by staining the cells with propidium iodide (PI) with FACS analysis for PI and GFP. The PI-negative/GFP-positive cells were recorded as viable cells. Percentage of viable doxycycline treated cells was expressed relative to percentage of viable untreated cells that was assigned as 100%. Each line was assayed in replicate in 3 independent experiments, and data are presented as mean±SEM. For statistical analysis unpaired two-tailed *t*-test was used. (C) Immunoblotting to detect the indicated BCL-2 family proteins, KRAS, cleaved caspase 3, and BIM_S variants 24 hours after the addition of doxycycline to the medium (1 μg/ml) in NSCLC cell lines expressing the lentiviral doxycycline-inducible BIM_S variants. β-ACTIN served as a loading control.

Importantly, BIM_S2A is known to stabilize MCL-1 while inhibiting its activity consistent with the elevated levels of MCL-1 observed by immunoblotting when BIM_S2A was

expressed (Lee et al., 2008). This is thought to occur by stabilizing MCL-1 by competing for binding to its E3-ligase MULE, which also binds to the BH3-domain of MCL-1. This might lead to a reduced ubiquitination of MCL-1 and therefore reduced degradation by the proteasome (Warr et al., 2005; Zhong et al., 2005). The BIM_S2A sensitive cell lines H2170 and H358 both express high level of BCL-X_L and BCL-2 (H2170), indicating that BCL-2 and BCL-X_L are not critical factors for the survival of these cell lines. This is consistent with the ABT-737 survival data.

Together, these data suggest that neutralization of MCL-1 activity is able to induce significant apoptotic cell death in NSCLC cell lines that express the protein irrespective of whether alternative pro-survival BCL-2 proteins are expressed, clearly identifying MCL-1 as the most important BCL-2 member in these cells.

3.4 Generation of a *Kras^{G12D}*-driven lung cancer mouse model and confirmation of adenoviral CRE functionality

An appropriate mouse model that closely recapitulates the clinical situation is an important tool to understand the mechanism of the disease and to provide new therapeutic strategies. In order to assess the functional role of MCL-1 in lung tumorigenesis under physiologically relevant conditions, I utilized a conditional knock-in mouse model based on inducible expression of oncogenic *Kras^{G12D}* specifically in the lung. The mouse model harboring a conditionally inducible *lox-STOP-lox-Kras^{G12D}* allele (*lsl-Kras$^{G12D/+}$* on the C57BL/6 background) was previously established (Jackson et al., 2001). In this model, endogenous expression of *Kras^{G12D}* is controlled by loxP sites flanked STOP cassettes. Upon expression of CRE recombinase *Kras^{G12D}* expression is induced. In order to evaluate the role of MCL-1 promoting the survival and development of *Kras^{G12D}* driven lung tumors, the *lsl-Kras$^{G12D/+}$* mice were intercrossed with *Mcl-1$^{fl/+}$* or *Mcl-1$^{fl/fl}$* mice (Opferman et al., 2003). This line harbors a loxP flanked exon 1 of *Mcl-1*, which results in the genetic deletion of *Mcl-1* upon CRE activity. To achieve simultaneous expression of mutated *Kras* and inactivation of *Mcl-1* via removal of the loxP site flanked elements, specifically in the lung, CRE expression was delivered through recombinant adenoviral particles (AdenoCRE) applied via intranasal infection (Figure 7A). Cohorts of *lsl-Kras$^{G12D/+}$ Mcl-1$^{fl/+}$* and *lsl-Kras$^{G12D/+}$ Mcl-1$^{fl/fl}$* mice and controls (*lsl-Kras$^{G12D/+}$ Mcl-1$^{+/+}$)* were infected with AdenoCRE and sacrificed at various time points for tumor analysis. As anticipated all mice developed multiple primary lung tumors following AdenoCRE infection (described below).

The *lsl-Kras^{G12D}* mouse model results in the formation of lung adenocarcinoma in mice (Jackson et al., 2001). We further verified the model using a

lung adenocarcinoma marker TTF-1 (Figure 7B) (Travis et al., 2013a). Following AdenoCRE infection using 5*10^6 PFU, *lsl-Kras*$^{G12D/+}$ mice were sacrificed at 6, 12 and 16 weeks post-infection and the lungs were stained for TTF-1. At these time points, *Kras*^{G12D} initiated lesions were positive for TTF-1 supporting the development of primary lung cancer lesions (Figure 7B).

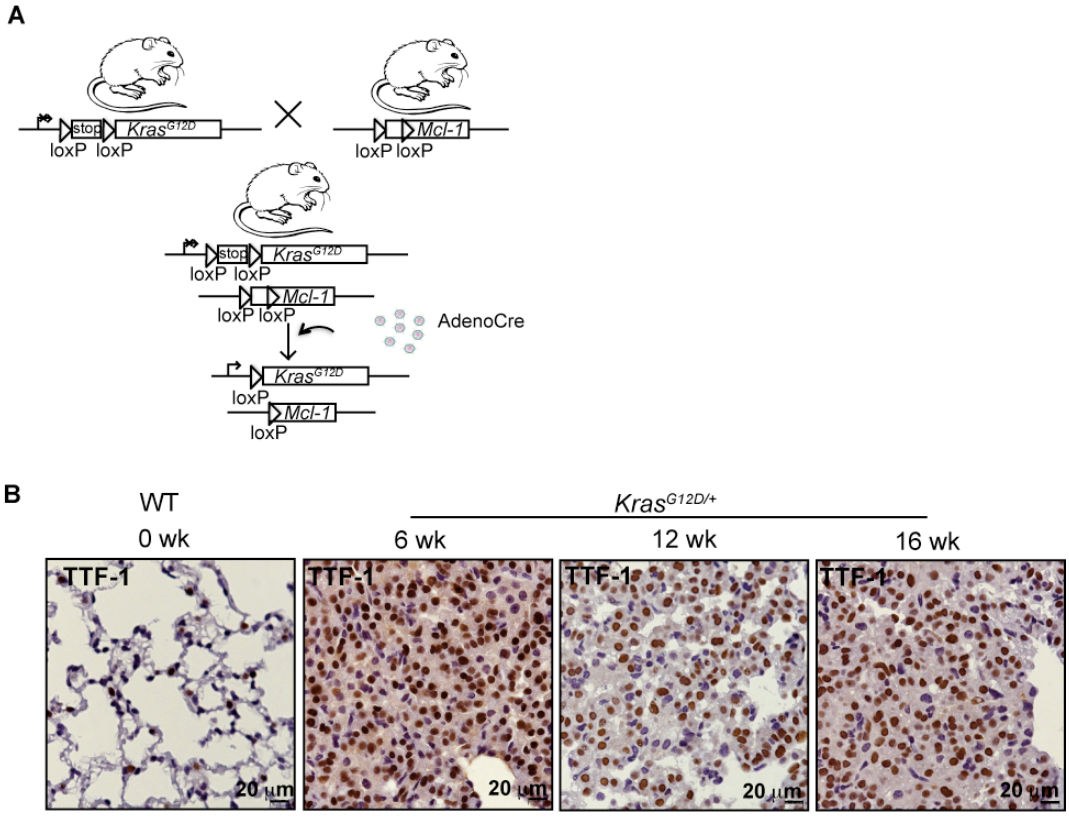

Figure 7. Generation of a KRAS-driven pulmonary adenocarcinoma mouse model (A) Schematic diagram of generation and infection of *lsl-Kras*$^{G12D/+}$ *Mcl-1*$^{fl/+}$ or *lsl-Kras*$^{G12D/+}$ *Mcl-1*$^{fl/fl}$ mouse model. (B) TTF-1 staining of WT and *Kras*$^{G12D/+}$ lungs at indicated time points after infection with 5*10^6 PFU of AdenoCRE.

As this model is dependent on the functionality of CRE recombinase, we tested the infection of the AdenoCRE virus. We utilized a reporter mouse model systems harboring *lox-STOP-lox LacZ* under control of the ROSA26 promoter. Transgenic *ROSA26 lsl-LacZ*$^{fl//fl}$ mice (Soriano, 1999) were infected with 5*10^8 PFU of AdenoCRE via intranasal instillation. Seventy-two hours after the infection, the expression of *LacZ* within the lung was investigated by performing a X-Gal staining on the lung sections. We found *LacZ* expression as a result of the removal of the STOP element subsequently resulting in the production of β-galactosidase. In the presence of β-galactosidase, X-gal, a chromogenic dye, is cleaved and produces an insoluble blue dye (Figure 8A). The staining showed expression of *LacZ* in individual

cells, which are indicated by an arrow within the figure (Figure 8B). This confirms that AdenoCRE was functional and infects individual cells upon intranasal delivery, which closely recapitulates the human situation where single cells undergo oncogenic transformation and give rise to lung cancers.

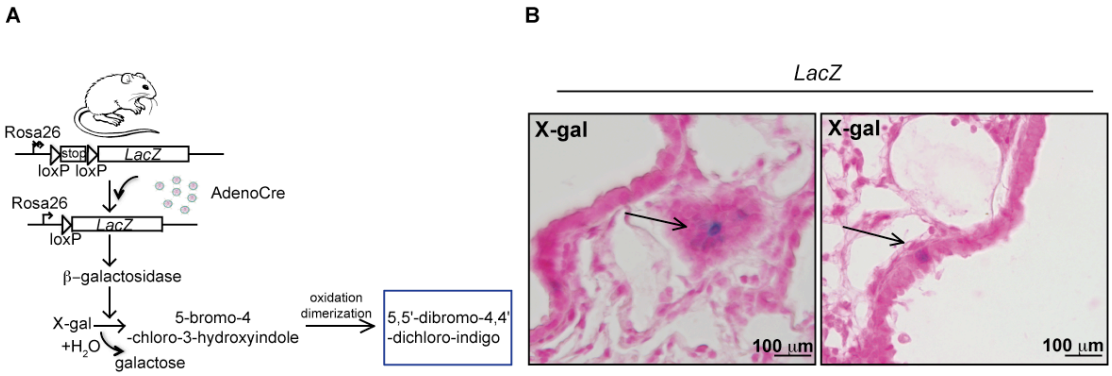

Figure 8. Verification of adenoviral CRE functionality. (A) Infection model of ROSA26 *lsl-LacZ*$^{fl/fl}$ mice with AdenoCRE. (B) X-gal staining of *LacZ* lungs 72 hours after infection with 5*10^8 PFU AdenoCRE. Two representative images of X-gal staining are shown. Arrows indicate individual cells expressing *LacZ.*

3.5 Deletion of *Mcl-1* and structural integrity of the lung

MCL-1 is critical for the normal development and maintenance of multiple hematopoietic and non-hematopeitic organs, and furthermore, deletion of *Mcl-1* affects multiple organs most likely due to increased apoptosis and mitochondrial damage (described in section 1.3.4). A therapeutic approach based on the pharmacologic inhibition of MCL-1 is therefore only feasible in case of low (or no) toxicity of MCL-1 inhibition within the physiologically healthy lung tissue. Therefore, I sought to identify the dependence of the normal lung tissue on MCL-1 for maintaining its normal structure. For this purpose, 6-8 weeks old *Mcl-1*$^{fl/+}$ mice were infected with 5*10^6 PFU of AdenoCRE and at 19 weeks post-infection, the mice were sacrificed and the lungs were harvested (Figure 9A). During this period of time the infected mice did not exhibit any sign of disease or difficulty of breathing. On examination, macroscopically the lungs appeared normal (data not shown) and microscopically, H&E staining of the *Mcl-1*$^{\Delta/+}$ lungs did not show any structural abnormalities (Figure 9C-F). Even at larger magnification, we were not able to detect any structural change, unexpected cellular infiltrates, abnormal architecture or thickening of membranes within the lungs of *Mcl-1*$^{fl/+}$ mice (Figure 9C-F). This data shows that heterozygous deletion of *Mcl-1* does not adversely affect the structural integrity and function of the lung and that pharmacologic inhibition of MCL-1 might be feasible *in vivo*.

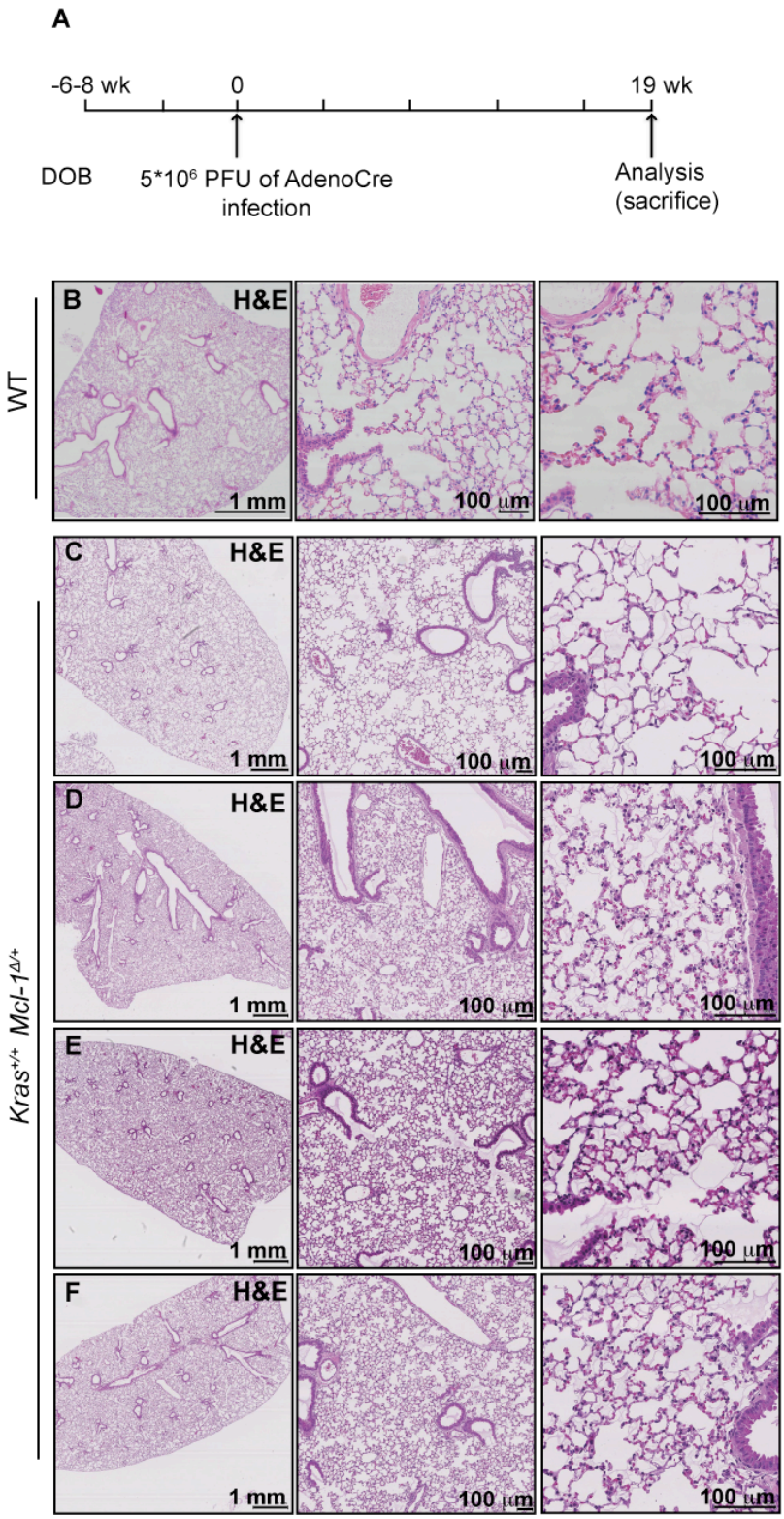

Figure 9. *Mcl-1* deletion does not impact on the structural integrity of the lung. (A) Timeline diagram of infection of the mouse model. DOB – date of birth. (B) H&E staining of a WT lung section without AdenoCRE infection with different magnifications (on the right) (C-E) H&E stainings of 4 independent *Mcl-1*$^{\Delta/+}$ lung sections with different magnifications (on the right) at 19 weeks post-infection with 5*10^6 PFU of AdenoCRE.

3.6 Characterization of *Mcl-1* deletion in mutant KRAS driven tumorigenesis

To determine the effect of genetic ablation of *Mcl-1 in* mutant *Kras*^{G12D} driven lung tumorigenesis, cohorts of *lsl-Kras*$^{G12D/+}$ *Mcl-1*$^{fl/+}$ and *lsl-Kras*$^{G12D/+}$ *Mcl-1*$^{+/+}$ mice were infected with 5*10^6 PFU of AdenoCRE by intranasal instillation and sacrificed at 19 weeks post-infection. On examination, lungs of both genotypes exhibited numerous lesions (arrows) on their surface (Figure 10A).

H&E staining of the lung sections showed multiple lesions mainly ranging from adenoma to adenocarcinoma showing cytologic features of malignancy such as nuclear hyperchromatism, nuclear pleomorphism (double arrows), prominent nucleoli (asterisk) and nuclear molding (single arrows), and hyperplasia and atypical hyperplasia (Figure 10B). The origin of the lesions was investigated by performing immunohistochemistry with specific markers for pneumocyte type II and Clara cells. In both genotypes, adenomas and adenocarcinomas were found be positive for the surfactant protein – C (SP-C), which is a pneumocyte type II marker, but negative for Clara cell antigen (CC10). Moreover, some lesions at the border of bronchiole/alveoli contained both CC10 positive cells and SP-C positive cells. The staining with SP-C and CC10 indicates that, consistent with previous reports (Jackson et al., 2001), the lesions originated from pneumocyte type II and Clara cell or their precursors defining them as primary adenocarcinoma of the lungs (Figure 10C).

To verify the histological type of the lesions from *lsl-Kras*$^{G12D/+}$ *Mcl-1*$^{+/+}$ and *lsl-Kras*$^{G12D/+}$ *Mcl-1*$^{fl/+}$ mice, the lesions were further examined with mucin staining using AB-PAS, a marker for lung adenocarcinoma (Travis et al., 2013a). At 19 weeks post-infection, AB-PAS staining showed mucin production within the tumors (Figure 10D) from both *Kras*$^{G12D/+}$ *Mcl-1*$^{+/+}$ *and Kras*$^{G12D/+}$ *Mcl-1*$^{\Delta/+}$ lesions. These data confirm that *Kras*^{G12D} driven lesions in the lung are lung adenocarcinoma and that the genetic deletion of one allele of *Mcl-1* did not affect the histological type of the tumors.

3.7 *Mcl-1* deletion reduces tumor burden

In order to assess the role of MCL-1 in tumor development I investigated the effect of deletion of *Mcl-1* on tumor growth. Cohorts of *lsl-Kras*$^{G12D/+}$ *Mcl-1*$^{+/+}$, *lsl-Kras*$^{G12D/+}$ *Mcl-1*$^{fl/+}$, and *lsl-Kras*$^{G12D/+}$ *Mcl-1*$^{fl/fl}$ mice were sacrificed at 19 weeks after infection with 5*10^6 PFU of AdenoCRE and lungs were harvested and further investigated. Using 3 serial H&E stained lung sections, separated by 100 μm, per animal (to ensure full coverage of the entire lung), I analysed the tumor burden of the diseased lungs by the following parameters: lesion number per section and tumor area (μm^2) per lung area (μm^2) of all sections. Using these parameters, I took into account the

different distribution patterns of the malignant lesions (Figure 11A). Already by low-resolution microscopic magnification a reduction in the total amount of lung cancer lesions was visible in sections from *lsl-Kras*$^{G12D/+}$ *Mcl-1*$^{fl/+}$ and *lsl-Kras*$^{G12D/+}$ *Mcl-1*$^{fl/fl}$ mice (Figure 11A). Moreover, the size of lesions was reduced in *lsl-Kras*$^{G12D/+}$ *Mcl-1*$^{fl/+}$ and *lsl-Kras*$^{G12D/+}$ *Mcl-1*$^{fl/fl}$ mice compared to controls (Figure 11A). The grading of the tumor lesions was assessed by published histological parameters (Nikitin et al., 2004) and revealed that the distribution of different histological type of lesions ranging from atypical adenomatous hyperplasia to adenocarcinoma remained largely identical in fully or partially *Mcl-1*-deleted mice compared to control animals (collaboration with PD. Dr. Specht, Institut für Allgemeine Pathologie und Pathologische Anatomie, MRI, TUM) (for criteria, see section 2.13) (Figure 11A).

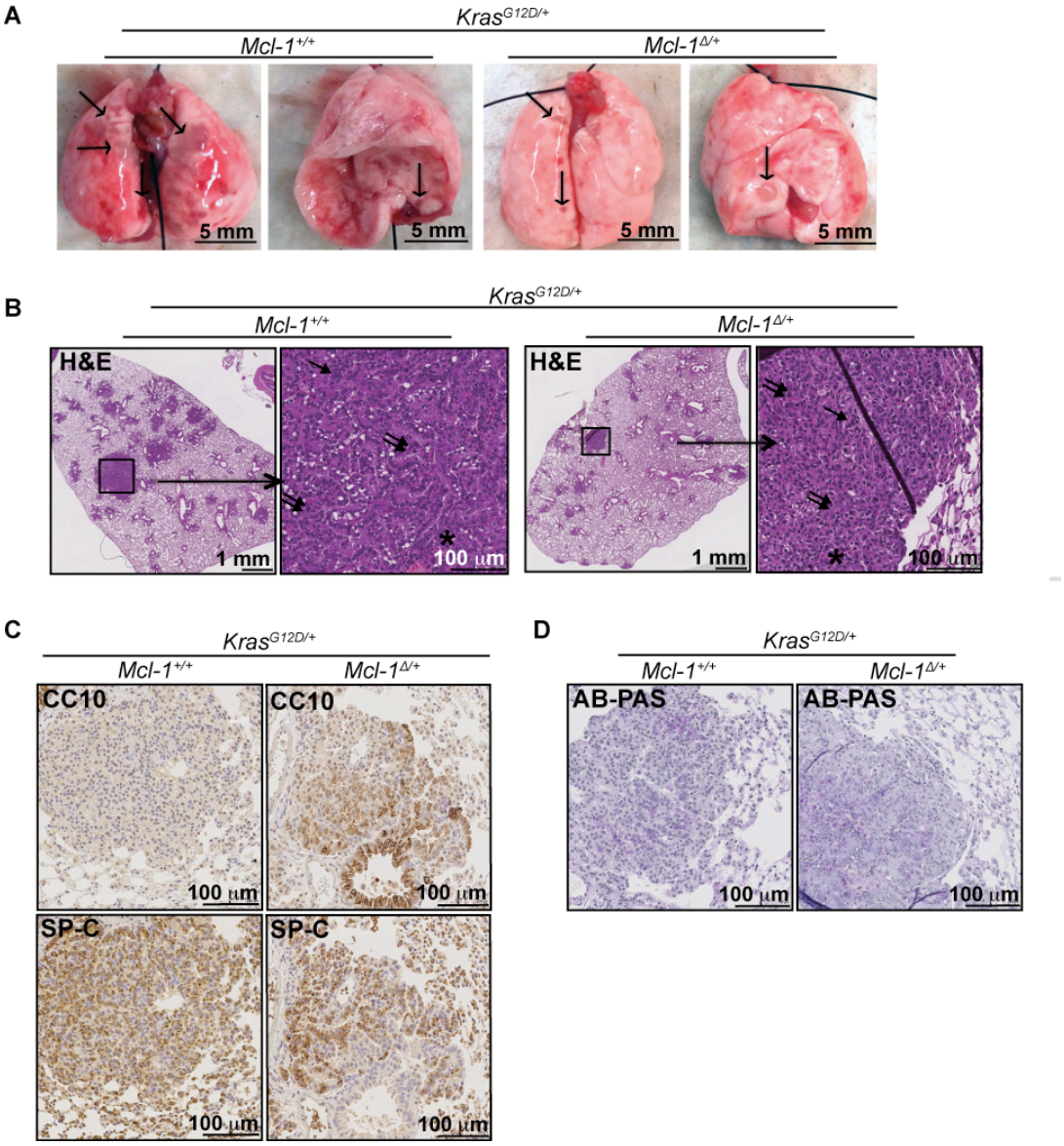

Figure 10. Characterization of *Mcl-1* deletion in tumorigenesis. (A) Representative lungs of the indicated genotypes 19 weeks after infection with 5*10^6 PFU of AdenoCRE. Tumors are indicated by arrows. (B) H&E staining of tumor bearing lung tissue. Higher magnifications

of lesions marked with squares are shown on the right. Tumors showed pleomorphic nuclei (double arrows), prominent nucleoli (the field of cells indicated by asterisk) and nuclear molding (single arrows). (C) CC10 and SP-C staining and (D) AB-PAS staining of the *Kras*$^{G12D/+}$ *Mcl-1*$^{+/+}$ and *Kras*$^{G12D/+}$ *Mcl-1*$^{\Delta/+}$ lesions 19 weeks after 5*10^6 PFU of AdenoCRE infection.

Using the Tissue IA image analysis software (Slidepath, Leica microsystems) to accurately calculate the lesion numbers and the tumor area per total lung area on each slide, I was able to quantify tumor development in mice that lack MCL-1 completely or partially and compare this to the lesion numbers observed in WT controls. By comparing the number of lesions on the sections of diseased lungs of *lsl-Kras*$^{G12D/+}$ *Mcl-1*$^{fl/+}$ mice to the number of lesions in the lungs of *lsl-Kras*$^{G12D/+}$ *Mcl-1*$^{+/+}$ control mice, I found a significant reduction in the number of lesions after deletion of only one allele of *Mcl-1* (Figure 11B). Furthermore, analysis of the ratio between the tumor area compared to the total lung area revealed that the deletion of a single allele of *Mcl-1* was sufficient to significantly reduce the overall tumor burden compared to the *lsl-Kras*^{G12D} *Mcl-1*$^{+/+}$ mice (Figure 11C).

Despite the reduction in the number of lesions in *lsl-Kras*$^{G12D/+}$ *Mcl-1*$^{fl/fl}$ mice compared to controls, the tumor burden measured as tumor area to lung area remained elevated in these mice when compared to controls (Figure 11C). This was caused by the appearance of individual lesions that grew to substantial sizes primarily in *lsl-Kras*$^{G12D/+}$ *Mcl-1*$^{fl/fl}$ mice but not in controls. The elevation in tumor burden was therefore caused by the relatively large size of individual lesions observed only in *lsl-Kras*$^{G12D/+}$ *Mcl-1*$^{fl/fl}$ mice but not by an overall increase in lesion numbers (detailed description below, see also Figure 12).

To verify the genetic deletion of *Mcl-1* and to correlate the differences observed between the three genotypes to the levels of MCL-1, a RNA *in situ* hybridization-based RNAscope assay was performed. This method was chosen due to the lack of a functional antibody for detecting mouse MCL-1 by IHC (Figure 11D). By RNA *in situ* hybridization, I showed that the mRNA expression of *Mcl-1* was reduced in *Kras*$^{G12D/+}$ *Mcl-1*$^{\Delta/+}$ and *Kras*$^{G12D/+}$ *Mcl-1*$^{\Delta/\Delta}$ lesions in comparison to controls. *Kras*$^{G12D/+}$ *Mcl-1*$^{\Delta/\Delta}$ lesions contained some cells expressing *Mcl-1* mRNA, which were structurally not similar to the tumor cells and were found specifically in septae between papillary structures. Therefore these cells were excluded from the analysis as they could be attributed to non-neoplastic cells likely representing from infiltrating cells and endothelial cells of the vasculature (Figure 11E). Importantly, *Mcl-1* expression was elevated within the lesions (Figure 11D). This is consistent with the notion that MCL-1 is overexpressed in lung cancer samples from patients (described also in section 1.3.5).

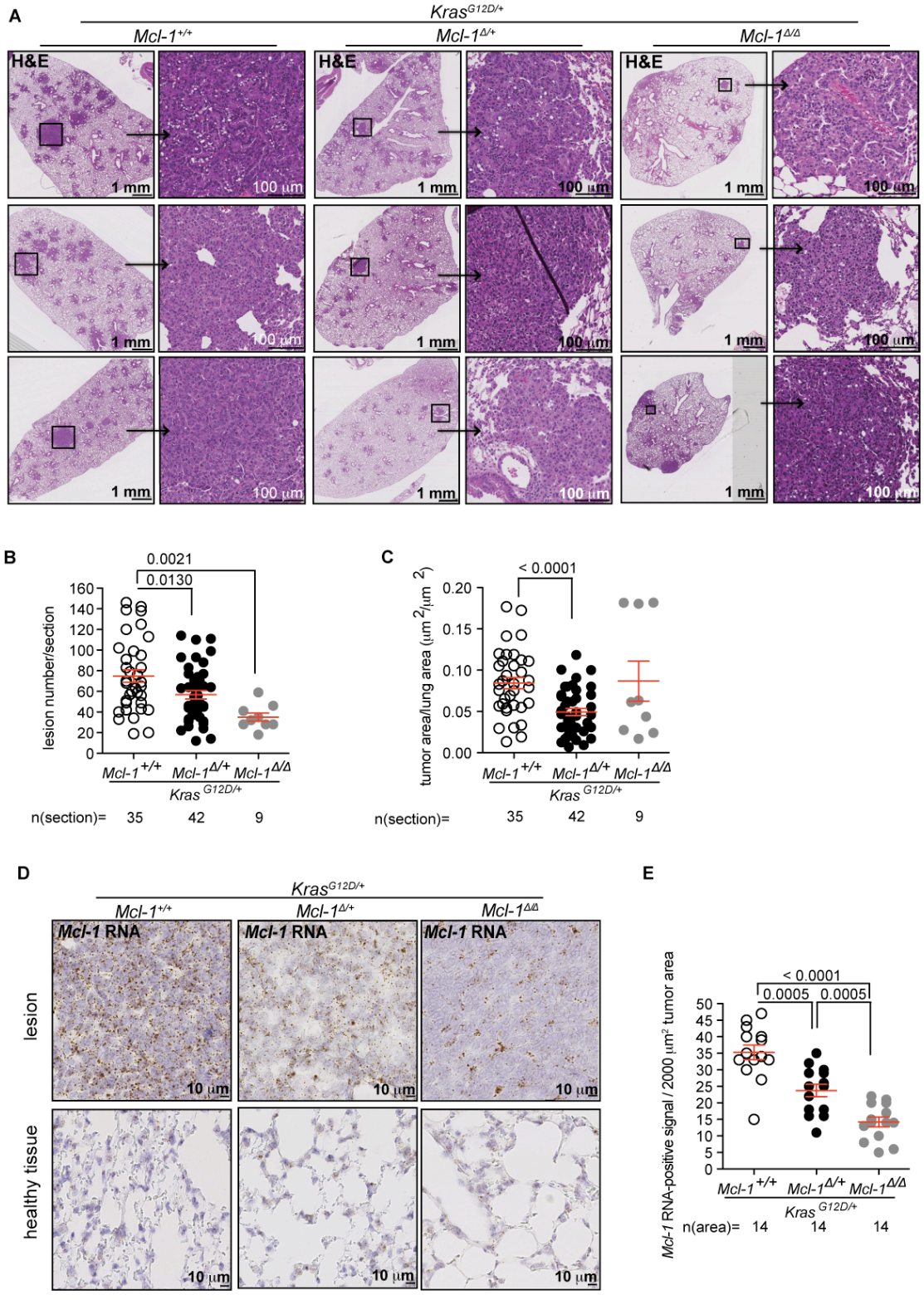

Figure 11. *Mcl-1* deletion reduces tumor burden. (A) H&E staining of three lung tissue sections from 3 mice for each genotype at 19 weeks post-infection with $5*10^6$ PFU of AdenoCRE. Higher magnifications of the marked lesions are shown on the right (B) Number of the lesions per section (C) Tumor area to lung area ratio on the sections. Three H&E stained sections of the lungs, each separated by 100 µm, were analyzed per animal. N number equals number of sections. (D) *Mcl-1* RNA *in situ* hybridization in the representative lesions and adjacent healthy tissue in the lungs of all three genotypes. (E) Quantification of

positive signal for *Mcl-1* RNA per 2000 μm^2 tumor area. N number equals number of lesion area. Determination of the lesions and lung area were performed with Tissue IA image analysis software (Slidepath, Leica microsystems). Data are presented as mean±SEM. For statistical analysis, unpaired two-tailed *t*-test and Mann Whitney test (lesion number/section *Kras*$^{G12D/+}$ *Mcl-1*$^{+/+}$ vs *Kras*$^{G12D/+}$ *Mcl-1*$^{\Delta/\Delta}$) were used.

Taken together, these data demonstrate that loss of a single allele of *Mcl-1* is sufficient to significantly diminish tumor burden by decreasing both the number of lesions and overall tumor burden. Intriguingly complete deletion of *Mcl-1* also reduces lesion numbers, but conversely resulted in the appearance of individual large tumor nodules.

3.8 Deletion of *Mcl-1* triggers formation of large anaplastic tumors

The appearance of individual very large tumor lesions specifically in the lungs of *lsl-Kras*$^{G12D/+}$ *Mcl-1*$^{fl/fl}$ mice prompted me to perform a detailed analysis of the size of the tumor lesions. I analyzed the sizes of the largest lesions found from mice of all three genotypes at 19 weeks post-infection with $5*10^6$ PFU of AdenoCRE. Exceptionally large tumors (over 8 mm^2 ($8*10^6$ μm^2)) were observed only in the *lsl-Kras*$^{G12D/+}$ *Mcl-1*$^{fl/fl}$ mice (Figure 12A). The size of the largest tumors harboring WT alleles, a heterozyously deleted allele or null allele of *Mcl-1* were 3 mm^2, 3.58 mm^2 and 8.23 mm^2, respectively (Figure 12B). The presence of the large tumors was further confirmed by ultra high-resolution micro-CT of the entire lungs of all three genotypes with the aid of 1% iodine metal in absolute ethanol (I2E) as contrast agent (Metscher, 2009) in a collaboration by Pidassa Bidola (IMETUM / Chair of Biomedical Physics, TUM) (Figure 12C).

Furthermore, the bulky lesions from all three genotypes exhibited advanced features such as enlarged, pleomorphic nuclei, prominent nucleoli, nuclear molding and hyperchromatism (Figure 12A). In addition, histological analysis of *Kras*$^{G12D/+}$ *Mcl-1*$^{\Delta/\Delta}$ and *Kras*$^{G12D/+}$ *Mcl-1*$^{\Delta/+}$ large lesions presented with a higher grade phenotype than controls, which was exemplified by multinucleate giant tumor cells (marked with arrows) and a stromal desmoplasia *(*marked with asterisk) (*Kras*$^{G12D/+}$ *Mcl-1*$^{\Delta/+}$*)*, the latter is used as a criterion to classify advanced lesion (Jackson et al., 2005). Moreover, tumor necrosis was identified in *Mcl-1*-deleted lesion (marked with double arrow), which is indicative of the diagnosis of adenocarcinoma (Figure 12A). Next to the histological parameter described before (section 3.6), the size of the tumor lesions also represents one of the criteria for adenocarcinoma (Nikitin et al., 2004).

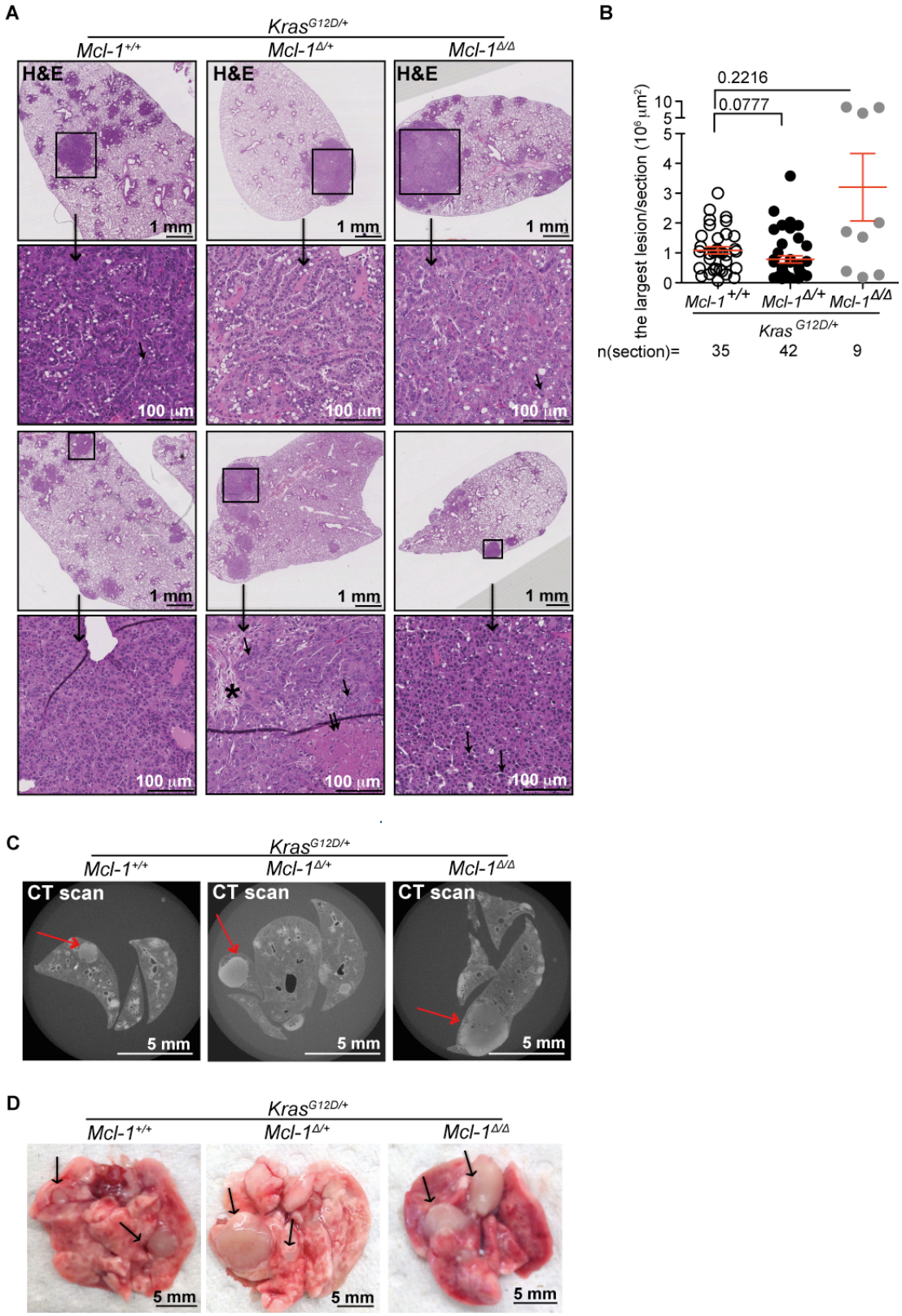

Figure 12. *Mcl-1* deletion triggers formation of large tumors. (A) Representative H&E staining of diseased lungs of the indicated genotypes at 19 weeks post-infection. Asterisk indicates desmoplastic stroma. Single arrows mark multinucleate giant tumor cells. Double arrow indicates necrosis. (B) Size of the largest lesion per section. N number equals number of section. Three sections per animal, each separated by 100 μm, were assessed. Data are represented as mean±SEM. For statistical analysis, unpaired two-tailed *t*-test and Mann

Whitney test (*Kras*$^{G12D/+}$ *Mcl-1*$^{+/+}$ vs *Kras*$^{G12D/+}$ *Mcl-1*$^{\Delta/\Delta}$) were used. The lesion sizes were determined by Tissue IA image analysis software (Slidepath, Leica microsystems). (D) Cross-sections of the reconstructed image of the contrast agent stained lungs at 19 weeks post-infection measured by absorption-based X-ray microCT (VersaXRM-500). Arrows indicate the largest tumor observed in the lungs. (E) Macroscopic view of the lungs at 30 weeks post-infection. The arrows indicate the large tumors on the surface of the lungs.

Further analysis of *Mcl-1* deleted lesions at a later time point (30 weeks post-infection) demonstrated that the extensive size of individual tumors was still present as compared to *Kras*$^{G12D/+}$ *Mcl-1*$^{+/+}$ control lesions (Figure 12D) indicating that the size difference of the lesions persisted overtime.

Taken together these data show that despite an overall reduction in the number of lesions in *lsl-Kras*$^{G12D/+}$ *Mcl-1*$^{fl/fl}$ and *lsl-Kras*$^{G12D/+}$ *Mcl-1*$^{fl/+}$ mice, complete deletion of *Mcl-1* can mediate the formation of individual very large and de-differentiated tumor lesions. This finding is suggestive of the acquisition of additional mutations in these lesions that drive tumor growth and block differentiation.

3.9 *Mcl-1* deletion results in an elevated activation of STAT3

In order to understand the molecular mechanisms causing the reduced tumor burden in mice deficient for one or two alleles of *Mcl-1*, I assessed tumor lesions for apoptosis and proliferation. MCL-1 is a potent anti-apoptotic protein likely affecting the apoptotic threshold in lung cancer cells. I therefore asked whether *Mcl-1* deletion mediated an increase in apoptosis by staining for cleaved and activated caspase 3 present within tumor sections (Figure 13A). However, no significant increase in the number of apoptotic cell was observed after deletion of one or both alleles of *Mcl-1* as compared to *Kras*$^{G12D/+}$ *Mcl-1*$^{+/+}$ lesions (Figure 13B). The failure to observe any difference in apoptotic cells in lung cancer lesions can be explained either by a non-apoptotic function of MCL-1 in this context. However, we favor the conclusion that the different levels of apoptosis are unlikely detectable in lung cancer lesions at 19 weeks after the initiation by CRE recombinase. Apoptotic cells are rapidly engulfed by immune cells such as macrophages effectively masking the effect of MCL-1 deletion several weeks after the tumor formation.

Next, the proliferation rate of cells within the tumors was examined by IHC using the proliferation marker, Ki67 (Figure 13C). The expression of Ki67 is strictly associated with cell proliferation and is present during all active phases of the cell cycle but is absent in resting cells (Scholzen and Gerdes, 2000). Quantification of Ki67 positive cells revealed that heterozygous deletion of *Mcl-1* slightly reduced proliferating cells numbers whereas proliferation was similar upon homozygous deletion of *Mcl-1* to control (Figure 13D).

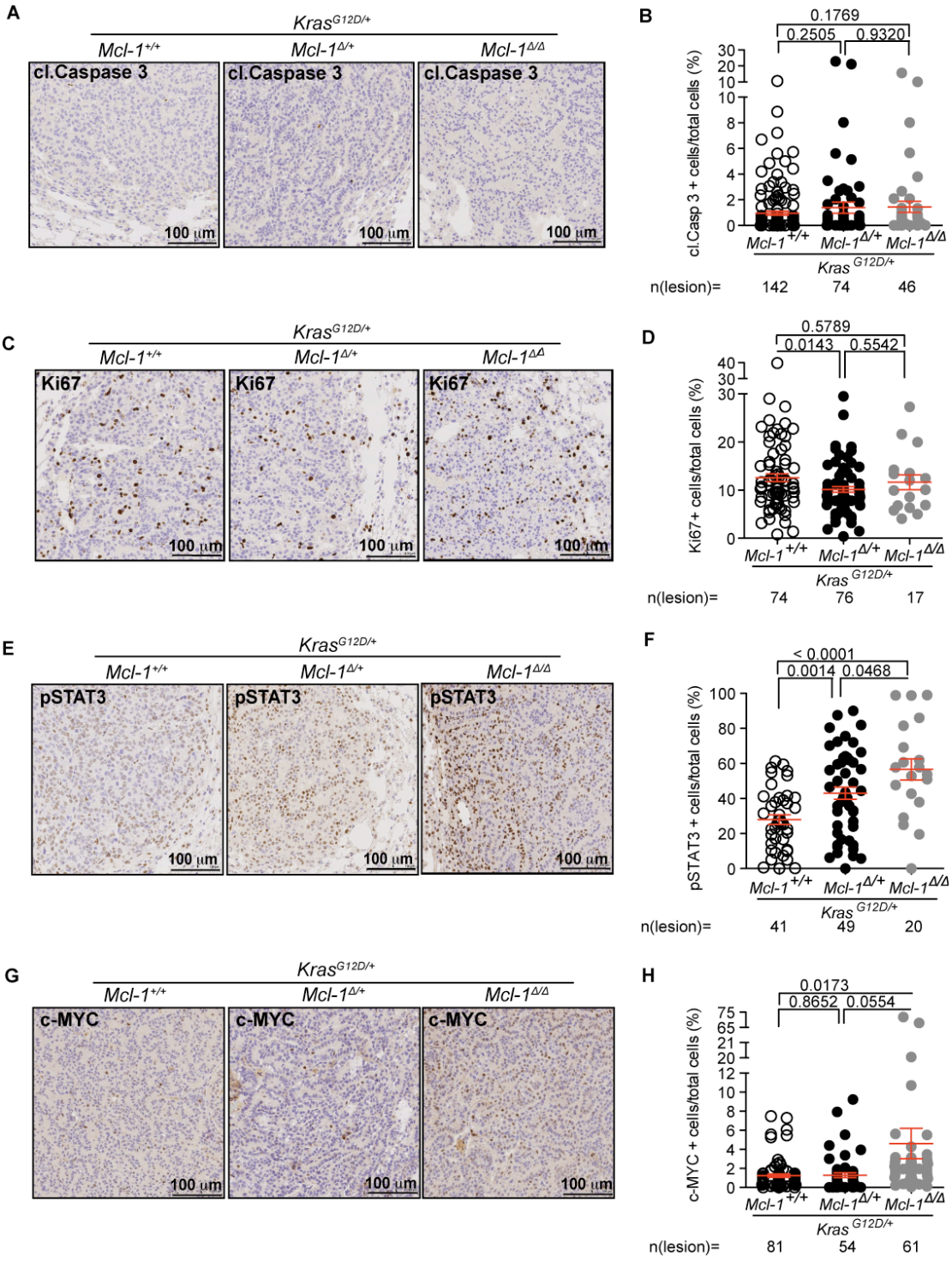

Figure 13. *Mcl-1* deletion results in an elevated activation of STAT3. (A, B) cleaved caspase 3 staining, (C, D) Ki67 staining, (E, F) pSTAT3 staining, and (G, H) c-MYC staining of *Kras*$^{G12D/+}$ *Mcl-1*$^{+/+}$, *Kras*$^{G12D/+}$ *Mcl-1*$^{\Delta/+}$, and *Kras*$^{G12D/+}$ *Mcl-1*$^{\Delta/\Delta}$ lesions and quantification of the staining. All quantifications were represented as percentage of positive cells relative to all cells in the assessed lesions at 19 weeks post-infection. For cleaved caspase 3 staining all lesions, and for Ki67, pSTAT3 and c-MYC staining approximately 8 lesions per sections were analyzed. Data are presented as mean±SEM. Statistical analysis was performed using unpaired two-tailed *t*-test and Mann Whitney test (*Kras*$^{G12D/+}$ *Mcl-1*$^{+/+}$ vs *Kras*$^{G12D/+}$ *Mcl-1*$^{\Delta/\Delta}$).

Phosphorylated STAT3 induces expression of genes that promote various cellular processes such as survival, proliferation, migration and transformation (Yu et al., 2014). Interestingly, *Mcl-1* deletion triggered activation of STAT3, a known stimulator of *Mcl-1* transcription (described in section 1.3.3) (Figure 13E). Activation of STAT3 was elevated in *Mcl-1* deleted lesions of mice harboring only one allele of *Mcl-1* and even more in mice where *Mcl-1* was deleted completely (Figure 13F). To assess the effect of activated STAT3 on one of its most potent target genes to promote tumor progression, IHC was performed for c-MYC expression in these lesions (Figure 13G). c-MYC is a target of pSTAT3 (Kiuchi et al., 1999) and is involved in a wide range of cellular process including cellular growth, proliferation, angiogenesis and de-differentiation (Pelengaris et al., 2002; Tansey, 2014). In line with an elevated pSTAT3 expression, c-MYC expression was also elevated in $Kras^{G12D/+}$ $Mcl\text{-}1^{\Delta/\Delta}$ lesions (Figure 13H).

Additionally, I checked for infiltration of immune cells to the tumor site in order to account for anti-tumor effects mediated by immune cells. T-lymphocytes measured by expression of CD3 and macrophages measured by expression of F4/80 were observed within and around the lesions of all three genotypes, but no significant differences in the infiltration of these cells were detected (Figure 14B and F). Slightly more B-lymphocytes measured by expression of B220 were recruited to $Kras^{G12D/+}$ $Mcl\text{-}1^{\Delta/\Delta}$ lesions (Figure 14D), whereas no myeloid cells were detected (MPO) in any of the lesions from the three genotypes (Figure 14E).

Taken together, these data showed that loss of *Mcl-1* during tumor initiation results in an elevation in activated JAK-STAT signaling and an elevation of c-MYC expression. Both observations likely drive the progression of the lesions despite no relevant changes in apoptosis, proliferation or immune cell invasion in the tumors after deletion of *Mcl-1*.

3.10 Treatment response to chemotherapy in lung cancer harboring deletions of *Mcl-1*

NSCLC often exhibit a striking insensitivity to chemotherapy, especially when compared to SCLC. However, most patients are diagnosed at advanced stages of the disease. Therapeutic options in advanced stage patients are substantially limited as surgery is usually not beneficial anymore. Systemic chemotherapy, targeted drugs or individualized irradiation regimens represent options for this patient population (National Cancer Institute: PDQ® Non-Small Cell Lung Cancer Treatment. Bethesda, MD: National Cancer Institute, (Heist and Engelman, 2012)).

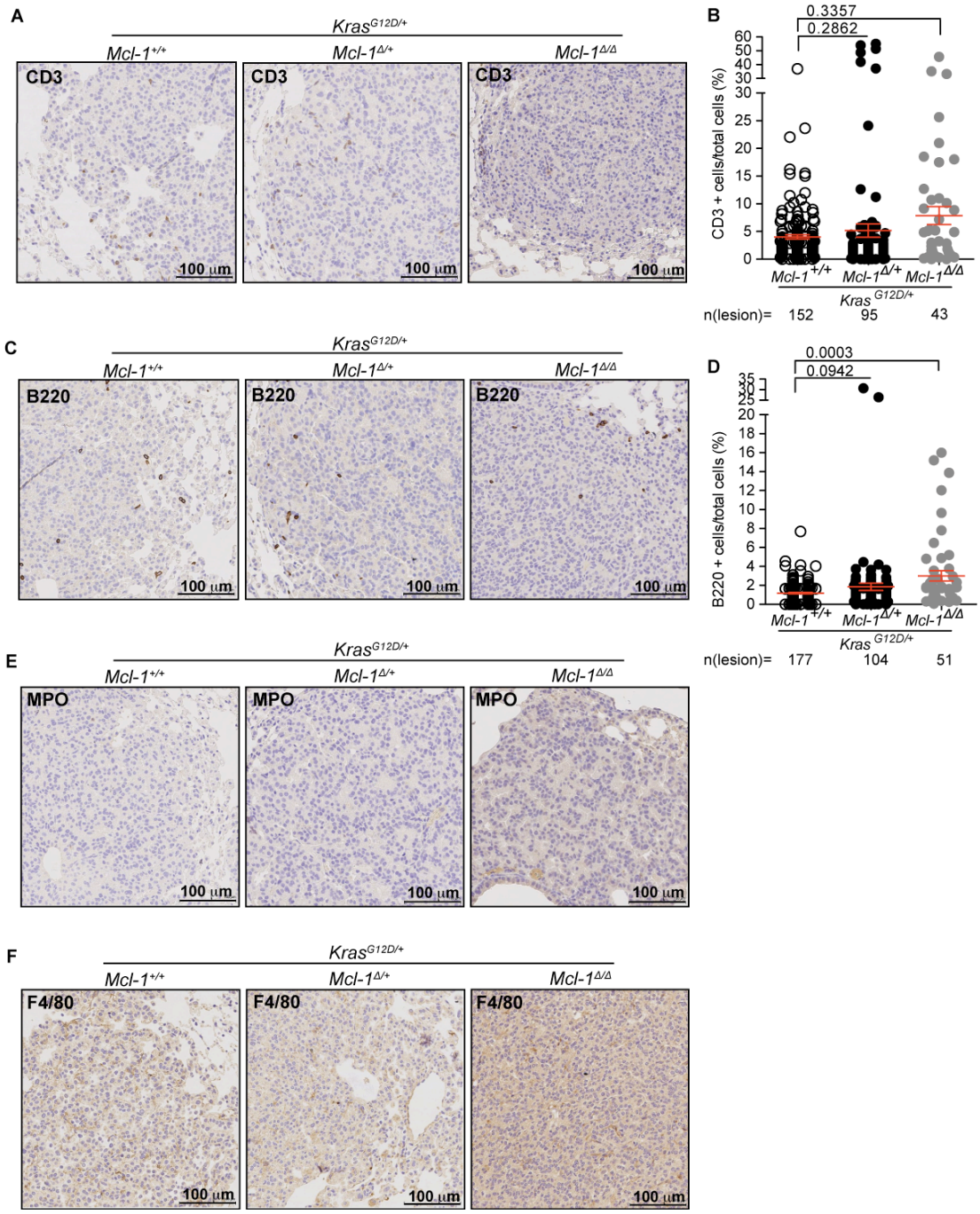

Figure 14. Characterization of immune cells infiltration into the tumor site. (A) CD3 staining of lung tumors and (B) quantification of CD3 positive cells at the site of the lesions. (C) B220 staining of the lesions in the lung. (D) Quantification of B220 positive cells. (E, F) MPO and F4/80 staining of the lesions in the lungs. All quantifications were represented as percentage of positive cells relative to all cells in the assessed lesions at 19 weeks post-infection. For CD3 and B220 staining all lesions per sections were analyzed. Data are presented as mean±SEM. Statistical analysis was performed using unpaired two-tailed *t*-test and Mann Whitney test (*Kras*$^{G12D/+}$ *Mcl-1*$^{+/+}$ vs *Kras*$^{G12D/+}$ *Mcl-1*$^{\Delta/\Delta}$).

Furthermore, MCL-1 is often overexpressed in NSCLC and overexpression of MCL-1 has been shown to mediate resistance to chemotherapy in a variety cancers (described in section 1.3.5). Therefore, I aimed to examine whether the reduction of

MCL-1 expression would improve tumor responses to targeted drugs or chemotherapy. For this aim, I chose to use only heterozygous deletion of *Mcl-1.* This strategy aims to mimic pharmaceutical inhibition of MCL-1 and sidesteps the observed aggravation of disease after complete inhibition of MCL-1. I investigated the impact of *Mcl-1* deletion on the response to the chemotherapeutic drug cisplatin and the BH3-mimetic drug ABT-263.

3.10.1 Pharmacologic inhibition of BCL-2, BCL-X_L and BCL-W does not confer additional treatment response

The previous data have shown (Figure 11B) that the genetic deletion of *Mcl-1* reduced the number of lesions in mice. We therefore wanted to characterize the relevance of the alternative pro-survival BCL-2 family members such as BCL-2, BCL-X_L and BCL-W for the sustained survival of lung cancer lesions. Published data have shown that genetic amplifications of the genomic locus harboring *BCL-X_L* is frequently amplified in many human cancer specimen, however the functional relevance in our mouse model was unclear (Beroukhim et al., 2010). Pharmacologic inhibition of pro-survival BCL-2 family members other than MCL-1 and A1 is readily available by the virtue of BH3-mimetic compounds, which effectively mimic the BH3 domain of pro-apoptotic BH3-only proteins thereby inhibiting the function of the pro-survival BCL-2 family members (Oltersdorf et al., 2005). The BH3-mimetic compound ABT-737 inhibits BCL-2, BCL-X_L and BCL-W but only its derivate ABT-263, effectively binding the same proteins, is orally bioavailable and can therefore be fed to mice (Tse et al., 2008). Moreover, it was observed that MCL-1 confers resistance to ABT-737 in our NSCLC cell line models (Figure 5B) suggesting that genetic ablation of MCL-1 *in vivo* using the loxP-CRE system might overcome the resistance and sensitize the lung cancer lesions to ABT-263. *lsl-Kras$^{G12D/+}$Mcl-1$^{+/+}$* or *lsl-Kras$^{G12D/+}$ Mcl-1$^{fl/+}$* lung tumor-bearing mice were treated *p.o.* with ABT-263 (100 mg/kg daily) for 2 weeks starting at 29 weeks post-infection. The treatment period was followed by an observational period of 2 weeks. The mice were subjected to computed tomography imaging (X-ray based micro-CT (FMT-XCT)) at baseline, after 2 weeks of treatment and after the observational period of additional 2 weeks to monitor for treatment response (Figure 15A).

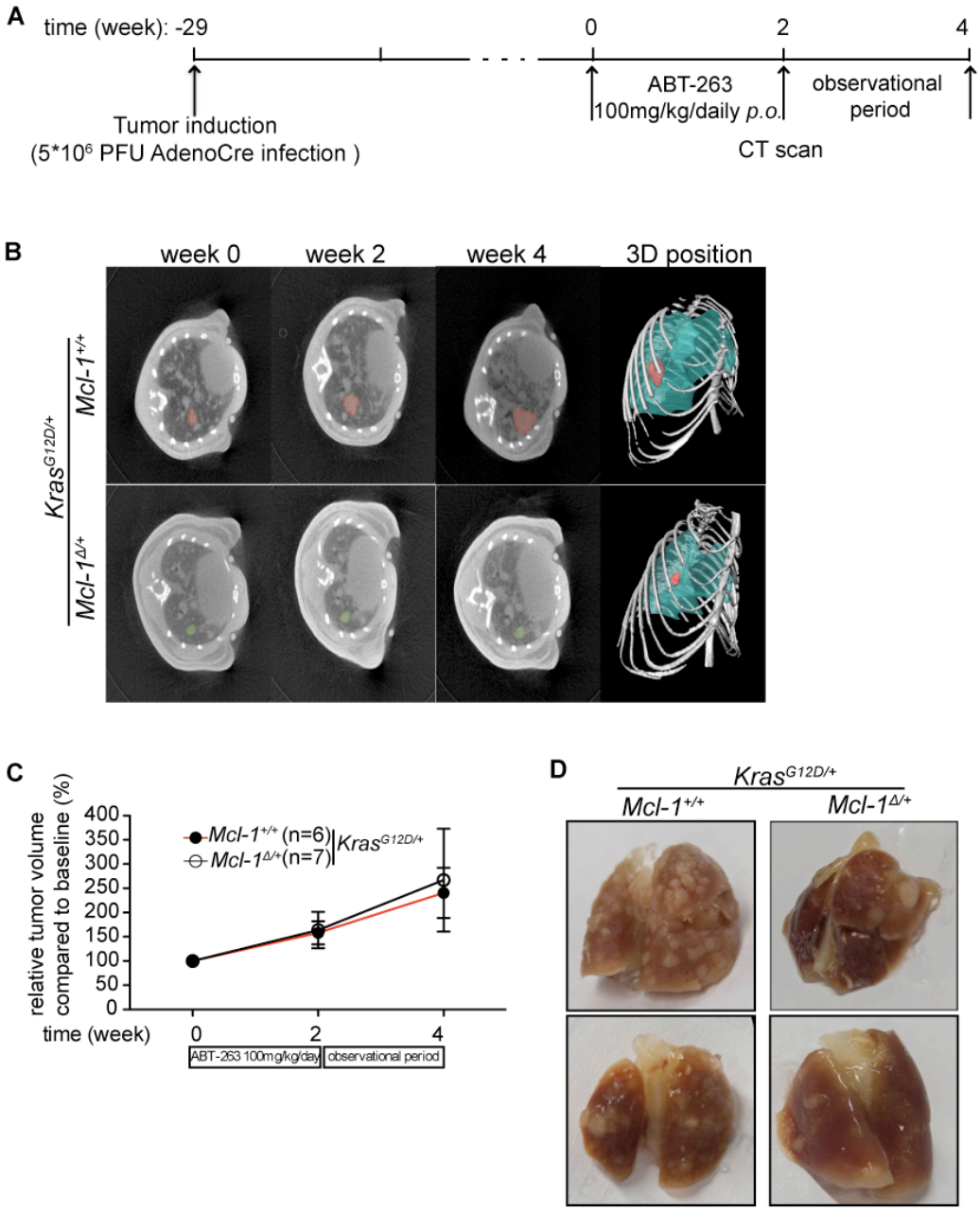

Figure 15. Acute inhibition of BCL-2, BCL-X_L and BCL-W in established lung tumors. (A) Experimental set-up for ABT-263 treatment of *lsl-Kras*$^{G12D/+}$ *Mcl-1*$^{+/+}$ and *lsl-Kras*$^{G12D/+}$ *Mcl-1*$^{fl/+}$ mice. (B) Representative micro-CT lung reconstructions with individual lung tumors pseudocolored at the beginning (week 0) and the end of treatment (week 2), and the end of observational period (week 4). (C) The dynamics of tumor volume at indicated time points. Data are presented as percentage of the measured tumor volume compared to the tumor volume at baseline (week 0) as mean±SEM. N number equals individual tumors from 4 mice per genotype. (D) Macroscopic view of representative lungs after the experiment.

To follow the disease progression over time, individual tumors, whose boundaries were clearly identified at baseline, were focused. The calculated tumor volume of

these lesions was followed throughout the experiment (Figure 15B). The tumor response to inhibition of BCL-2, BCL-X_L and BCL-W by ABT-263 was measured by comparing the tumor volumes of the 2nd (after treatment) and 3rd (after observational period) CT scan relative to the initial tumor volume (at baseline). The analysis of the CT scans revealed that ABT-263 did not confer a differential effect on the tumor size in either genotype (Figure 15C). This parameter, however, only describes the change of the tumor size of the summary of lesions detected per animal. It does not define the total size and number of lesions present since imaging by CT scanning does not possess a sufficiently high resolution to also acquire accurate data on the overall tumor burden. *Kras*$^{G12D/+}$ *Mcl-1*$^{\Delta/+}$ individual lesions did not progress in size as much as observed in the control group (Figure 15B), however statistical analysis of several lesions did not show an overall difference (Figure 15C). After the end of the experiment, the lungs were harvested and further analyzed. Consistent with our data described above, the lungs from mice harboring a deleted allele of *Mcl-1* showed fewer lesions while control lungs exhibited multiple lesions on their surface (Figure 15D). This result shows that despite an overall reduction in the number of lesions in *lsl-Kras*$^{G12D/+}$ *Mcl-1*$^{fl/+}$ mice, the additional inhibition of BCL-2, BCL-X_L and BCL-W in fully established adenocarcinoma of the lung does not impact on tumor cell survival. This suggests that the remaining levels of MCL-1 might suffice for continued tumor cell survival.

3.10.2 Characterization of *Mcl-1* deletion on the effect of cisplatin treatment

Cisplatin is a commonly used chemotherapeutic in lung cancer treatment. All major treatment regimens for adenocarcinoma, squamous cell carcinoma, and even small cell carcinoma of the lung are based on cisplatin in first-line treatment. I therefore explored whether a reduction in *Mcl-1* expression level would improve cisplatin efficiency *in vivo*. To this end, lung tumor-bearing mice with or without heterozygous deletions of *Mcl-1* were treated *i.p.* with a single dose of cisplatin (7mg/kg) 24 weeks after tumor induction by AdenoCRE infection (Figure 16A). The treatment response was monitored with ^{18}F-FDG PET/CT at baseline and on day 2 and 4 after treatment (Figure 16A). ^{18}F-FDG uptake is a method that provides functional information based on the increased glucose uptake and glycolysis of cancer cells and depicts the metabolism of malignant tissue (Almuhaideb et al., 2011). To define treatment response, ^{18}F-FDG uptake after the treatment was monitored and calculated relative to the values before treatment. This imaging modality was chosen to obtain rapid information based on metabolism to judge treatment response. In *Kras*$^{G12D/+}$ *Mcl-1*$^{+/+}$

lesions, the tumoral ^{18}F-FDG uptake was elevated on day 2 compared to baseline values and decreased on day 4 after cisplatin treatment. In contrast, in tumors with heterozygous deletion of *Mcl-1* ^{18}F-FDG uptake lacked the elevation observed in controls and remained relatively constant over time (Figure 16C). In order to check for the level of apoptosis induced by cisplatin, cleaved caspase 3 positive cells as parameter of apoptotic cells at a given time point, were enumerated with IHC on day 2 and 4 after treatment. Although the number of apoptotic cells was similar in *Kras*$^{G12D/+}$ *Mcl-1*$^{+/+}$ and *Kras*$^{G12D/+}$ *Mcl-1*$^{\Delta/+}$ tumors on day 2 (Figure 16D), a significant reduction in cleaved caspase 3 positive cells was observed on day 4 only in *Kras*$^{G12D/+}$ *Mcl-1*$^{\Delta/+}$ lesions (Figure 16E). The reduced ^{18}F-FDG uptake of *Kras*$^{G12D/+}$ *Mcl-1*$^{\Delta/+}$ tumors after cisplatin suggests that these tumors are not as metabolically active compared to *Kras*$^{G12D/+}$ *Mcl-1*$^{+/+}$ tumors. The reduction in glucose metabolism, albeit not statistically significant, indicates a treatment response in these tumor lesions supporting the notion that *Mcl-1* serves as a valid target in these tumors. The data on the levels of cleaved caspase 3 within the tumor lesions showed a significant reduction upon *Mcl-1* deletion specifically on day 4. This finding indicates a reduced number of apoptotic cells at that time point. In the light of the reduced glucose uptake on day 2, the reduction in apoptotic cells might be explained by a more accelerated phagocytic removal of these cells from the lesions. The data presented here are encouraging to further study MCL-1 inhibition in combination with cisplatin treatment as a therapeutic principle in adenocarcinoma of the lung.

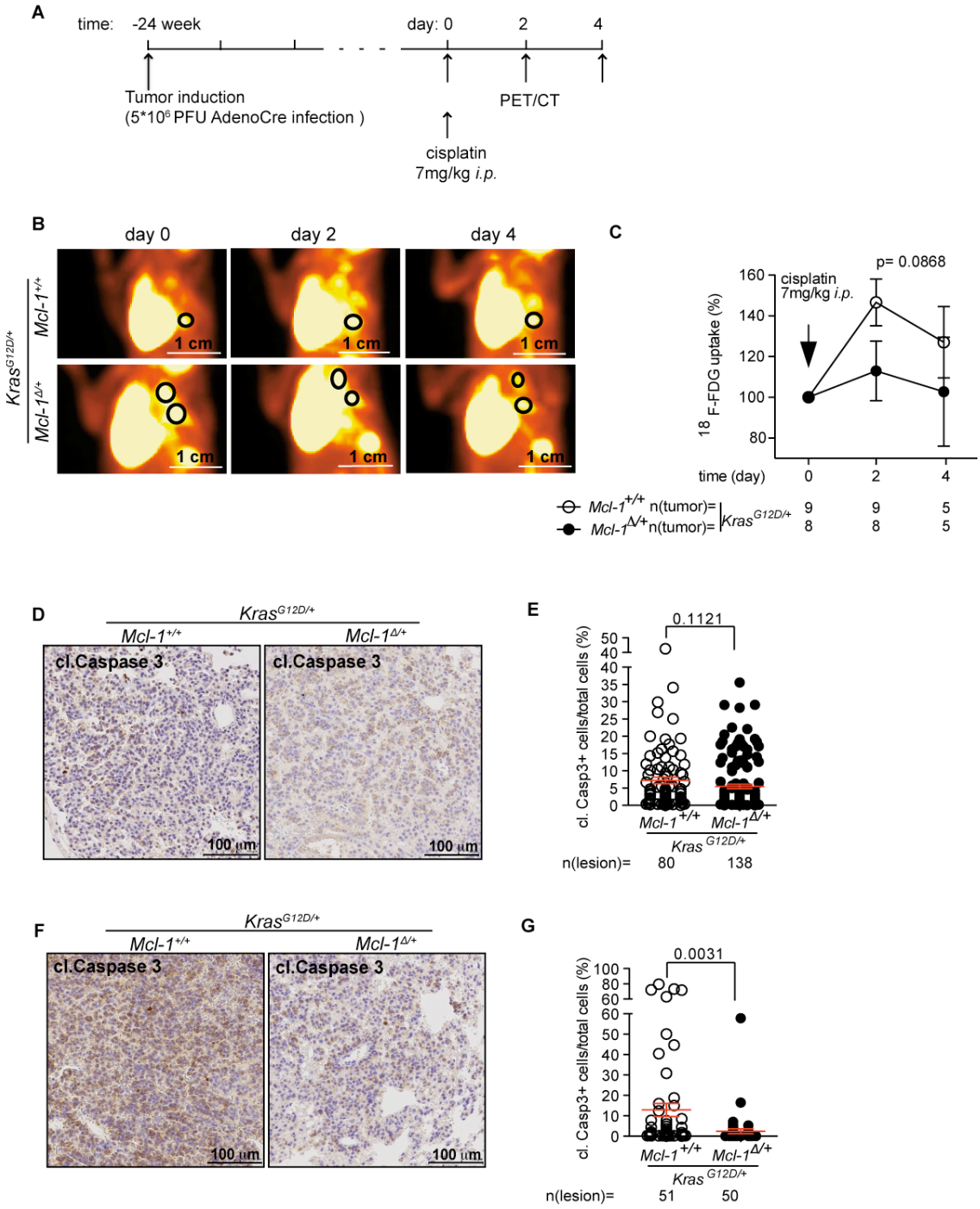

Figure 16. Comparison of the cisplatin efficiency after MCL-1 deletion. (A) Schematic overview of the experiment. (B) Representative ^{18}F-FDG PET lung tumor (marked with circles) reconstruction. (C) Dynamic of ^{18}F-FDG uptake of lung tumors on indicated days relative to uptake on day 0. Black arrow indicates cisplatin treatment. N number equals individual tumors from 5/6 (day 0 and day 2), and 3 (day 4) mice per genotype. Representative cleaved caspase 3 staining and quantification of cleaved caspase 3 positive cells in the lesions on day 2 (D, E) and on day 4 (F, G) after cisplatin treatment. N number equals lesion number. Data are presented as mean±SEM. Unpaired two-tailed *t*- test was used for statistical analysis.

4. DISCUSSION

Lung cancer is one of the most commonly diagnosed cancers and it is responsible for one-fifth of all cancer deaths worldwide (Globalcan 2012, International Agency for Research on Cancer, World Health Organization). At the time of diagnosis most patients have advanced stage disease (Travis et al., 2013b) making chemotherapy and targeted therapy the treatment options of choice. Despite these treatments, prognosis of the disease remains poor and patients often develop resistance to therapy (Buettner et al., 2013; Schiller, 2001). Within the group of lung cancer, adenocarcinoma is the most common form diagnosed. Thirty three percent of lung adenocarcinomas harbor mutations in *KRAS* that render this protein constitutively active (The Cancer Genome Atlas Research Network, 2014). Mutated KRAS activates multiple effector pathways that promote oncogenic transformation and tumor progression. However, targeting KRAS in the clinical setting is, at least until now, impossible. This identifies the need to develop additional strategies to target this disease based on the molecular make-up of the individual tumor (de Castro Carpeño and Belda-Iniesta, 2013)

Malignant transformation of cells induces a range of pro-apoptotic stresses, which activate the apoptotic program (Cory et al., 2003; Youle and Strasser, 2008). These stresses range from hypoxia, deprivation of nutrients and growth factors, violation of cell cycle checkpoints, telomere erosion, endoplasmic reticulum stress to oncogenic signaling (Hanahan and Weinberg, 2011). Interestingly, cancer cells block the apoptotic program effectively evading cell death induction despite the presence of apoptotic stimuli. The molecular mechanism by which cancer cells protect themselves from apoptotic cell death remained elusive for a long time.

One mechanism described already in 1984 was the chromosomal translocation between chromosome 14 and 18, which resulted in the constitutively elevated expression of the pro-survival BCL-2 family member BCL-2 under control of the immunoglobulin heavy chain enhancer elements (Pegoraro et al., 1984; Tsujimoto et al., 1984). This genetic aberration was the first description of the deregulated expression of pro-survival BCL-2 proteins primarily found indolent B-cell lymphoma such as follicular lymphoma.

After many years of research, it took until approximately 2010 to identify additional genetic changes that directly and frequently caused the deregulation of pro-survival BCL-2 family members in human cancer specimen. A study in over 3000 human cancers identified a high frequency of copy number amplification of

chromosome 1 (1q21.2). The pro-survival BCL-2 family member *MCL-1* is located at 1q21.2 suggesting that copy number gains of *MCL-1* might result in elevated expression levels and subsequent protection of cancer cells against intrinsic apoptotic stresses. Genetic silencing by knockdown of *MCL-1* in human lung cancer cell lines that harbored copy number gains at that locus proved that MCL-1 was indeed critically required to protect these cell lines from cell death (Beroukhim et al., 2010). In addition, genetic amplifications of the locus harboring the pro-survival *BCL-2* family member *BCL-X$_L$* were also frequently detected. This finding suggests a common mechanism of selection for tumor cells that are capable of protecting themselves from intrinsic apoptotic stimuli by elevated expression of pro-survival BCL-2 family members. Of note, the corresponding molecular mechanism of apoptotic blockade, namely the reduced expression of pro-apoptotic BCL-2 family members by copy number losses, was also observed with high frequency in the same study. Copy number losses of the *BAX/BAK*-homologue *BOK* were identified in a multitude of cancer specimen rendering it one of the most frequently deleted tumor suppressor genes detected (Beroukhim et al., 2010).

This data was supported by the finding that RNA and protein expression of MCL-1 were elevated in 45 primary NSCLC specimens in comparison to matched healthy lung tissue correlating with an reduced overall survival of patients (Luo et al., 2012). Moreover, elevated levels of MCL-1 are often considered responsible for promoting resistance to chemotherapeutics and radiation therapy (Michels et al., 2014; Palve and Teni, 2012). Together this previously published data clearly identifies the pro-survival BCL-2 group of proteins as potential future targets of targeted cancer therapy.

A major drawback for functional studies on the relevance of MCL-1 is the paucity of pharmacologic inhibitors. Whereas potent inhibitors of pro-survival BCL-2, BCL-X$_L$ and BCL-W are readily available (namely ABT-737 and the orally available compound ABT-263), no specific inhibitors for MCL-1 have yet been identified. Large unstructured sections of the MCL-1 protein, lacking in large parts a rigid three-dimensional tertiary structure, make it especially difficult to create inhibitors that bind to the BH3 domain at low nanomolar concentrations and in the context of a viable cell.

Several approaches to reduce MCL-1 levels have been employed to study the functional consequences of its deletion in cells or in animal models. The reduction in MCL-1 levels by antisense oligonucleotide treatment or ectopic expression of the MCL-1-inhibiting BH3-only protein NOXA have shown to induce

apoptosis and sensitize lung cancer cells to chemotherapeutic agents and radiation (Song et al., 2005; Whitsett et al., 2014). In addition, MCL-1 levels have been depleted in multiple different cancer cell lines by inhibition of transcription or translation, as well as induction of degradation. This is exemplified by the inhibition of *MCL-1* transcription *in vitro* using the cyclin-dependent kinase inhibitor Flavopiridol in multiple myeloma cells (Gojo et al., 2002). This approach, however, was not specific and it is difficult to pinpoint the observed effects to the reduction in MCL-1 levels only. Moreover, the reduction of MCL-1 levels was achieved with the multi-kinase inhibitor BAY43-9006. This compound downregulated MCL-1 primarily by inhibiting the translation of MCL-1 as transcription and stability were not affected. Using several human leukemia cell lines such as U937 or human primary acute leukemia blasts *in vitro*, a substantial reduction in MCL-1 levels was observed following 6-8 hours treatment with BAY43-9006 (Rahmani et al., 2005). The same was achieved in lung cancer cell lines, in which BAY43-9006 reduced MCL-1 levels in a time- and dose-dependent manner as early as 3 hours after treatment (Yu et al., 2005). These strategies for inhibiting MCL-1 succeeded in inducing apoptosis *in vitro,* however, these agents have a broad specificity *in vivo*, which might not necessarily only depend on the inhibition of MCL-1. The emergence of side effects caused by off-target effects also likely impede on the clinical relevance of multi-kinase inhibitors.

In order to verify the functional relevance of MCL-1 and due to the lack of specific pharmacologic inhibitors, I utilized a strategy that targets the alternative pro-survival BCL-2 family member such as BCL-2, BCL-X_L and BCL-W using ABT-737. The sensitivity of NSCLC cell lines to inhibition by ABT-737 indicates the relevance of BCL-2, BCL-X_L and BCL-W to sustained NSCLC cell survival. All tested NSCLC cell lines were relatively insensitive to ABT-737, which shows that survival is likely mediated by MCL-1. This approach was validated in MEF proficient or deficient for *Mcl-1*. Consistent with previously published data, we found that *Mcl-1*$^{-/-}$ MEF were sensitive to ABT-737 while WT MEF were resistant, confirming that MCL-1 promotes ABT-737 resistance (Figure 4B and C) (van Delft et al., 2006).

In order to circumvent the fact that specific pharmacologic inhibitors of MCL-1 were not available to test the requirement of MCL-1 in the set of human NSCLC cell lines, I ectopically overexpressed the endogenous inhbitor of MCL-1 using mutated versions of the BH3-only protein BIM. The mutations induced are located within the BH3 domain of BIM and alter the binding specificity of the protein so that we can target the mutated BIM to individual pro-survival BCL-2 family members (Figure 6A) (Chen et al., 2005; Kelly et al., 2014; Lee et al., 2008). As MCL-1 confers resistance to ABT-737 induced-apoptosis in NSCLC cell lines (Figure 5B), I wanted to confirm

the functional relevance of MCL-1 by expressing individual BIM mutants in NSCLC cell lines, which express high or low levels of MCL-1. The abundance of MCL-1 clearly correlated with the level of cell death induced by the MCL-1 inhibiting BIM mutant (BIM_S2A). This indicates that MCL-1 potently protects NSCLC cell lines that express relevant levels of this protein against apoptosis and that inhibition of its function was capable of driving cell death. Notably, it was found the presence of alternative pro-survival BCL-2 family members, irrespective of their expression levels, did not affect the survival of NSCLC cell lines when MCL-1 was inhibited, clearly showing that functional blockade of MCL-1 *in vivo* might serves as a promising tool to target lung adenocarcinoma.

These results are consistent with several other studies that demonstrated a critical role of MCL-1 in promoting cancer cell survival. RNA interference with siRNA against *MCL-1*, induced apoptosis in lung cancer cell line that had high levels of MCL-1 supporting our finding by an alternative methodology (Zhang et al., 2011). Downregulation of MCL-1 in NSCLC cell lines that harbor genetic amplifications of chromosome 1q21 using shRNA also supported a critical function of MCL-1 for sustained cancer cell survival *in vitro* (Beroukhim et al., 2010). Consistent with MCL-1 being critical for resistance to ABT-737, MCL-1-expressing NSLCL cell lines remained insensitive to the treatment with ABT-737. In this study, overexpression of NOXA, which inhibits MCL-1, overcame resistance to ABT-737 furthermore pinpointing towards a critical survival function mediated by MCL-1 (Wesarg et al., 2007).

Our data obtained in cell culture supported the notion that MCL-1 inhibition was capable of killing lung cancer cell lines. We therefore set out to verify this observation within the context of the whole organism. I utilized a murine lung cancer model that is based on the expression of mutated KRAS. This genetic lesion is one of the most prevalent genetic aberrations observed in patients diagnosed with adenocarcinoma of the lung (The Cancer Genome Atlas Research Network, 2014) and therefore represents an excellent model to draw conclusions for future translation into the clinical context.

Our mouse model is based on the expression of mutated KRAS similar to what is frequently observed in patients. To monitor the effects of mutated KRAS on apoptosis, I initially addressed the response of WT and *Mcl-1*$^{-/-}$ MEF to *Kras*^{G12D} expression. Transcriptionally, *Kras*^{G12D} expression in WT MEF resulted in the upregulation of various pro-survival *Bcl-2* members such as *A1, Bcl-x*$_L$ and *Mcl-1* (Figure 4D and E). Notably, in both *Kras*^{G12D} expression models (MEF + ectopic

Kras^{G12D} or MEF from *lsl-Kras*$^{G12D/+}$ mice + AdenoCRE infection), *Mcl-1* was consistently upregulated (Figure 4D and E). Expression of the constitutively active *Kras*^{G12D} in *Mcl-1*$^{-/-}$ MEF conferred a modest protection against cell death induced by ABT-737 when directly compared to the expression of WT *Kras* (Figure 4B and C). This points towards an anti-apoptotic effect of constitutive KRAS signaling and further supports the notion that re-activation of apoptosis e.g. by genetic deletion of *Mcl-1* might have therapeutic potential.

Constitutively active RAS signaling activates multiple effector pathways, which regulate various cellular activities such as cellular survival (described in section 1.2). The data in Figure 4 show that *Kras*^{G12D} promotes cell survival, at least partially, by up-regulating BCL-2 family members by a transcriptional mechanism. However, this is unlikely the only anti-apoptotic effect of mutant KRAS signaling. *Kras*^{G12D} is also capable of promoting survival independent of BCL-2 protein expression e.g. by activation of NF-κB through PI3K-AKT signaling (Finco et al., 1997; Mayo and Baldwin, 2000), or by expression of repressors of apoptosis through the RAF-MEK-ERK pathway (Wu et al., 2010).

To translate the findings of the *in vitro* studies into the context of the whole organism and to further investigate the functional relevance of MCL-1 *in vivo,* I established a *Kras*^{G12D}-driven murine adenoma / adenocarcinoma mouse model. The hypothesis that inhibition (or genetic deletion) of MCL-1 might perturb tumor development in mutant *Kras*-driven lung tumors under physiological conditions was tested using the *lsl-Kras*^{G12D} mouse model originally established in the Jack´s lab (Jackson et al., 2001). Tumor induction with AdenoCRE infection in *lsl-Kras*^{G12D} *Mcl-1*^{floxed} compound mutant mice allowed for the analysis of the role of MCL-1 *in vivo*. Using these mice, it was shown that the oncogenic *Kras*-driven lung tumors in this model resemble many aspects of early adenocarcinoma of patients (Figure 10 and 12). To fully recapitulate advanced stage human lung adenocarcinoma with its capacity of metastasizing to alternative organs, an additional *p53* mutations and/or deletion is required to generate a murine model (Jackson et al., 2005). This feature is not represented in our mouse model. However, it is important to note that in a recent data set published by the cancer genome atlas research network focusing on the molecular profiling of lung adenocarcinoma, 50 out of 74 *KRAS*-mutated lung adenocarcinoma did not harbor additional *p53* mutations, which accounts for 68 % of samples (The Cancer Genome Atlas Research Network, 2014). Therefore, our *Kras*-driven lung tumor model is clinically relevant to those patients with *KRAS* mutant adenocarcinoma without *p53* co-mutations. More importantly, our model focuses on the initiation of the tumor within the lungs since *Mcl-1* is co-deleted when *Kras*^{G12D}

expression is initiated. This argues that early events during malignant transformation are depicted in which additional aberrations of *p53* might not yet play an important role.

The route of delivery of the virus represents another advantage of our model system over xenograft or cell culture-based systems. Adenoviral-mediated delivery of CRE mimics the development of human tumors by causing sporadic activation of the *Kras* oncogene only in individual cells that remain surrounded by normal tissue in the context of an otherwise healthy animal. This infection method therefore recapitulates the origin of the disease in humans, where individual mutant cells give rise to malignant tumors.

AdenoCRE mediated tumor induction resulted in the formation of lesions in the lungs of *Mcl-1*-deleted animals, which originated from pneumocyte type II or both pneumocyte type II and Clara cell or their progenitors as previously published (Jackson et al., 2001). Furthermore, mucin positivity of the lung cancer lesions confirmed that the origin of the lesions as adenocarcinoma (Figure 10) (Travis et al., 2013a). Together, my mouse model system closely recapitulates the human situation and is therefore well suited to study the effects of MCL-1 inhibition *in vivo*.

Heterozygous deletion of *Mcl-1* was sufficient to diminish tumor burden, predominantly by decreasing the number of lesions formed. This effect on the number of lesions was clearly enhanced upon homozygous deletion of *Mcl-1* (Figure 11A and B). The efficient reduction in tumor burden upon *Mcl-1* deletion is the first report of this function in epithelial cancers and therefore represents an important step towards the concept of re-activating apoptosis in cancer.

The findings in this study are consistent with studies of *Mcl-1* depletion in tumor initiation and maintenance that have so far been predominantly studied in hematopoietic malignancies. For examples, haploinsufficiency of *Mcl-1* retarded the development of *Myc*-induced acute myeloid leukemia (AML), however this mouse model does not recapitulate a frequently observed AML subtype (Xiang et al., 2010). Using a clinically more relevant AML model based on the retroviral expression of mixed-lineage leukemia (MLL)-based oncogenic fusions or the oncogenic fusion AML1-ETO (also known as RUNX1/MTG8), Glaser and colleagues showed that *Mcl-1* deletion did not only impair tumor development but also affected tumor maintenance as removal of one allele of *Mcl-1* significantly reduced the viability of fully established AML cells (Glaser et al., 2012). Moreover, homozygous deletion of *Mcl-1* regressed *Myc*-driven B-cell lymphoma and prolonged survival of lymphoma-bearing mice *in vivo*. Even heterozygous loss of *Mcl-1* was highly detrimental for the

sustained growth of *Myc*-driven B-cell lymphoma clearly identifying this protein as an interesting target in hematopoietic malignancies (Kelly et al., 2014).

My presented results suggest that the dependency of tumor cells on the sustained activity of MCL-1 is not only critical for hematopoietic cancers but also for epithelial tumors. Therefore, MCL-1 may serve as a promising new target for future cancer therapy in a variety of neoplasm.

It is important to emphasize the observation that individual large and anaplastic tumor lesions were observed at low frequency when both alleles of *Mcl-1* were deleted. Some $Kras^{G12D/+}Mcl\text{-}1^{\Delta/\Delta}$ tumors were capably of extending to large sizes despite the complete genetic deletion of *Mcl-1*. Both heterozygous but more prominently homozygous *Mcl-1* deletion mediated the formation of advanced, relatively large, and de-differentiated lung lesions potentially because additional genetic events occurred in these lesions. The development of compensatory mechanisms overcoming the induction of apoptosis driven by the genetic loss of *Mcl-1* likely resulted in the development of these large tumors (Figure 12). Transformed cells have been proposed to be more dependent on MCL-1 compared to normal cells, as untransformed cells tolerate reduced levels of MCL-1 significantly better (Figure 9) (Opferman et al., 2005; Vikstrom et al., 2010). Our data show that malignantly transformed cells either die in response to *Mcl-1* deletion as evidenced by the reduced number of tumor lesions and the reduced tumor burden of diseased mice (Figure 11B and C). Alternatively, individual malignant lesions may develop new survival strategies and even progress to more advanced tumors when MCL-1 is absent (Figure 12).

We have to be cautious in over interpreting this concept since our mouse model system only sheds light on the very early stages of disease development and the initiation process of malignant transformation. The activity of CRE to drive mutant KRAS signaling occurs in parallel to the genetic deletion of *Mcl-1*, effectively rendering cells prone to cell death when KRAS signaling becomes activated. This was in line with our hypothesis that continued protection against apoptosis was required for tumor formation and my mouse model therefore provides data specifically on this aspect of carcinogenesis. However in the clinical setting of cancer patients, it will be impossible to apply MCL-1 inhibiting compounds to patients at that stage of disease development. Instead, pharmacologic inhibition of MCL-1 will only be possible when the tumors become clinically apparent. The exact functional consequences of a complete and sustained MCL-1 inhibition (by genetic deletion in the mouse or pharmacologic inhibition in patients) can therefore not be concluded from our data.

The current push of pharmaceutical companies for the development of MCL-1 specific inhibitors is therefore likely suited to serve the purpose to reduce the main tumor bulk in fully established lung cancers, whereas it is unclear whether this approach will drive the development of individual resistant and more aggressive clones from the tumor, which might eventually result in disease relapse. This, however, is similar to alternative targeted therapies currently in clinical use such as EGFR inhibition, which might also result in the development of resistant clones (Jackman et al., 2010). Whereas my study might warn against the continued uncritical use of MCL-1 inhibitors in the treatment of adenocarcinoma of the lung in patients, it will be the most important to elucidate the molecular mechanisms by which *Mcl-1* deletion contributes to the development of anaplastic tumors.

In order to elucidate the molecular mechanisms that cause the observed phenotype, apoptosis and proliferation were assessed in *Mcl-1*-deleted tumors. As MCL-1 mostly functions as a pro-survival protein, downregulation of MCL-1 often results in an elevated level of apoptosis in tumor cells. In the established $Kras^{G12D/+}$ $Mcl\text{-}1^{\Delta/+}$ and $Kras^{G12D/+}$ $Mcl\text{-}1^{\Delta/\Delta}$ lesions, apoptosis was not increased as compared to controls when assessed 19 weeks after tumor induction (Figure 13A and B). This time point might be too late to detect differences in apoptosis within the cancer lesions. Nevertheless, the overall reduction in lesion numbers 19 weeks after disease initiation support the notion that elevated levels of apoptosis are present during the early developmental stages of the tumors (Figure 11B). The tumors that were capable of forming visible lesions at such a late time point likely have escaped apoptosis induction rendering them largely resistant to cell death.

Furthermore, expression of the proliferation marker Ki67 was reduced upon heterozygous deletion of *Mcl-1* (Figure 13D). Consistently, Perciavalle and colleagues have shown that *Mcl-1* deletion in MEF and hepatocytes slowed down the proliferation accompanied by mitochondrial defects (Perciavalle et al., 2012). As genetic ablation of *Mcl-1* impairs both anti-apoptotic and mitochondrial functions (Perciavalle and Opferman, 2013), our data do not allow for a clear distinction between both outcomes. Unexpectedly, the proliferation rate remained unchanged in *Mcl-1* homozygously deleted lesions in comparison to control tumors. This phenomenon might be explained by the acquisition of escape mechanisms protecting against apoptosis in $Kras^{G12D/+}Mcl\text{-}1^{\Delta/\Delta}$ tumors, which renders these lesions more proliferative.

Interestingly, activation of STAT3 was elevated in both *Mcl-1* heterozygously and homozygously deleted lesions (Figure 13F). Activated (phosphorylated) STAT3

(pSTAT3) regulates genes transcription promoting cell proliferation, survival, angiogenesis and metastasis and inhibits anti-tumor-immunity (Yu et al., 2014; Yu et al., 2009). Interestingly, pSTAT3 regulates *MCL-1* transcription. Activation of STAT3 (phosphorylation on serine 727) was shown to upregulate *MCL-1* expression in human primary macrophages while suppression of STAT3 phosphorylation reduced MCL-1 levels and lead to apoptosis (Liu et al., 2003). Consistently, the dominant-negative form of STAT3 decreased both mRNA and protein levels of BCL-2 and MCL-1 resulting in activation of caspase 3 in intestinal epithelial cells (Bhattacharya et al., 2005). Furthermore, in multiple cancers STAT3 is constitutively activated (Al Zaid Siddiquee and Turkson, 2008). Furhermore, pSTAT3 induced *MCL-1* expression in human myeloma cell lines (Puthier et al., 1999), and in chronic lymphocytic leukemia B cells (Lee et al., 2005) in response to IL-6 and VEGF, respectively. STAT3 is also persistently activated in primary glioblastoma multiforme (GB) and GB cell lines, and the Janus kinase inhibitor AG490 mediated-inhibition of STAT3 activation triggered apoptosis in U251 (GB cell line) cells by the reduction in BCL-X_L, BCL-2 and MCL-1 protein levels (Rahaman et al., 2002).

Notably, in my study both heterozygous and homozygous deletion of *Mcl-1* resulted in elevated activation of STAT3. This suggests a compensatory mechanism activated by the reduction of MCL-1 protein levels, which might indirectly contribute to tumor progression. Furthermore, expression of c-MYC, a target of pSTAT3 (Kiuchi et al., 1999) was elevated in *Mcl-1* homozygously deleted lesions (Figure 13H). c-MYC is a transcription factor that is involved in a wide range of cellular processes such as cellular growth, proliferation, angiogenesis and de-differentiation (Pelengaris et al., 2002; Tansey, 2014). Therefore, overexpression of c-MYC might support the tumor progression observed in individual lesions. Taken together, upregulated activation of STAT3 and its target c-MYC might serve as a compensatory mechanism to adapt to the loss of *Mcl-1* as well as to contribute to tumor progression and survival.

A critical consideration for the clinical use of MCL-1 inhibiting strategies as anti-neoplastic agents is their effect on physiologically healthy tissue. The characterization of the effects of MCL-1 deletion should therefore not be limited to tumor tissue only. A specific interest needs to be placed on the tolerance of healthy tissue to MCL-1 downregulation/inhibition. It is important to note that the complete deletion of *Mcl-1* induces damage in several critical organs such as the hematopoietic system, cardiomyocytes and hepatocytes (described in section 1.3.4) (Arbour et al., 2008; Opferman et al., 2005; Opferman et al., 2003; Steimer et al.,

2009; Thomas et al., 2013; Vick et al., 2009; Wang et al., 2013). However, heterozygous deletion of *Mcl-1,* which mimics to some degree the clinically achievable inhibition of the protein by pharmacologic blockade, did not cause apparent abnormalities in several studies including heterozygous deletion of *Mcl-1* in bone marrow (hematopoietic stem cells), liver (Opferman et al., 2005), in activated and in naive B-cells (Vikstrom et al., 2010). Notably, lung tissue remained completely unaffected by the partial deletion of *Mcl-1* over a time frame of 19 weeks (Figure 9C-F). Several sections of different *Mcl-1* $^{\Delta/+}$ mice showed no pulmonary pathology after AdenoCRE-mediated deletion of *Mcl*-1 in healthy lungs. These findings suggest that partial inhibition of MCL-1 unlikely affects healthy lung tissue rendering this protein a valuable target for potential future lung cancer therapy.

A growing body of evidence indicates that MCL-1 (over-)expression confers resistance to therapy and associates with poor prognosis in NSCLC patients. For example, expression of MCL-1 correlated with advanced stage disease in NSCLC patients and a poor prognosis (Whitsett et al., 2014). *In vitro*, MCL-1 expression conferred chemo- and radioresistance and depletion of MCL-1 expression by genetic and pharmacological approaches re-sensitized NSCLC cell lines to these treatment modalities (Whitsett et al., 2014). To address whether the reduction of MCL-1 expression sensitizes NSCLC to anti-neoplastic treatment *in vivo*, I utilized two different treatment approaches, based either on the *i.p.* injection of cisplatin or, alternatively, on the oral gavage with ABT-263 in mice harboring *Mcl-1* heterozygously deleted lesions and controls animals.

MCL-1 is not inhibited by ABT-263 (or ABT-737 *in vitro*) suggesting that resistance ot ABT-263 might be overcome by treating *lsl-Kras*$^{G12D/+}$ *Mcl-1*$^{fl/+}$ mice with this compound when compared to control mice (van Delft et al., 2006). However, additional inhibition of BCL-2, BCL-X_L and BCL-W by ABT-263 did not induce significant tumor regression in the established *Kras*$^{G12D/+}$ *Mcl-1*$^{\Delta/+}$ lesions *in vivo* when directly compared to control mice (Figure 15C). This finding shows that the inhibition of pro-survival BCL-2 family members other than MCL-1 did not impact on the survival of lung cancer cells at the tested time points *in vivo*. The remaining level of MCL-1 might block apoptosis induction effectively rendering ABT-263 insensitive. Alternatively, compensatory upregulation of MCL-1 in response to ABT-263, similar to what was observed in SCLC cells or hepatocytes, might block ABT-263-mediated cell death induction (Tahir et al., 2007; Wang et al., 2014a). The complete genetic deletion of *Mcl-1* might eventually result in an elevated toxicity of ABT-263, however

this approach is clinically not feasible due to the observed systemic toxicity (described in section 1.3.4).

In line with this data, the ectopic expression of the MCL-1-inhibiting BH3-only protein NOXA in ABT-737 resistant NSCLC cell lines overcame the apoptotic resistance of these cells (Wesarg et al., 2007). This finding was supported by the sensitizing effect of targeting MCL-1 by RNA interference, by ERK inhibition (which destabilizes MCL-1), or NOXA expression (Konopleva et al., 2006) in AML blasts or in T-leukemic cells (Rooswinkel et al., 2012). In summary, my data show that additional inhibition of pro-survival BCL-2 family proteins other than MCL-1 (and potentially also A1) did not impact on the survival of lung cancer lesions *in vivo.*

We therefore tested an alternative established treatment concept using cisplatin (cis-diamminedichloroplatinum (II)), which is one of the most widely used chemotherapeutic drugs in lung cancer (Socinski, 2004). It is used as first line therapy for NSCLC and SCLC and it is included in combination regimens for adjuvant therapy of early stages of NSCLC (Dasari and Bernard Tchounwou, 2014). Cisplatin binds to the purine bases on the DNA and forms intrastrand and interstrand crosslinks. These modifications (platinated adducts) distort DNA helix and impair replication and transcription, which lead to stalled replication forks and the formation of double-strand breaks. Subsequently, cell cycle checkpoints are activated resulting in cell cycle arrest to repair DNA damage or to induce apoptosis (Wang and Lippard, 2005). Although treatment with cisplatin is often effective in cancers during the first courses of therapy, intrinsic and acquired resistance to cisplatin during later cycles of exposure or during relapse poses a limiting factor (Galanski, 2006). Cisplatin resistant cells (obtained by chronic exposure of parental cells to sublethal concentration of cisplatin) including NSCLC cell lines have shown resistance to cisplatin induced-apoptosis by upregulation of MCL-1. In turn, depletion of MCL-1 by RNA interference or treatment with the pan-BCL-2 inhibitor obatoclax induced apoptosis in those cells, supporting a critical role of MCL-1 in cisplatin-resistant NSCLC cell lines (Michels et al., 2014).

Consequently, I aimed to identify the efficiency of cisplatin in tumors with reduced levels of MCL-1 in direct comparison to tumors that were proficient in MCL-1 *in vivo*. In control *Kras*$^{G12D/+}$ *Mcl-1*$^{+/+}$ tumors, the ^{18}F-FDG uptake as a marker of metabolic activity and subsequent survival of the cancer cells, increased until day 2 and dropped on day 4 in response to cisplatin treament (Figure 16C). The delayed response of the tumors to cisplatin treatment is likely explained by the normal cell cycle process in which cells undergo cell cycle arrest at G2, which occurs approximately within 48 hours of the administration of cisplatin. After this time point

cells are released from the arrest or killed (Marcu and Bezak, 2012). On day 4 after cisplatin treatment, a significantly elevated level of apoptosis was observed in *Kras*$^{G12D/+}$*Mcl-1*$^{+/+}$ tumors directly correlated with a drop in ^{18}F-FDG uptake, showing that apoptosis was efficiently induced in control tumors (Figure 16F and G).

In contrast, the dynamics of ^{18}F-FDG uptake after cisplatin treatment in *Mcl-1* heterozygously deleted tumors remained relatively stable over time (Figure 16C). The appearance (day 2) and disappearance (day 4) of apoptotic cells in response to cisplatin specifically in *Kras*$^{G12D/+}$ *Mcl-1*$^{\Delta/+}$ lesions (Figure 16F and G) likely reflects the induction of apoptosis and subsequent clearance of apoptotic cells from the tissue. This in turn results in a reduced metabolic activity (lower level of ^{18}F-FDG uptake) and supports the notion that treatment-induced apoptosis was stimulated more readily in MCL-1 targeted tumors compared to control tumors. Further investigations will focus on the macrophage markers in the tumor lesions to better define the molecular mechanisms controlling metabolims and apoptosis in response to cisplatin.

An alternative explanation suggests that increased chemotherapy-induced senescence, similar to what was observed in a colon cancer cell line in response to the silencing of *MCL-1* by shRNA, might result in a reduced ^{18}F-FDG uptake (Bolesta et al., 2012). Cisplatin might therefore have induced senescence instead of apoptosis in *Mcl-1*-deleted lesions. Subsequently, these lesions exhibit a growth arrest exemplified by the failure to increase the ^{18}F-FDG uptake over time (Campisi and d'Adda di Fagagna, 2007). Further characterization of the levels of senescence markers such as p21 in these lesions will be used to verify this possibility.

Yet another alternative might be that tumor lesions become metabolically inactive after deletion of *Mcl-1* rendering any chemotherapy less active in these tumors. An intrinsically reduced level of metabolic activity might explain the reduced glucose uptake observed in *Mcl-1*-deleted lesions. Recent data suggests that MCL-1 might have a direct impact on metabolism. It was found that *Mcl-1* deletion in MEF reduced ATP levels as well as the mitochondrial membrane potential, which drives ATP synthesis. In addition, *Mcl-1* deletion also triggered the aberrant assembly of the respiratory complex (supercomplex IV), which enhances electron transport, and prevented F_1F_0-ATP synthase oligomerization. This results in disorganization of mitochondrial cristae and consequently in a decreased ATP synthesizing capacity (Perciavalle et al., 2012).

In summary, this experiment shows that the ^{18}F-FDG uptake, as a parameter of metabolic activity, is reduced in *Kras*$^{G12D/+}$ *Mcl-1*$^{\Delta/+}$ lesions compared to control tumors suggesting that the combination of chemotherapy with MCL-1 inhibition might

be a powerful way to enhace the efficacy of conventional chemotherapy. However, further characterization is required to better understand the molecular mechanisms controlling senescence and apoptosis in lung cancer lesions in response to MCL-1 inhibition *in vivo*.

Together, I have shown that lung cancer cell lines expressing MCL-1 critically depend on its sustained activity irrespective of whether they express alternative pro-survival BCL-2 family proteins. Using the mouse model described above, I have shown that the genetic deletion of *Mcl-1* results in a significant reduction of tumor burden, decreased number of tumor lesions, reduced glucose uptake in lung cancer lesions after chemotherapy treatment, but no toxicity on healthy lung tissue. However, the appearance of individual large anaplastic lesions in mice expressing constitutively active mutant KRAS after complete deletion of MCL-1 argues that escape mechanisms in individual tumor exist. I hypothesize that the sustained inhibition of MCL-1 might select for the presence of more aggressive tumors *in vivo*. In summary, my data argue that the pharmacologic inhibition of MCL-1 might serve as a novel therapeutic principle when selection for more aggressive clones can be circumvented either by interruption of MCL-1 inhibiting treatment or by better understanding (and subsequent inhibition) of the molecular escape mechanisms.

STUDY IMPLICATIONS AND FURTHER QUESTIONS

The pro-survival BCL-2 proteins, including MCL-1, have long been desirable targets for treatment of cancer because of their potent inhibition of apoptotic cell death (Adams and Cory, 2007; Cory et al., 2003) and their contribution to tumor development and maintenance (Czabotar et al., 2014; Kelly and Strasser, 2011). Inhibition of BCL-2 by a specific compound termed ABT-199 has recently entered clinical trials for B-cell neoplasia with an exceptionally high efficacy and low toxicity.

Our data fit with the initial hypothesis that sustained blockade of apoptosis by MCL-1 is important for KRAS-driven adenocarincoma development in the lung of experimental mice. This data is highly interesting because it describes the first *in vivo* model of solid (epithelial) cancers in which targeting of MCL-1 is efficacious. Targeting MCL-1 pharmacologically appears to be a highly attractive possibility for future lung cancer therapy, despite the difficulties in designing a robust inhibitor for systemic application at the moment.

However, in rare occasions *Mcl-1* deletion mediated the formation of relatively large and histologically advanced tumors in some mice. This suggests the development of escape mechanisms, especially when both alleles of *Mcl-1* are deleted and cautions against the uncritical use of potential MCL-1 inhibitory compounds.

A possible compensatory mechanism that we have observed was the upregulation of STAT3 activation in tumor lesions from mice with (partially or fully) *Mcl-1*-deleted tumors. Additional STAT signaling inhibition might overcome this compensatory proliferation. Neverthelesse, further characterizations of the molecular mechanisms driving the development of large analplastic tumor lesions in these mice is mandatory before a clinical assessment of MCL-1 inhibiting strategies will become a clinical reality.

5. ABBREVIATIONS

A1	BCL-2 related protein A1
AB-PAS	alcian blue- periodic acid schiff
ALK	anaplastic lymphoma kinase
AML	acute myeloid leukemia
AP-1	activating protein-1
APAF1	apoptotic protease activating factor-1
Asp	aspartic acid
ATP	adenosine triphosphate
ATS	American thoracic society
BAD	BCL-2-associated death promoter
BAK	BCL-2 antagonist/killer
BAX	BCL-2-ssociated X protein
BCA assay	bicinchoninic acid assay
BCL-2	B-cell lymphoma - 2
BCL-2L10	BCL-2-like 10
BCL-2L11	BCL-2-like 11
BCL-2L2	BCL-2-like 2
BCL-X_L	B-cell lymphoma - extra large
BH domain	BCL-2 homology domain
BID	BH3 interacting-domain death agonist
BIM	BCL-2- interacting mediator of cell death
BIM_{EL}	BIM-extra long
BIM_S	BIM short
BOK	BCL-2-related ovarian killer
BRAF	v-raf murine sarcoma viral oncogene homologue B
CC10	Clara cell antigen 10
CCSP	Clara cell secretory protein
CDK	cyclin-dependent kinase
CREB	cAMP response-element binding protein
CT	computed tomography
DMEM	Dulbecco's modified eagle medium
DMSO	dimethyl sulfoxide
DNA	deoxyribonucleic acid
dox	doxycycline
EDTA	ethylenediaminetetraacetic acid
EGFR	epidermal groeth factor
EML4	echinoderm microtubule-associated protein-like 4
ERK	extracellular regulated kinase
ERS	European respiratory society
ETC	electron transport chain
^{18}F-FDG	2-deoxy-2-[^{18}F] fluoro-D-glucose
FACS	fluorescence-activated cell sorting
FASL	FAS ligand
FBS	fetal bovine serum
FFPE	formalin-fixed paraffin embedded
FGFR2	fiborblast growth factor receptor-2
FOX	forkhead box
GAP	GTPase-activating protein
GDP	guanosine diphosphate
GEF	guanine nucleotide-exchange factors

GFP	green fluorescent protein
GM-CSF	granulocyte-macrophage colony-stimulating factor
GrB	Granzyme B
GRB2	growth-factor receptor-bound protein-2
GRFs	guanine nucleotide releasing proteins
GSK-3	glycogen synthase kinase-3
GTP	guanosine triphosphate
GTPase	guanine triphosphatase
H&E	hematoxylin-eosin stain
HEK293T	Human embryonic kidney 293T cells
HGF	hepatocyte growth factor
HIF-1α	hypoxia-inducible factor-1 apha
HRAS	Harvey rat sarcoma viral oncogene homologue
I2E	1% iodine (I_2) dissolved in absolute ethanol (I2E)
IASLC	International association for the study of lung cancer
IGF	insulin-like growth factor
IHC	immunohistochemistry
IL	interleukin
ISH	*in situ* hybridization
JAK	Janus kinase
JNK	c-Jun N-terminal kinase
kDa	kilodalton
KRAS	Kirsten rat sarcoma viral oncogene homologue
MAPK	mitogen-activated protein kinase
MAPKK	mitogen-activated protein kinase kinase
MAPKKK	mitogen-activated protein kinase kinase kinase
MCL-1	myeloid cell leukemia -1
MCL-1ES	MCL-1 extra short
MCL-1S	MCL-1 short
MEF	murine embryonic fibroblast
MEK	MAPK/ ERK kinase
MET	*MNNG-HOS* transforming gene
MLL	mixed-lineage leukemia
MPP	mitochondrial processing peptidase
MULE	MCL-1 Ubiquitin Ligase E3
N-RAS	neuroblastoma RAS viral (v-ras) oncogene homologue
NF-1	neurofibromin-1
NF-κB	nuclear factor kappa B
NOXA	latin for *damage*
NSCLC	non-small cell lung cancer
PAS	pulmonary adenoma susceptibility
PBS	phosphate-buffered saline
PCNA	proliferating cell nuclear antigen
PD-ECGF	platelet-derived endothelial cell growth factor
PDGFR	platelet derived growth factor receptor
PEST	sequences that are rich in **p**roline, glutamic acid (**e**), **s**erine, and **t**hreonine
PET	positron emission tomography
PFA	paraformaldehyde
PFU	particle forming unit
PH	pleckstrin homology
PI	propodium iodide
PI3K	phosphoinositide 3-kinase
PIP2	phosphatidylinositol-4,5-biphosphate
PIP3	phosphatidylinositol 3,4,5- triphosphate

PLD	phospholipase D
PMAIP1	Phorbol-12-myristate-13-acetate-induced protein 1
PTEN	phosphatase and tensin homolog
PUMA	p53 upregulated modulator of apoptosis
qPCR	quantitative real-time polymerase chain reaction
RAF	rapidly accelerated fibrosarcoma
RAL	RAS-like
RALGDS	RAL guanine nucleotide dissociation stimulator
RALGEF	RAL guanine exchange factor
RAS	Rat Sarcoma viral oncogene homologue
RB	retinoblastoma
RGL	RALGDS-like
RMA	robust multi-array average
RT	room temperature
RTK	receptor tyrosine kinase
rtTA	reverse tet transactivator
SAPK	stress-activated protein kinase
SCLC	small cell lung cancer
SDS-PAGE	sodium dodecyl sulfate polyacrylamide gel electrophoresis
Ser	serine
SH	Src homology
snMCL-1	short nuclear form of MCL-1
SOS	son of sevenless
SP-C	surfactant protein-C
STAT	signal transducer and activators of transcription
STK11	serine/threonine kinase 11
tBID	truncated BH3 interacting-domain death agonist
tet-O	tet-operator
Thr	threonine
TIAM1	T-cell lymphoma invasion and metastasis-1
TM	transmembrane
TNF	tumor necrosis factor
TPA	12-O-Tetradecanoylphorbol-13-Acetate
TRAIL	TNF-related apoptosis-inducing ligand
TRE	tet-responsive promoter element
TTF-1	thyroid transcription factor-1
UICC	Union for International Cancer Control
VEGF	vascular endothelial growth factor
WT	wild type

ACKNOWLEDGEMENTS

I owe my deepest gratitude to everyone who has made this work possible.

Especially, I wish to express my gratitude to my supervisor PD. Dr. Philipp Jost for accepting me to work on this project in his group and for his guidance, encouragement, and scientific inspirations.

I would like to thank Prof. Dr. Mathias Heikenwälder for his impressive support, supervision, and invaluable ideas. Much appreciation goes to my mentor Prof. Dr. Jens Siveke for his inputs. I also thank Dr. Martina Anton for her scientific collaborations and her input in this work. I wish to thank PD. Dr. Katja Specht for her input in histological evaluation of the tumors.

I would like to whole-heartedly thank all members of the AG Jost research group for their excellent practical assistance, helpful suggestions and great working atmosphere. I thank Dr. Monica Yabal for her guidance, and proofreading this manuscript. I also wish to thank Sabine Spinner, who has been my “first mentor”, and Ulrike Höckendorf for her invaluable discussions and advices, and Nicole Müller and Stephanie Rott, who have been there to share my ups and downs with the “emergency package”, for their endless helpfulness that I could always count on.

I especially thank everyone in the Heikenwälder group, who has been willing to help. Specifically, I would like to thank Judith Bauer, Ruth Hillermann, and Daniel Kull for their inputs and priceless assistance.

Much appreciation goes to Zhoulei Li, Xiaopeng Ma, Pidassa Bidola, and Jolanta Slawska for their expertise in imaging and data analysis.

I would like to thank Prof. Dr. Tobias Dechow, Dr. Anja Baumgart, and Kerstin Behnke, who have made my first months in Germany as easy as possible, for their invaluable guidance not only concerning lab life but also in everyday life.

I am grateful to all colleagues from the AG Ruland research group for their continued help and friendly working environment.

My absolutely sincere gratitude goes to my family. My parents have always believed in me and supported to pursue all my goals. My brother has always pushed me to step forward and tirelessly encouraged me. Finally, I thank my best friend and fiancé for his support in any situation and being there sharing my wins and losses.

REFERENCES

Abulwerdi, F., Liao, C., Liu, M., Azmi, A.S., Aboukameel, A., Mady, A.S., Gulappa, T., Cierpicki, T., Owens, S., Zhang, T.*, et al.* (2014). A novel small-molecule inhibitor of mcl-1 blocks pancreatic cancer growth in vitro and in vivo. Molecular cancer therapeutics *13*, 565-575.

Adams, J.M., and Cory, S. (2007). The Bcl-2 apoptotic switch in cancer development and therapy. Oncogene *26*, 1324-1337.

Ahrendt, S.A., Hu, Y., Buta, M., McDermott, M.P., Benoit, N., Yang, S.C., Wu, L., and Sidransky, D. (2003). p53 mutations and survival in stage I non-small-cell lung cancer: results of a prospective study. Journal of the National Cancer Institute *95*, 961-970.

Aichberger, K.J., Mayerhofer, M., Krauth, M.T., Skvara, H., Florian, S., Sonneck, K., Akgul, C., Derdak, S., Pickl, W.F., Wacheck, V.*, et al.* (2005). Identification of mcl-1 as a BCR/ABL-dependent target in chronic myeloid leukemia (CML): evidence for cooperative antileukemic effects of imatinib and mcl-1 antisense oligonucleotides. Blood *105*, 3303-3311.

Akgul, C., Moulding, D.A., White, M.R.H., and Edwards, S.W. (2000a). In vivo localisation and stability of human Mcl-1 using green fluorescent protein (GFP) fusion proteins. FEBS letters *478*, 72-76.

Akgul, C., Turner, P.C., White, M.R.H., and Edwards*, S.W. (2000b). Functional analysis of the human MCL-1 gene. CMLS, Cell Mol Life Sci *57*, 684-691.

Al Zaid Siddiquee, K., and Turkson, J. (2008). STAT3 as a target for inducing apoptosis in solid and hematological tumors. Cell research *18*, 254-267.

Albanese, C., Johnson, J., Watanabe, G., Eklund, N., Vu, D., Arnold, A., and Pestell, R.G. (1995). Transforming p21ras mutants and c-Ets-2 activate the cyclin D1 promoter through distinguishable regions. The Journal of biological chemistry *270*, 23589-23597.

Alessi, D.R., Saito, Y., Campbell, D.G., Cohen, P., Sithanandam, G., Rapp, U., Ashworth, A., Marshall, C.J., and Cowley, S. (1994). Identification of the sites in MAP kinase kinase-1 phosphorylated by p74raf-1. The EMBO journal *13*, 1610-1619.

Almoguera, C., Shibata, D., Forrester, K., Martin, J., Arnheim, N., and Perucho, M. (1988). Most human carcinomas of the exocrine pancreas contain mutant c-K-ras genes. Cell *53*, 549-554.

Almuhaideb, A., Papathanasiou, N., and Bomanji, J. (2011). 18F-FDG PET/CT imaging in oncology. Annals of Saudi medicine *31*, 3-13.

Arbour, N., Vanderluit, J.L., Le Grand, J.N., Jahani-Asl, A., Ruzhynsky, V.A., Cheung, E.C., Kelly, M.A., MacKenzie, A.E., Park, D.S., Opferman, J.T.*, et al.* (2008). Mcl-1 is a key regulator of apoptosis during CNS development and after DNA damage. The Journal of neuroscience : the official journal of the Society for Neuroscience *28*, 6068-6078.

Bader, A.G., Kang, S., Zhao, L., and Vogt, P.K. (2005). Oncogenic PI3K deregulates transcription and translation. Nature reviews Cancer *5*, 921-929.

Bae, J., Leo, C.P., Hsu, S.Y., and Hsueh, A.J. (2000). MCL-1S, a splicing variant of the antiapoptotic BCL-2 family member MCL-1, encodes a proapoptotic protein possessing only the BH3 domain. The Journal of biological chemistry *275*, 25255-25261.

Bass, A.J., Watanabe, H., Mermel, C.H., Yu, S., Perner, S., Verhaak, R.G., Kim, S.Y., Wardwell, L., Tamayo, P., Gat-Viks, I.*, et al.* (2009). SOX2 is an amplified lineage-survival oncogene in lung and esophageal squamous cell carcinomas. Nature genetics *41*, 1238-1242.

Bergers, G., and Benjamin, L.E. (2003). Tumorigenesis and the angiogenic switch. Nature reviews Cancer *3*, 401-410.

Bergethon, K., Shaw, A.T., Ou, S.H., Katayama, R., Lovly, C.M., McDonald, N.T., Massion, P.P., Siwak-Tapp, C., Gonzalez, A., Fang, R.*, et al.* (2012). ROS1 rearrangements define a unique molecular class of lung cancers. Journal of clinical oncology : official journal of the American Society of Clinical Oncology *30*, 863-870.

Beroukhim, R., Mermel, C.H., Porter, D., Wei, G., Raychaudhuri, S., Donovan, J., Barretina, J., Boehm, J.S., Dobson, J., Urashima, M.*, et al.* (2010). The landscape of somatic copy-number alteration across human cancers. Nature *463*, 899-905.

Bhattacharya, S., Ray, R.M., and Johnson, L.R. (2005). STAT3-mediated transcription of Bcl-2, Mcl-1 and c-IAP2 prevents apoptosis in polyamine-depleted cells. The Biochemical journal *392*, 335-344.

Billard, C. (2013). BH3 mimetics: status of the field and new developments. Molecular cancer therapeutics *12*, 1691-1700.

Bingle, C.D., Craig, R.W., Swales, B.M., Singleton, V., Zhou, P., and Whyte, M.K. (2000). Exon skipping in Mcl-1 results in a bcl-2 homology domain 3 only gene product that promotes cell death. The Journal of biological chemistry *275*, 22136-22146.

Birchmeier, C., Birchmeier, W., Gherardi, E., and Vande Woude, G.F. (2003). Met, metastasis, motility and more. Nature reviews Molecular cell biology *4*, 915-925.

Bogart, J.A., Herndon, J.E., 2nd, Lyss, A.P., Watson, D., Miller, A.A., Lee, M.E., Turrisi, A.T., and Green, M.R. (2004). 70 Gy thoracic radiotherapy is feasible concurrent with chemotherapy for limited-stage small-cell lung cancer: analysis of Cancer and Leukemia Group B study 39808. International journal of radiation oncology, biology, physics *59*, 460-468.

Bolesta, E., Pfannenstiel, L.W., Demelash, A., Lesniewski, M.L., Tobin, M., Schlanger, S.E., Nallar, S.C., Papadimitriou, J.C., Kalvakolanu, D.V., and Gastman, B.R. (2012). Inhibition of Mcl-1 promotes senescence in cancer cells: implications for preventing tumor growth and chemotherapy resistance. Molecular and cellular biology *32*, 1879-1892.

Borner, M.M., Brousset, P., Pfanner-Meyer, B., Bacchi, M., Vonlanthen, S., Hotz, M.A., Altermatt, H.J., Schlaifer, D., Reed, J.C., and Betticher, D.C. (1999). Expression of apoptosis regulatory proteins of the Bcl-2 family and p53 in primary resected non-small-cell lung cancer. British journal of cancer *79*, 952-958.

Bos, J.L., Fearon, E.R., Hamilton, S.R., Vries, M.V.-d., van Boom, J.H., van der Eb, A.J., and Vogelstein, B. (1987). Prevalence of ras gene mutations in human colorectal cancers. Nature *327*, 293-297.

Bos, J.L., Toksoz, D., Marshall, C.J., Verlaan-de Vries, M., Veeneman, G.H., van der Eb, A.J., van Boom, J.H., Janssen, J.W.G., and Steenvoorden, A.C.M. (1985). Amino-acid substitutions at codon 13 of the N-ras oncogene in human acute myeloid leukaemia. Nature *315*, 726-730.

Bowtell, D., Fu, P., Simon, M., and Senior, P. (1992). Identification of murine homologues of the Drosophila son of sevenless gene: potential activators of ras. Proceedings of the National Academy of Sciences of the United States of America *89*, 6511-6515.

Brose, M.S., Volpe, P., Feldman, M., Kumar, M., Rishi, I., Gerrero, R., Einhorn, E., Herlyn, M., Minna, J., Nicholson, A.*, et al.* (2002). BRAF and RAS mutations in human lung cancer and melanoma. Cancer research *62*, 6997-7000.

Buday, L., and Downward, J. (1993). Epidermal growth factor regulates p21ras through the formation of a complex of receptor, Grb2 adapter protein, and Sos nucleotide exchange factor. Cell *73*, 611-620.

Buettner, R., Wolf, J., and Thomas, R.K. (2013). Lessons learned from lung cancer genomics: the emerging concept of individualized diagnostics and treatment. Journal of clinical oncology : official journal of the American Society of Clinical Oncology *31*, 1858-1865.

Campisi, J., and d'Adda di Fagagna, F. (2007). Cellular senescence: when bad things happen to good cells. Nature reviews Molecular cell biology *8*, 729-740.

Catalogue of Somatic Mutations in Cancer (COSMIC) of the Welcome Trust Sanger Institute, Cambridge, UK. http://cancer.sanger.ac.uk/cancergenome/projects/cosmic, accessed September, 2014

Certo, M., Del Gaizo Moore, V., Nishino, M., Wei, G., Korsmeyer, S., Armstrong, S.A., and Letai, A. (2006). Mitochondria primed by death signals determine cellular addiction to antiapoptotic BCL-2 family members. Cancer cell *9*, 351-365.

Chang, F., Steelman, L.S., Lee, J.T., Shelton, J.G., Navolanic, P.M., Blalock, W.L., Franklin, R.A., and McCubrey, J.A. (2003). Signal transduction mediated by the Ras/Raf/MEK/ERK pathway from cytokine receptors to transcription factors: potential targeting for therapeutic intervention. Leukemia *17*, 1263-1293.

Chao, J.R., Wang, J.M., Lee, S.F., Peng, H.W., Lin, Y.H., Chou, C.H., Li, J.C., Huang, H.M., Chou, C.K., Kuo, M.L.*, et al.* (1998). mcl-1 is an immediate-early gene activated by the granulocyte-macrophage colony-stimulating factor (GM-CSF) signaling pathway and is one component of the GM-CSF viability response. Molecular and cellular biology *18*, 4883-4898.

Chen, L., Willis, S.N., Wei, A., Smith, B.J., Fletcher, J.I., Hinds, M.G., Colman, P.M., Day, C.L., Adams, J.M., and Huang, D.C. (2005). Differential targeting of prosurvival Bcl-2 proteins by their BH3-only ligands allows complementary apoptotic function. Molecular cell *17*, 393-403.

Chen, Z., Sasaki, T., Tan, X., Carretero, J., Shimamura, T., Li, D., Xu, C., Wang, Y., Adelmant, G.O., Capelletti, M.*, et al.* (2010). Inhibition of ALK, PI3K/MEK, and HSP90 in murine lung adenocarcinoma induced by EML4-ALK fusion oncogene. Cancer research *70*, 9827-9836.

Chien, Y., and White, M.A. (2003). RAL GTPases are linchpin modulators of human tumour-cell proliferation and survival. EMBO reports *4*, 800-806.

Chittenden, T., Flemington, C., Houghton, A.B., Ebb, R.G., Gallo, G.J., Elangovan, B., Chinnadurai, G., and Lutz, R.J. (1995). A conserved domain in Bak, distinct from BH1 and BH2, mediates cell death and protein binding functions. The EMBO journal *14*, 5589-5596.

Clohessy, J.G., Zhuang, J., and Brady, H.J. (2004). Characterisation of Mcl-1 cleavage during apoptosis of haematopoietic cells. British journal of haematology *125*, 655-665.

Cooper, C.S., Park, M., Blair, D.G., Tainsky, M.A., Huebner, K., Croce, C.M., and Vande Woude, G.F. (1984). Molecular cloning of a new transforming gene from a chemically transformed human cell line. Nature *311*, 29-33.

Corcoran, R.B., Cheng, K.A., Hata, A.N., Faber, A.C., Ebi, H., Coffee, E.M., Greninger, P., Brown, R.D., Godfrey, J.T., Cohoon, T.J.*, et al.* (2013). Synthetic lethal interaction of combined BCL-XL and MEK inhibition promotes tumor regressions in KRAS mutant cancer models. Cancer cell *23*, 121-128.

Cory, S., Huang, D.C., and Adams, J.M. (2003). The Bcl-2 family: roles in cell survival and oncogenesis. Oncogene *22*, 8590-8607.

Coulthard, L.R., White, D.E., Jones, D.L., McDermott, M.F., and Burchill, S.A. (2009). p38(MAPK): stress responses from molecular mechanisms to therapeutics. Trends in molecular medicine *15*, 369-379.

Crawford, M., Batte, K., Yu, L., Wu, X., Nuovo, G.J., Marsh, C.B., Otterson, G.A., and Nana-Sinkam, S.P. (2009). MicroRNA 133B targets pro-survival molecules MCL-1 and BCL2L2 in lung cancer. Biochemical and biophysical research communications *388*, 483-489.

Croxton, R., Ma, Y., Song, L., Haura, E.B., and Cress, W.D. (2002). Direct repression of the Mcl-1 promoter by E2F1. Oncogene *21*, 1359-1369.

Czabotar, P.E., Lee, E.F., van Delft, M.F., Day, C.L., Smith, B.J., Huang, D.C., Fairlie, W.D., Hinds, M.G., and Colman, P.M. (2007). Structural insights into the degradation of Mcl-1 induced by BH3 domains. Proceedings of the National Academy of Sciences of the United States of America *104*, 6217-6222.

Czabotar, P.E., Lessene, G., Strasser, A., and Adams, J.M. (2014). Control of apoptosis by the BCL-2 protein family: implications for physiology and therapy. Nature reviews Molecular cell biology *15*, 49-63.

Dang, T.P., Gazdar, A.F., Virmani, A.K., Sepetavec, T., Hande, K.R., Minna, J.D., Roberts, J.R., and Carbone, D.P. (2000). Chromosome 19 Translocation, Overexpression of Notch3, and Human Lung Cancer. Journal of the National Cancer Institute *92*, 1355-1357.

Dasari, S., and Bernard Tchounwou, P. (2014). Cisplatin in cancer therapy: Molecular mechanisms of action. European Journal of Pharmacology *740*, 364-378.

Datta, S.R., Dudek, H., Tao, X., Masters, S., Fu, H., Gotoh, Y., and Greenberg, M.E. (1997). Akt phosphorylation of BAD couples survival signals to the cell-intrinsic death machinery. Cell *91*, 231-241.

Davies, H., Bignell, G.R., Cox, C., Stephens, P., Edkins, S., Clegg, S., Teague, J., Woffendin, H., Garnett, M.J., Bottomley, W.*, et al.* (2002). Mutations of the BRAF gene in human cancer. Nature *417*, 949-954.

De Biasio, A., Vrana, J.A., Zhou, P., Qian, L., Bieszczad, C.K., Braley, K.E., Domina, A.M., Weintraub, S.J., Neveu, J.M., Lane, W.S.*, et al.* (2007). N-terminal truncation of antiapoptotic MCL1, but not G2/M-induced phosphorylation, is associated with stabilization and abundant expression in tumor cells. The Journal of biological chemistry *282*, 23919-23936.

de Castro Carpeño, J., and Belda-Iniesta, C. (2013). KRAS mutant NSCLC, a new opportunity for the synthetic lethality therapeutic approach. Translational Lung Cancer Research *2*, 142-151.

DeGregori, J. (2006). Surprising dependency for retinoblastoma protein in ras-mediated tumorigenesis. Molecular and cellular biology *26*, 1165-1169.

del Peso, L., Gonzalez-Garcia, M., Page, C., Herrera, R., and Nunez, G. (1997). Interleukin-3-induced phosphorylation of BAD through the protein kinase Akt. Science (New York, NY) *278*, 687-689.

Detterbeck, F.C., Boffa, D.J., and Tanoue, L.T. (2009). The new lung cancer staging system. Chest *136*, 260-271.

Devereux, T.R., and Kaplan, N.L. (1998). Use of quantitative trait loci to map murine lung tumor susceptibility genes. Experimental lung research *24*, 407-417.

Dewson, G., Kratina, T., Sim, H.W., Puthalakath, H., Adams, J.M., Colman, P.M., and Kluck, R.M. (2008). To trigger apoptosis, Bak exposes its BH3 domain and homodimerizes via BH3:groove interactions. Molecular cell *30*, 369-380.

Dewson, G., Ma, S., Frederick, P., Hockings, C., Tan, I., Kratina, T., and Kluck, R.M. (2012). Bax dimerizes via a symmetric BH3:groove interface during apoptosis. Cell death and differentiation *19*, 661-670.

Ding, Q., He, X., Hsu, J.M., Xia, W., Chen, C.T., Li, L.Y., Lee, D.F., Liu, J.C., Zhong, Q., Wang, X.*, et al.* (2007a). Degradation of Mcl-1 by beta-TrCP mediates glycogen synthase kinase 3-induced tumor suppression and chemosensitization. Molecular and cellular biology *27*, 4006-4017.

Ding, Q., He, X., Xia, W., Hsu, J.M., Chen, C.T., Li, L.Y., Lee, D.F., Yang, J.Y., Xie, X., Liu, J.C.*, et al.* (2007b). Myeloid cell leukemia-1 inversely correlates with glycogen synthase kinase-3beta activity and associates with poor prognosis in human breast cancer. Cancer research *67*, 4564-4571.

Ding, Q., Huo, L., Yang, J.Y., Xia, W., Wei, Y., Liao, Y., Chang, C.J., Yang, Y., Lai, C.C., Lee, D.F.*, et al.* (2008). Down-regulation of myeloid cell leukemia-1 through inhibiting Erk/Pin 1 pathway by sorafenib facilitates chemosensitization in breast cancer. Cancer research *68*, 6109-6117.

Domina, A.M., Vrana, J.A., Gregory, M.A., Hann, S.R., and Craig, R.W. (2004). MCL1 is phosphorylated in the PEST region and stabilized upon ERK activation in viable cells, and at additional sites with cytotoxic okadaic acid or taxol. Oncogene *23*, 5301-5315.

Dosaka-Akita, H., Cagle, P.T., Hiroumi, H., Fujita, M., Yamashita, M., Sharma, A., Kawakami, Y., and Benedict, W.F. (2000). Differential retinoblastoma and p16INK4A protein expression in neuroendocrine tumors of the lung. Cancer *88*, 550-556.

Downward, J., Riehl, R., Wu, L., and Weinberg, R.A. (1990). Identification of a nucleotide exchange-promoting activity for p21ras. Proceedings of the National Academy of Sciences of the United States of America *87*, 5998-6002.

Engelman, J.A., Chen, L., Tan, X., Crosby, K., Guimaraes, A.R., Upadhyay, R., Maira, M., McNamara, K., Perera, S.A., Song, Y.*, et al.* (2008). Effective use of PI3K and MEK inhibitors to treat mutant Kras G12D and PIK3CA H1047R murine lung cancers. Nature medicine *14*, 1351-1356.

Evans, T.L. (2001). Lung Cancer. The Oncologist *6*, 407-414.

Farago, A.F., Snyder, E.L., and Jacks, T. (2012). SnapShot: Lung cancer models. Cell *149*, 246-246 e241.

Fasbender, A., Lee, J.H., Walters, R.W., Moninger, T.O., Zabner, J., and Welsh, M.J. (1998). Incorporation of adenovirus in calcium phosphate precipitates enhances gene transfer to airway epithelia in vitro and in vivo. The Journal of clinical investigation *102*, 184-193.

Festing, M.F., Lin, L., Devereux, T.R., Gao, F., Yang, A., Anna, C.H., White, C.M., Malkinson, A.M., and You, M. (1998). At least four loci and gender are associated with susceptibility to the chemical induction of lung adenomas in A/J x BALB/c mice. Genomics *53*, 129-136.

Festing, M.F., Yang, A., and Malkinson, A.M. (1994). At least four genes and sex are associated with susceptibility to urethane-induced pulmonary adenomas in mice. Genetical research *64*, 99-106.

Finco, T.S., Westwick, J.K., Norris, J.L., Beg, A.A., Der, C.J., and Baldwin, A.S., Jr. (1997). Oncogenic Ha-Ras-induced signaling activates NF-kappaB transcriptional activity, which is required for cellular transformation. The Journal of biological chemistry *272*, 24113-24116.

Fletcher, J.I., Meusburger, S., Hawkins, C.J., Riglar, D.T., Lee, E.F., Fairlie, W.D., Huang, D.C.S., and Adams, J.M. (2008). Apoptosis is triggered when prosurvival Bcl-2 proteins cannot restrain Bax. Proceedings of the National Academy of Sciences.

Fong, K.M., Sekido, Y., Gazdar, A.F., and Minna, J.D. (2003). Lung cancer. 9: Molecular biology of lung cancer: clinical implications. Thorax *58*, 892-900.

Franke, T.F., Kaplan, D.R., Cantley, L.C., and Toker, A. (1997). Direct regulation of the Akt proto-oncogene product by phosphatidylinositol-3,4-bisphosphate. Science (New York, NY) *275*, 665-668.

Friberg, A., Vigil, D., Zhao, B., Daniels, R.N., Burke, J.P., Garcia-Barrantes, P.M., Camper, D., Chauder, B.A., Lee, T., Olejniczak, E.T.*, et al.* (2013). Discovery of potent myeloid cell leukemia 1 (Mcl-1) inhibitors using fragment-based methods and structure-based design. Journal of medicinal chemistry *56*, 15-30.

Fujise, K., Zhang, D., Liu, J., and Yeh, E.T. (2000). Regulation of apoptosis and cell cycle progression by MCL1. Differential role of proliferating cell nuclear antigen. The Journal of biological chemistry *275*, 39458-39465.

Fujita, J., Yoshida, O., Yuasa, Y., Rhim, J.S., Hatanaka, M., and Aaronson, S.A. (1984). Ha-ras oncogenes are activated by somatic alterations in human urinary tract tumours. Nature *309*, 464-466.

Galanski, M. (2006). Recent developments in the field of anticancer platinum complexes. Recent patents on anti-cancer drug discovery *1*, 285-295.

Gariboldi, M., Manenti, G., Canzian, F., Falvella, F.S., Radice, M.T., Pierotti, M.A., Della Porta, G., Binelli, G., and Dragani, T.A. (1993). A major susceptibility locus to murine lung carcinogenesis maps on chromosome 6. Nature genetics *3*, 132-136.

Gavathiotis, E., Suzuki, M., Davis, M.L., Pitter, K., Bird, G.H., Katz, S.G., Tu, H.C., Kim, H., Cheng, E.H., Tjandra, N.*, et al.* (2008). BAX activation is initiated at a novel interaction site. Nature *455*, 1076-1081.

Glaser, S.P., Lee, E.F., Trounson, E., Bouillet, P., Wei, A., Fairlie, W.D., Izon, D.J., Zuber, J., Rappaport, A.R., Herold, M.J.*, et al.* (2012). Anti-apoptotic Mcl-1 is essential for the development and sustained growth of acute myeloid leukemia. Genes & development *26*, 120-125.

Globalcan 2012, International Agency for Research on Cancer, World Health Organization http://globocan.iarc.fr/Pages/fact_sheets_cancer.aspx, accessed September, 2014

Gojo, I., Zhang, B., and Fenton, R.G. (2002). The cyclin-dependent kinase inhibitor flavopiridol induces apoptosis in multiple myeloma cells through transcriptional repression and down-regulation of Mcl-1. Clinical cancer research : an official journal of the American Association for Cancer Research *8*, 3527-3538.

Guerra, C., Mijimolle, N., Dhawahir, A., Dubus, P., Barradas, M., Serrano, M., Campuzano, V., and Barbacid, M. (2003). Tumor induction by an endogenous K-ras oncogene is highly dependent on cellular context. Cancer cell *4*, 111-120.

Hagemann, C., and Blank, J.L. (2001). The ups and downs of MEK kinase interactions. Cellular Signalling *13*, 863-875.

Han, J., Goldstein, L.A., Gastman, B.R., Froelich, C.J., Yin, X.M., and Rabinowich, H. (2004). Degradation of Mcl-1 by granzyme B: implications for Bim-mediated mitochondrial apoptotic events. The Journal of biological chemistry *279*, 22020-22029.

Hanahan, D., and Weinberg, R.A. (2011). Hallmarks of cancer: the next generation. Cell *144*, 646-674.

Heist, R.S., and Engelman, J.A. (2012). SnapShot: non-small cell lung cancer. Cancer cell *21*, 448 e442.

Hinds, M.G., Lackmann, M., Skea, G.L., Harrison, P.J., Huang, D.C.S., and Day, C.L. (2003). The structure of Bcl-w reveals a role for the C-terminal residues in modulating biological activity. The EMBO journal *22*, 1497-1507.

Hitomi, M., and Stacey, D.W. (1999). Cyclin D1 production in cycling cells depends on Ras in a cell-cycle-specific manner. Current Biology *9*, 1075-S1072.

Ho, V.M., Schaffer, B.E., Karnezis, A.N., Park, K.S., and Sage, J. (2009). The retinoblastoma gene Rb and its family member p130 suppress lung adenocarcinoma induced by oncogenic K-Ras. Oncogene *28*, 1393-1399.

Huang, C.R., and Yang-Yen, H.F. (2010). The fast-mobility isoform of mouse Mcl-1 is a mitochondrial matrix-localized protein with attenuated anti-apoptotic activity. FEBS letters *584*, 3323-3330.

Huang, D.C., and Strasser, A. (2000). BH3-Only proteins-essential initiators of apoptotic cell death. Cell *103*, 839-842.

Huang, H.M., Huang, C.J., and Yen, J.J. (2000). Mcl-1 is a common target of stem cell factor and interleukin-5 for apoptosis prevention activity via MEK/MAPK and PI-3K/Akt pathways. Blood *96*, 1764-1771.

Iglesias-Serret, D., Pique, M., Gil, J., Pons, G., and Lopez, J.M. (2003). Transcriptional and translational control of Mcl-1 during apoptosis. Archives of biochemistry and biophysics *417*, 141-152.

Ihrie, R.A., Reczek, E., Horner, J.S., Khachatrian, L., Sage, J., Jacks, T., and Attardi, L.D. (2003). Perp is a mediator of p53-dependent apoptosis in diverse cell types. Current biology : CB *13*, 1985-1990.

Inoshita, S., Takeda, K., Hatai, T., Terada, Y., Sano, M., Hata, J., Umezawa, A., and Ichijo, H. (2002). Phosphorylation and inactivation of myeloid cell leukemia 1 by JNK in response to oxidative stress. The Journal of biological chemistry *277*, 43730-43734.

Ischenko, I., Zhi, J., Moll, U.M., Nemajerova, A., and Petrenko, O. (2013). Direct reprogramming by oncogenic Ras and Myc. Proceedings of the National Academy of Sciences of the United States of America *110*, 3937-3942.

Iwakawa, R., Kohno, T., Kato, M., Shiraishi, K., Tsuta, K., Noguchi, M., Ogawa, S., and Yokota, J. (2011). MYC amplification as a prognostic marker of early-stage lung adenocarcinoma identified by whole genome copy number analysis. Clinical cancer research : an official journal of the American Association for Cancer Research *17*, 1481-1489.

Jackman, D., Pao, W., Riely, G.J., Engelman, J.A., Kris, M.G., Janne, P.A., Lynch, T., Johnson, B.E., and Miller, V.A. (2010). Clinical definition of acquired resistance to epidermal growth factor receptor tyrosine kinase inhibitors in non-small-cell lung cancer. Journal of clinical oncology : official journal of the American Society of Clinical Oncology *28*, 357-360.

Jackson, E.L., Olive, K.P., Tuveson, D.A., Bronson, R., Crowley, D., Brown, M., and Jacks, T. (2005). The differential effects of mutant p53 alleles on advanced murine lung cancer. Cancer research *65*, 10280-10288.

Jackson, E.L., Willis, N., Mercer, K., Bronson, R.T., Crowley, D., Montoya, R., Jacks, T., and Tuveson, D.A. (2001). Analysis of lung tumor initiation and progression using conditional expression of oncogenic K-ras. Genes & development *15*, 3243-3248.

Jamil, S., Sobouti, R., Hojabrpour, P., Raj, M., Kast, J., and Duronio, V. (2005). A proteolytic fragment of Mcl-1 exhibits nuclear localization and regulates cell growth by interaction with Cdk1. The Biochemical journal *387*, 659-667.

Janssen, J.W., Steenvoorden, A.C., Collard, J.G., and Nusse, R. (1985). Oncogene activation in human myeloid leukemia. Cancer research *45*, 3262-3267.

Ji, H., Ramsey, M.R., Hayes, D.N., Fan, C., McNamara, K., Kozlowski, P., Torrice, C., Wu, M.C., Shimamura, T., Perera, S.A.*, et al.* (2007). LKB1 modulates lung cancer differentiation and metastasis. Nature *448*, 807-810.

Johnson, J.L., Pillai, S., and Chellappan, S.P. (2012). Genetic and Biochemical Alterations in Non-Small Cell Lung Cancer. Biochemistry Research International *2012*, 18.

Johnson, L., Mercer, K., Greenbaum, D., Bronson, R.T., Crowley, D., Tuveson, D.A., and Jacks, T. (2001). Somatic activation of the K-ras oncogene causes early onset lung cancer in mice. Nature *410*, 1111-1116.

Jorda, M., Gomez-Fernandez, C., Garcia, M., Mousavi, F., Walker, G., Mejias, A., Fernandez-Castro, G., and Ganjei-Azar, P. (2009). P63 differentiates subtypes of nonsmall cell carcinomas of lung in cytologic samples: implications in treatment selection. Cancer *117*, 46-50.

Joseph, T., Bryant, A., Frankel, P., Wooden, R., Kerkhoff, E., Rapp, U.R., and Foster, D.A. (2002). Phospholipase D overcomes cell cycle arrest induced by high-intensity Raf signaling. Oncogene *21*, 3651-3658.

Kaiser, U., Schilli, M., Haag, U., Neumann, K., Kreipe, H., Kogan, E., and Havemann, K. (1996). Expression of bcl-2--protein in small cell lung cancer. Lung cancer (Amsterdam, Netherlands) *15*, 31-40.

Kaufmann, S.H., Karp, J.E., Svingen, P.A., Krajewski, S., Burke, P.J., Gore, S.D., and Reed, J.C. (1998). Elevated expression of the apoptotic regulator Mcl-1 at the time of leukemic relapse. Blood *91*, 991-1000.

Kawano, O., Sasaki, H., Endo, K., Suzuki, E., Haneda, H., Yukiue, H., Kobayashi, Y., Yano, M., and Fujii, Y. (2006). PIK3CA mutation status in Japanese lung cancer patients. Lung cancer (Amsterdam, Netherlands) *54*, 209-215.

Kelly, G.L., Grabow, S., Glaser, S.P., Fitzsimmons, L., Aubrey, B.J., Okamoto, T., Valente, L.J., Robati, M., Tai, L., Fairlie, W.D.*, et al.* (2014). Targeting of MCL-1 kills MYC-driven mouse and human lymphomas even when they bear mutations in p53. Genes & development *28*, 58-70.

Kelly, P.N., and Strasser, A. (2011). The role of Bcl-2 and its pro-survival relatives in tumourigenesis and cancer therapy. Cell death and differentiation *18*, 1414-1424.

Keohavong, P., DeMichele, M.A., Melacrinos, A.C., Landreneau, R.J., Weyant, R.J., and Siegfried, J.M. (1996). Detection of K-ras mutations in lung carcinomas: relationship to prognosis. Clinical cancer research : an official journal of the American Association for Cancer Research *2*, 411-418.

Khwaja, A., Rodriguez-Viciana, P., Wennstrom, S., Warne, P.H., and Downward, J. (1997). Matrix adhesion and Ras transformation both activate a phosphoinositide 3-OH kinase and protein kinase B/Akt cellular survival pathway. The EMBO journal *16*, 2783-2793.

Kim, J.H., and Bae, J. (2013). MCL-1ES induces MCL-1L-dependent BAX- and BAK-independent mitochondrial apoptosis. PloS one *8*, e79626.

Kim, J.H., Sim, S.H., Ha, H.J., Ko, J.J., Lee, K., and Bae, J. (2009). MCL-1ES, a novel variant of MCL-1, associates with MCL-1L and induces mitochondrial cell death. FEBS letters *583*, 2758-2764.

Kiuchi, N., Nakajima, K., Ichiba, M., Fukada, T., Narimatsu, M., Mizuno, K., Hibi, M., and Hirano, T. (1999). STAT3 is required for the gp130-mediated full activation of the c-myc gene. The Journal of experimental medicine *189*, 63-73.

Kluck, R.M., Bossy-Wetzel, E., Green, D.R., and Newmeyer, D.D. (1997). The release of cytochrome c from mitochondria: a primary site for Bcl-2 regulation of apoptosis. Science (New York, NY) *275*, 1132-1136.

Kobayashi, S., Lee, S.H., Meng, X.W., Mott, J.L., Bronk, S.F., Werneburg, N.W., Craig, R.W., Kaufmann, S.H., and Gores, G.J. (2007). Serine 64 phosphorylation enhances the antiapoptotic function of Mcl-1. The Journal of biological chemistry *282*, 18407-18417.

Kodama, Y., Taura, K., Miura, K., Schnabl, B., Osawa, Y., and Brenner, D.A. (2009). Antiapoptotic effect of c-Jun N-terminal Kinase-1 through Mcl-1 stabilization in TNF-induced hepatocyte apoptosis. Gastroenterology *136*, 1423-1434.

Kong-Beltran, M., Seshagiri, S., Zha, J., Zhu, W., Bhawe, K., Mendoza, N., Holcomb, T., Pujara, K., Stinson, J., Fu, L.*, et al.* (2006). Somatic mutations lead to an oncogenic deletion of met in lung cancer. Cancer research *66*, 283-289.

Konishi, J., Kawaguchi, K.S., Vo, H., Haruki, N., Gonzalez, A., Carbone, D.P., and Dang, T.P. (2007). γ-Secretase Inhibitor Prevents Notch3 Activation and Reduces Proliferation in Human Lung Cancers. Cancer research *67*, 8051-8057.

Konopleva, M., Contractor, R., Tsao, T., Samudio, I., Ruvolo, P.P., Kitada, S., Deng, X., Zhai, D., Shi, Y.X., Sneed, T.*, et al.* (2006). Mechanisms of apoptosis sensitivity and resistance to the BH3 mimetic ABT-737 in acute myeloid leukemia. Cancer cell *10*, 375-388.

Koukourakis, M.I., Giatromanolaki, A., O'Byrne, K.J., Comley, M., Whitehouse, R.M., Talbot, D.C., Gatter, K.C., and Harris, A.L. (1997). Platelet-derived endothelial cell growth factor expression correlates with tumour angiogenesis and prognosis in non-small-cell lung cancer. British journal of cancer *75*, 477-481.

Kozopas, K.M., Yang, T., Buchan, H.L., Zhou, P., and Craig, R.W. (1993). MCL1, a gene expressed in programmed myeloid cell differentiation, has sequence similarity to BCL2. Proceedings of the National Academy of Sciences of the United States of America *90*, 3516-3520.

Kuwana, T., Bouchier-Hayes, L., Chipuk, J.E., Bonzon, C., Sullivan, B.A., Green, D.R., and Newmeyer, D.D. (2005). BH3 domains of BH3-only proteins differentially regulate Bax-mediated mitochondrial membrane permeabilization both directly and indirectly. Molecular cell *17*, 525-535.

Kvansakul, M., Yang, H., Fairlie, W.D., Czabotar, P.E., Fischer, S.F., Perugini, M.A., Huang, D.C., and Colman, P.M. (2008). Vaccinia virus anti-apoptotic F1L is a novel Bcl-2-like domain-swapped dimer that binds a highly selective subset of BH3-containing death ligands. Cell death and differentiation *15*, 1564-1571.

Kwon, M.C., and Berns, A. (2013). Mouse models for lung cancer. Molecular oncology *7*, 165-177.

Kyriakis, J.M., and Avruch, J. (1996). Protein kinase cascades activated by stress and inflammatory cytokines. BioEssays : news and reviews in molecular, cellular and developmental biology *18*, 567-577.

Lambert, J.M., Lambert, Q.T., Reuther, G.W., Malliri, A., Siderovski, D.P., Sondek, J., Collard, J.G., and Der, C.J. (2002). Tiam1 mediates Ras activation of Rac by a PI(3)K-independent mechanism. Nature cell biology *4*, 621-625.

Le Gouill, S., Podar, K., Amiot, M., Hideshima, T., Chauhan, D., Ishitsuka, K., Kumar, S., Raje, N., Richardson, P.G., Harousseau, J.-L.*, et al.* (2004). VEGF induces Mcl-1 up-regulation and protects multiple myeloma cells against apoptosis, Vol 104.

Lee, E.F., Czabotar, P.E., van Delft, M.F., Michalak, E.M., Boyle, M.J., Willis, S.N., Puthalakath, H., Bouillet, P., Colman, P.M., Huang, D.C*., et al.* (2008). A novel BH3 ligand that selectively targets Mcl-1 reveals that apoptosis can proceed without Mcl-1 degradation. The Journal of cell biology *180*, 341-355.

Lee, Y.K., Shanafelt, T.D., Bone, N.D., Strege, A.K., Jelinek, D.F., and Kay, N.E. (2005). VEGF receptors on chronic lymphocytic leukemia (CLL) B cells interact with STAT 1 and 3: implication for apoptosis resistance. Leukemia *19*, 513-523.

Leon, J., Guerrero, I., and Pellicer, A. (1987). Differential expression of the ras gene family in mice. Molecular and cellular biology *7*, 1535-1540.

Letai, A., Bassik, M.C., Walensky, L.D., Sorcinelli, M.D., Weiler, S., and Korsmeyer, S.J. (2002). Distinct BH3 domains either sensitize or activate mitochondrial apoptosis, serving as prototype cancer therapeutics. Cancer cell *2*, 183-192.

Leu, C.M., Chang, C., and Hu, C. (2000). Epidermal growth factor (EGF) suppresses staurosporine-induced apoptosis by inducing mcl-1 via the mitogen-activated protein kinase pathway. Oncogene *19*, 1665-1675.

Li, H., Cho, S.N., Evans, C.M., Dickey, B.F., Jeong, J.W., and DeMayo, F.J. (2008). Cre-mediated recombination in mouse Clara cells. Genesis (New York, NY : 2000) *46*, 300-307.

Li, H., Zhu, H., Xu, C.J., and Yuan, J. (1998). Cleavage of BID by caspase 8 mediates the mitochondrial damage in the Fas pathway of apoptosis. Cell *94*, 491-501.

Li, P., Nijhawan, D., Budihardjo, I., Srinivasula, S.M., Ahmad, M., Alnemri, E.S., and Wang, X. (1997). Cytochrome c and dATP-dependent formation of Apaf-1/caspase-9 complex initiates an apoptotic protease cascade. Cell *91*, 479-489.

Li, Z., Graf, N., Herrmann, K., Junger, A., Aichler, M., Feuchtinger, A., Baumgart, A., Walch, A., Peschel, C., Schwaiger, M*., et al.* (2012). FLT-PET Is Superior to FDG-PET for Very Early Response Prediction in NPM-ALK-Positive Lymphoma Treated with Targeted Therapy. Cancer research *72*, 5014-5024.

Lin, L., Festing, M.F., Devereux, T.R., Crist, K.A., Christiansen, S.C., Wang, Y., Yang, A., Svenson, K., Paigen, B., Malkinson, A.M*., et al.* (1998). Additional evidence that the K-ras protooncogene is a candidate for the major mouse pulmonary adenoma susceptibility (Pas-1) gene. Experimental lung research *24*, 481-497.

Liu, H., Ma, Y., Cole, S.M., Zander, C., Chen, K.-H., Karras, J., and Pope, R.M. (2003). Serine phosphorylation of STAT3 is essential for Mcl-1 expression and macrophage survival, Vol 102.

Liu, X.H., Yu, E.Z., Li, Y.Y., and Kagan, E. (2006). HIF-1alpha has an anti-apoptotic effect in human airway epithelium that is mediated via Mcl-1 gene expression. Journal of cellular biochemistry *97*, 755-765.

Luciano, F., Jacquel, A., Colosetti, P., Herrant, M., Cagnol, S., Pages, G., and Auberger, P. (2003). Phosphorylation of Bim-EL by Erk1/2 on serine 69 promotes its degradation via the proteasome pathway and regulates its proapoptotic function. Oncogene *22*, 6785-6793.

Luo, L., Zhang, T., Liu, H., Lv, T., Yuan, D., Yao, Y., Lv, Y., and Song, Y. (2012). MiR-101 and Mcl-1 in non-small-cell lung cancer: expression profile and clinical significance. Medical oncology *29*, 1681-1686.

Luo, X., Budihardjo, I., Zou, H., Slaughter, C., and Wang, X. (1998). Bid, a Bcl2 Interacting Protein, Mediates Cytochrome c Release from Mitochondria in Response to Activation of Cell Surface Death Receptors. Cell *94*, 481-490.

Lynch, T.J., Bell, D.W., Sordella, R., Gurubhagavatula, S., Okimoto, R.A., Brannigan, B.W., Harris, P.L., Haserlat, S.M., Supko, J.G., Haluska, F.G*., et al.* (2004). Activating mutations in the epidermal growth factor receptor underlying responsiveness of non-small-cell lung cancer to gefitinib. The New England journal of medicine *350*, 2129-2139.

Malkinson, A.M. (1989). The genetic basis of susceptibility to lung tumors in mice. Toxicology *54*, 241-271.

Malkinson, A.M. (1999). Inheritance of pulmonary adenoma susceptibility in mice. Progress in experimental tumor research *35*, 78-94.

Malkinson, A.M., Nesbitt, M.N., and Skamene, E. (1985). Susceptibility to urethan-induced pulmonary adenomas between A/J and C57BL/6J mice: use of AXB and BXA recombinant inbred lines indicating a three-locus genetic model. Journal of the National Cancer Institute *75*, 971-974.

Malumbres, M., Hunt, S.L., Sotillo, R., Martin, J., Odajima, J., Martin, A., Dubus, P., Ortega, S., and Barbacid, M. (2003). Driving the cell cycle to cancer. Advances in experimental medicine and biology *532*, 1-11.

Marcu, L.G., and Bezak, E. (2012). Neoadjuvant cisplatin for head and neck cancer: Simulation of a novel schedule for improved therapeutic ratio. Journal of Theoretical Biology *297*, 41-47.

Marte, B.M., and Downward, J. (1997). PKB/Akt: connecting phosphoinositide 3-kinase to cell survival and beyond. Trends Biochem Sci *22*, 355-358.

Martin, G.A., Viskochil, D., Bollag, G., McCabe, P.C., Crosier, W.J., Haubruck, H., Conroy, L., Clark, R., O'Connell, P., Cawthon, R.M.*, et al.* (1990). The GAP-related domain of the neurofibromatosis type 1 gene product interacts with ras p21. Cell *63*, 843-849.

Masuya, D., Huang, C., Liu, D., Kameyama, K., Hayashi, E., Yamauchi, A., Kobayashi, S., Haba, R., and Yokomise, H. (2001). The intratumoral expression of vascular endothelial growth factor and interleukin-8 associated with angiogenesis in nonsmall cell lung carcinoma patients. Cancer *92*, 2628-2638.

Maurer, U., Charvet, C., Wagman, A.S., Dejardin, E., and Green, D.R. (2006). Glycogen synthase kinase-3 regulates mitochondrial outer membrane permeabilization and apoptosis by destabilization of MCL-1. Mol Cell *21*, 749-760.

Mayo, M.W., and Baldwin, A.S. (2000). The transcription factor NF-kappaB: control of oncogenesis and cancer therapy resistance. Biochimica et biophysica acta *1470*, M55-62.

Metscher, B.D. (2009). MicroCT for comparative morphology: simple staining methods allow high-contrast 3D imaging of diverse non-mineralized animal tissues. BMC physiology *9*, 11.

Meuwissen, R., and Berns, A. (2005). Mouse models for human lung cancer. Genes & development *19*, 643-664.

Meuwissen, R., Linn, S.C., Linnoila, R.I., Zevenhoven, J., Mooi, W.J., and Berns, A. (2003). Induction of small cell lung cancer by somatic inactivation of both Trp53 and Rb1 in a conditional mouse model. Cancer cell *4*, 181-189.

Meuwissen, R., Linn, S.C., van der Valk, M., Mooi, W.J., and Berns, A. (2001). Mouse model for lung tumorigenesis through Cre/lox controlled sporadic activation of the K-Ras oncogene. Oncogene *20*, 6551-6558.

Michels, J., Obrist, F., Vitale, I., Lissa, D., Garcia, P., Behnam-Motlagh, P., Kohno, K., Wu, G.S., Brenner, C., Castedo, M.*, et al.* (2014). MCL-1 dependency of cisplatin-resistant cancer cells. Biochemical pharmacology.

Minna, J.D., Roth, J.A., and Gazdar, A.F. (2002). Focus on lung cancer. Cancer cell *1*, 49-52.

Mirsadraee, S., Oswal, D., Alizadeh, Y., Caulo, A., and van Beek, E., Jr. (2012). The 7th lung cancer TNM classification and staging system: Review of the changes and implications. World journal of radiology *4*, 128-134.

Moll, U.M., and Petrenko, O. (2003). The MDM2-p53 interaction. Molecular cancer research : MCR *1*, 1001-1008.

Moodie, S.A., Willumsen, B.M., Weber, M.J., and Wolfman, A. (1993). Complexes of Ras.GTP with Raf-1 and mitogen-activated protein kinase kinase. Science (New York, NY) *260*, 1658-1661.

Morel, C., Carlson, S.M., White, F.M., and Davis, R.J. (2009). Mcl-1 integrates the opposing actions of signaling pathways that mediate survival and apoptosis. Molecular and cellular biology *29*, 3845-3852.

Moskalenko, S., Henry, D.O., Rosse, C., Mirey, G., Camonis, J.H., and White, M.A. (2002). The exocyst is a Ral effector complex. Nature cell biology *4*, 66-72.

Motoyama, N., Wang, F., Roth, K.A., Sawa, H., Nakayama, K., Nakayama, K., Negishi, I., Senju, S., Zhang, Q., Fujii, S.*, et al.* (1995). Massive cell death of immature hematopoietic cells and neurons in Bcl-x-deficient mice. Science (New York, NY) *267*, 1506-1510.

Mott, J.L., Kobayashi, S., Bronk, S.F., and Gores, G.J. (2007). mir-29 regulates Mcl-1 protein expression and apoptosis. Oncogene *26*, 6133-6140.

Moulding, D.A., Akgul, C., Derouet, M., White, M.R., and Edwards, S.W. (2001). BCL-2 family expression in human neutrophils during delayed and accelerated apoptosis. Journal of leukocyte biology *70*, 783-792.

Muchmore, S.W., Sattler, M., Liang, H., Meadows, R.P., Harlan, J.E., Yoon, H.S., Nettesheim, D., Chang, B.S., Thompson, C.B., Wong, S.L.*, et al.* (1996). X-ray and NMR structure of human Bcl-xL, an inhibitor of programmed cell death. Nature *381*, 335-341.

National Cancer Institute: PDQ® Non-Small Cell Lung Cancer Treatment. Bethesda, MD: National Cancer Institute. Date last modified 08/06/2014. http://www.cancer.gov/cancertopics/pdq/treatment/non-small-cell-lung/healthprofessional, accessed October, 2014

National Cancer Institute: PDQ® Small Cell Lung Cancer Treatment. Bethesda, MD: National Cancer Institute. Date last modified 08/06/2014. t:http://www.cancer.gov/cancertopics/pdq/treatment/small-cell-lung/healthprofessional, accessed October, 2014

Nettesheim, P., and Hammons, A.S. (1971). Induction of squamous cell carcinoma in the respiratory tract of mice. Journal of the National Cancer Institute *47*, 697-701.

Nguyen, M., Marcellus, R.C., Roulston, A., Watson, M., Serfass, L., Murthy Madiraju, S.R., Goulet, D., Viallet, J., Bélec, L., Billot, X.*, et al.* (2007). Small molecule obatoclax (GX15-070) antagonizes MCL-1 and overcomes MCL-1-mediated resistance to apoptosis. Proceedings of the National Academy of Sciences *104*, 19512-19517.

Nikitin, A.Y., Alcaraz, A., Anver, M.R., Bronson, R.T., Cardiff, R.D., Dixon, D., Fraire, A.E., Gabrielson, E.W., Gunning, W.T., Haines, D.C.*, et al.* (2004). Classification of proliferative pulmonary lesions of the mouse: recommendations of the mouse models of human cancers consortium. Cancer research *64*, 2307-2316.

O'Byrne, K.J., Koukourakis, M.I., Giatromanolaki, A., Cox, G., Turley, H., Steward, W.P., Gatter, K., and Harris, A.L. (2000). Vascular endothelial growth factor, platelet-derived endothelial cell growth factor and angiogenesis in non-small-cell lung cancer. British journal of cancer *82*, 1427-1432.

Obata, M., Nishimori, H., Ogawa, K., and Lee, G.H. (1996). Identification of the Par2 (Pulmonary adenoma resistance) locus on mouse chromosome 18, a major genetic determinant for lung carcinogen resistance in BALB/cByJ mice. Oncogene *13*, 1599-1604.

Oliver, T.G., Mercer, K.L., Sayles, L.C., Burke, J.R., Mendus, D., Lovejoy, K.S., Cheng, M.H., Subramanian, A., Mu, D., Powers, S.*, et al.* (2010). Chronic cisplatin treatment promotes enhanced damage repair and tumor progression in a mouse model of lung cancer. Genes & development *24*, 837-852.

Oltersdorf, T., Elmore, S.W., Shoemaker, A.R., Armstrong, R.C., Augeri, D.J., Belli, B.A., Bruncko, M., Deckwerth, T.L., Dinges, J., Hajduk, P.J.*, et al.* (2005). An inhibitor of Bcl-2 family proteins induces regression of solid tumours. Nature *435*, 677-681.

Oltvai, Z.N., Milliman, C.L., and Korsmeyer, S.J. (1993). Bcl-2 heterodimerizes in vivo with a conserved homolog, Bax, that accelerates programmed cell death. Cell *74*, 609-619.

Opferman, J.T., Iwasaki, H., Ong, C.C., Suh, H., Mizuno, S., Akashi, K., and Korsmeyer, S.J. (2005). Obligate role of anti-apoptotic MCL-1 in the survival of hematopoietic stem cells. Science (New York, NY) *307*, 1101-1104.

Opferman, J.T., Letai, A., Beard, C., Sorcinelli, M.D., Ong, C.C., and Korsmeyer, S.J. (2003). Development and maintenance of B and T lymphocytes requires antiapoptotic MCL-1. Nature *426*, 671-676.

Padua, R.A., Barrass, N.C., and Currie, G.A. (1985). Activation of N-ras in a human melanoma cell line. Molecular and cellular biology *5*, 582-585.

Paik, P.K., Arcila, M.E., Fara, M., Sima, C.S., Miller, V.A., Kris, M.G., Ladanyi, M., and Riely, G.J. (2011). Clinical characteristics of patients with lung adenocarcinomas harboring BRAF mutations. Journal of clinical oncology : official journal of the American Society of Clinical Oncology *29*, 2046-2051.

Palve, V.C., and Teni, T.R. (2012). Association of anti-apoptotic Mcl-1L isoform expression with radioresistance of oral squamous carcinoma cells. Radiation oncology (London, England) *7*, 135.

Pegoraro, L., Palumbo, A., Erikson, J., Falda, M., Giovanazzo, B., Emanuel, B.S., Rovera, G., Nowell, P.C., and Croce, C.M. (1984). A 14;18 and an 8;14 chromosome translocation in a cell line derived from an acute B-cell leukemia. Proceedings of the National Academy of Sciences of the United States of America *81*, 7166-7170.

Pelengaris, S., Khan, M., and Evan, G. (2002). c-MYC: more than just a matter of life and death. Nature reviews Cancer *2*, 764-776.

Pepper, C., Lin, T.T., Pratt, G., Hewamana, S., Brennan, P., Hiller, L., Hills, R., Ward, R., Starczynski, J., Austen, B.*, et al.* (2008). Mcl-1 expression has in vitro and in vivo significance in chronic lymphocytic leukemia and is associated with other poor prognostic markers. Blood *112*, 3807-3817.

Perciavalle, R.M., and Opferman, J.T. (2013). Delving deeper: MCL-1's contributions to normal and cancer biology. Trends in cell biology *23*, 22-29.

Perciavalle, R.M., Stewart, D.P., Koss, B., Lynch, J., Milasta, S., Bathina, M., Temirov, J., Cleland, M.M., Pelletier, S., Schuetz, J.D.*, et al.* (2012). Anti-apoptotic MCL-1 localizes to the mitochondrial matrix and couples mitochondrial fusion to respiration. Nature cell biology *14*, 575-583.

Petros, A.M., Medek, A., Nettesheim, D.G., Kim, D.H., Yoon, H.S., Swift, K., Matayoshi, E.D., Oltersdorf, T., and Fesik, S.W. (2001). Solution structure of the antiapoptotic protein bcl-2. Proceedings of the National Academy of Sciences of the United States of America *98*, 3012-3017.

Pezzella, F., Turley, H., Kuzu, I., Tungekar, M.F., Dunnill, M.S., Pierce, C.B., Harris, A., Gatter, K.C., and Mason, D.Y. (1993). bcl-2 Protein in Non-Small-Cell Lung Carcinoma. New England Journal of Medicine *329*, 690-694.

Politi, K., Zakowski, M.F., Fan, P.D., Schonfeld, E.A., Pao, W., and Varmus, H.E. (2006). Lung adenocarcinomas induced in mice by mutant EGF receptors found in human lung cancers respond to a tyrosine kinase inhibitor or to down-regulation of the receptors. Genes & development *20*, 1496-1510.

Prager, G.W., Poettler, M., Unseld, M., and Zielinski, C.C. (2011). Angiogenesis in cancer: anti-VEGF escape mechanisms. Translational Lung Cancer Research *1*, 14-25.

Puthier, D., Bataille, R., and Amiot, M. (1999). IL-6 up-regulates mcl-1 in human myeloma cells through JAK / STAT rather than ras / MAP kinase pathway. European journal of immunology *29*, 3945-3950.

Pylayeva-Gupta, Y., Grabocka, E., and Bar-Sagi, D. (2011). RAS oncogenes: weaving a tumorigenic web. Nature reviews Cancer *11*, 761-774.

Qiu, R.-G., Chen, J., Kirn, D., McCormick, F., and Symons, M. (1995). An essential role for Rac in Ras transformation. Nature *374*, 457-459.

Rahaman, S.O., Harbor, P.C., Chernova, O., Barnett, G.H., Vogelbaum, M.A., and Haque, S.J. (2002). Inhibition of constitutively active Stat3 suppresses proliferation and induces apoptosis in glioblastoma multiforme cells. Oncogene *21*, 8404-8413.

Rahmani, M., Davis, E.M., Bauer, C., Dent, P., and Grant, S. (2005). Apoptosis induced by the kinase inhibitor BAY 43-9006 in human leukemia cells involves down-regulation of Mcl-1 through inhibition of translation. The Journal of biological chemistry *280*, 35217-35227.

Regales, L., Balak, M.N., Gong, Y., Politi, K., Sawai, A., Le, C., Koutcher, J.A., Solit, D.B., Rosen, N., Zakowski, M.F*., et al.* (2007). Development of new mouse lung tumor models expressing EGFR T790M mutants associated with clinical resistance to kinase inhibitors. PloS one *2*, e810.

Rehm, S., Lijinsky, W., Singh, G., and Katyal, S.L. (1991). Mouse bronchiolar cell carcinogenesis. Histologic characterization and expression of Clara cell antigen in lesions induced by N-nitrosobis-(2-chloroethyl) ureas. The American journal of pathology *139*, 413-422.

Reissmann, P.T., Koga, H., Figlin, R.A., Holmes, E.C., and Slamon, D.J. (1999). Amplification and overexpression of the cyclin D1 and epidermal growth factor receptor genes in non-small-cell lung cancer. Lung Cancer Study Group. Journal of cancer research and clinical oncology *125*, 61-70.

Reissmann, P.T., Koga, H., Takahashi, R., Figlin, R.A., Holmes, E.C., Piantadosi, S., Cordon-Cardo, C., and Slamon, D.J. (1993). Inactivation of the retinoblastoma susceptibility gene in non-small-cell lung cancer. The Lung Cancer Study Group. Oncogene *8*, 1913-1919.

Rikova, K., Guo, A., Zeng, Q., Possemato, A., Yu, J., Haack, H., Nardone, J., Lee, K., Reeves, C., Li, Y*., et al.* (2007). Global Survey of Phosphotyrosine Signaling Identifies Oncogenic Kinases in Lung Cancer. Cell *131*, 1190-1203.

Rinkenberger, J.L., Horning, S., Klocke, B., Roth, K., and Korsmeyer, S.J. (2000). Mcl-1 deficiency results in peri-implantation embryonic lethality. Genes & development *14*, 23-27.

Rodenhuis, S., and Slebos, R.J. (1990). The ras oncogenes in human lung cancer. The American review of respiratory disease *142*, S27-30.

Rodenhuis, S., Slebos, R.J., Boot, A.J., Evers, S.G., Mooi, W.J., Wagenaar, S.S., van Bodegom, P.C., and Bos, J.L. (1988). Incidence and possible clinical significance of K-ras oncogene activation in adenocarcinoma of the human lung. Cancer research *48*, 5738-5741.

Rodriguez-Viciana, P., Warne, P.H., Dhand, R., Vanhaesebroeck, B., Gout, I., Fry, M.J., Waterfield, M.D., and Downward, J. (1994). Phosphatidylinositol-3-OH kinase as a direct target of Ras. Nature *370*, 527-532.

Rooswinkel, R.W., van de Kooij, B., Verheij, M., and Borst, J. (2012). Bcl-2 is a better ABT-737 target than Bcl-xL or Bcl-w and only Noxa overcomes resistance mediated by Mcl-1, Bfl-1, or Bcl-B. Cell death & disease *3*, e366.

Rosen, K., Rak, J., Jin, J., Kerbel, R.S., Newman, M.J., and Filmus, J. (1998). Downregulation of the pro-apoptotic protein Bak is required for the ras-induced transformation of intestinal epithelial cells. Current Biology *8*, S1.

Rudin, C.M., Durinck, S., Stawiski, E.W., Poirier, J.T., Modrusan, Z., Shames, D.S., Bergbower, E.A., Guan, Y., Shin, J., Guillory, J*., et al.* (2012). Comprehensive genomic analysis identifies SOX2 as a frequently amplified gene in small-cell lung cancer. Nature genetics *44*, 1111-1116.

Sameshima, Y., Matsuno, Y., Hirohashi, S., Shimosato, Y., Mizoguchi, H., Sugimura, T., Terada, M., and Yokota, J. (1992). Alterations of the p53 gene are common and critical events for the maintenance of malignant phenotypes in small-cell lung carcinoma. Oncogene *7*, 451-457.

Samuels, Y., Wang, Z., Bardelli, A., Silliman, N., Ptak, J., Szabo, S., Yan, H., Gazdar, A., Powell, S.M., Riggins, G.J*., et al.* (2004). High frequency of mutations of the PIK3CA gene in human cancers. Science (New York, NY) *304*, 554.

Schaffer, B.E., Park, K.S., Yiu, G., Conklin, J.F., Lin, C., Burkhart, D.L., Karnezis, A.N., Sweet-Cordero, E.A., and Sage, J. (2010). Loss of p130 accelerates tumor development in a mouse model for human small-cell lung carcinoma. Cancer research *70*, 3877-3883.

Scheffzek, K., Ahmadian, M.R., Kabsch, W., Wiesmuller, L., Lautwein, A., Schmitz, F., and Wittinghofer, A. (1997). The Ras-RasGAP complex: structural basis for GTPase activation and its loss in oncogenic Ras mutants. Science (New York, NY) *277*, 333-338.

Schiller, J.H. (2001). Current Standards of Care in Small-Cell and Non-Small-Cell Lung Cancer. Oncology *61(suppl 1)*, 3-13.

Scholzen, T., and Gerdes, J. (2000). The Ki-67 protein: From the known and the unknown. Journal of Cellular Physiology *182*, 311-322.

Schubbert, S., Shannon, K., and Bollag, G. (2007). Hyperactive Ras in developmental disorders and cancer. Nature reviews Cancer *7*, 295-308.

Schwickart, M., Huang, X., Lill, J.R., Liu, J., Ferrando, R., French, D.M., Maecker, H., O'Rourke, K., Bazan, F., Eastham-Anderson, J.*, et al.* (2010). Deubiquitinase USP9X stabilizes MCL1 and promotes tumour cell survival. Nature *463*, 103-107.

Seger, R., Ahn, N.G., Posada, J., Munar, E.S., Jensen, A.M., Cooper, J.A., Cobb, M.H., and Krebs, E.G. (1992). Purification and characterization of mitogen-activated protein kinase activator(s) from epidermal growth factor-stimulated A431 cells. The Journal of biological chemistry *267*, 14373-14381.

Shimkin, M.B., and Stoner, G.D. (1975). Lung tumors in mice: application to carcinogenesis bioassay. Advances in cancer research *21*, 1-58.

Shou, C., Farnsworth, C.L., Neel, B.G., and Feig, L.A. (1992). Molecular cloning of cDNAs encoding a guanine-nucleotide-releasing factor for Ras p21. Nature *358*, 351-354.

Sieghart, W., Losert, D., Strommer, S., Cejka, D., Schmid, K., Rasoul-Rockenschaub, S., Bodingbauer, M., Crevenna, R., Monia, B.P., Peck-Radosavljevic, M.*, et al.* (2006). Mcl-1 overexpression in hepatocellular carcinoma: a potential target for antisense therapy. Journal of hepatology *44*, 151-157.

Slebos, R.J., Kibbelaar, R.E., Dalesio, O., Kooistra, A., Stam, J., Meijer, C.J., Wagenaar, S.S., Vanderschueren, R.G., van Zandwijk, N., Mooi, W.J.*, et al.* (1990). K-ras oncogene activation as a prognostic marker in adenocarcinoma of the lung. The New England journal of medicine *323*, 561-565.

Socinski, M.A. (2004). Cytotoxic chemotherapy in advanced non-small cell lung cancer: a review of standard treatment paradigms. Clinical cancer research : an official journal of the American Association for Cancer Research *10*, 4210s-4214s.

Soda, M., Choi, Y.L., Enomoto, M., Takada, S., Yamashita, Y., Ishikawa, S., Fujiwara, S.-i., Watanabe, H., Kurashina, K., Hatanaka, H.*, et al.* (2007). Identification of the transforming EML4-ALK fusion gene in non-small-cell lung cancer. Nature *448*, 561-566.

Song, L., Coppola, D., Livingston, S., Cress, D., and Haura, E.B. (2005). Mcl-1 regulates survival and sensitivity to diverse apoptotic stimuli in human non-small cell lung cancer cells. Cancer biology & therapy *4*, 267-276.

Sordella, R., Bell, D.W., Haber, D.A., and Settleman, J. (2004). Gefitinib-Sensitizing EGFR Mutations in Lung Cancer Activate Anti-Apoptotic Pathways. Science (New York, NY) *305*, 1163-1167.

Soriano, P. (1999). Generalized lacZ expression with the ROSA26 Cre reporter strain. Nature genetics *21*, 70-71.

Soucek, L., Whitfield, J.R., Sodir, N.M., Masso-Valles, D., Serrano, E., Karnezis, A.N., Swigart, L.B., and Evan, G.I. (2013). Inhibition of Myc family proteins eradicates KRas-driven lung cancer in mice. Genes & development *27*, 504-513.

Stam, R.W., Den Boer, M.L., Schneider, P., de Boer, J., Hagelstein, J., Valsecchi, M.G., de Lorenzo, P., Sallan, S.E., Brady, H.J., Armstrong, S.A.*, et al.* (2010). Association of high-level MCL-1 expression with in vitro and in vivo prednisone resistance in MLL-rearranged infant acute lymphoblastic leukemia. Blood *115*, 1018-1025.

Steimer, D.A., Boyd, K., Takeuchi, O., Fisher, J.K., Zambetti, G.P., and Opferman, J.T. (2009). Selective roles for antiapoptotic MCL-1 during granulocyte development and macrophage effector function. Blood *113*, 2805-2815.

Stephens, P., Hunter, C., Bignell, G., Edkins, S., Davies, H., Teague, J., Stevens, C., O'Meara, S., Smith, R., Parker, A.*, et al.* (2004). Lung cancer: Intragenic ERBB2 kinase mutations in tumours. Nature *431*, 525-526.

Subramaniam, D., Natarajan, G., Ramalingam, S., Ramachandran, I., May, R., Queimado, L., Houchen, C.W., and Anant, S. (2008). Translation inhibition during cell cycle arrest and apoptosis: Mcl-1 is a novel target for RNA binding protein CUGBP2. American journal of physiology Gastrointestinal and liver physiology *294*, G1025-1032.

Suzuki, M., Youle, R.J., and Tjandra, N. (2000). Structure of Bax: coregulation of dimer formation and intracellular localization. Cell *103*, 645-654.

Tabin, C.J., and Weinberg, R.A. (1985). Analysis of viral and somatic activations of the cHa-ras gene. Journal of virology *53*, 260-265.

Tahir, S.K., Yang, X., Anderson, M.G., Morgan-Lappe, S.E., Sarthy, A.V., Chen, J., Warner, R.B., Ng, S.C., Fesik, S.W., Elmore, S.W.*, et al.* (2007). Influence of Bcl-2 family members on the cellular response of small-cell lung cancer cell lines to ABT-737. Cancer research *67*, 1176-1183.

Takeuchi, K., Choi, Y.L., Soda, M., Inamura, K., Togashi, Y., Hatano, S., Enomoto, M., Takada, S., Yamashita, Y., Satoh, Y.*, et al.* (2008). Multiplex reverse transcription-PCR screening for EML4-ALK fusion transcripts. Clinical cancer research : an official journal of the American Association for Cancer Research *14*, 6618-6624.

Tansey, W.P. (2014). Mammalian MYC Proteins and Cancer. New Journal of Science *2014*, 27.

Taparowsky, E., Shimizu, K., Goldfarb, M., and Wigler, M. (1983). Structure and activation of the human N-ras gene. Cell *34*, 581-586.

The Cancer Genome Atlas Research Network (2012). Comprehensive genomic characterization of squamous cell lung cancers. Nature *489*, 519-525.

The Cancer Genome Atlas Research Network (2014). Comprehensive molecular profiling of lung adenocarcinoma. Nature *511*, 543-550.

Thomas, L.W., Lam, C., and Edwards, S.W. (2010). Mcl-1; the molecular regulation of protein function. FEBS letters *584*, 2981-2989.

Thomas, R.L., Roberts, D.J., Kubli, D.A., Lee, Y., Quinsay, M.N., Owens, J.B., Fischer, K.M., Sussman, M.A., Miyamoto, S., and Gustafsson, A.B. (2013). Loss of MCL-1 leads to impaired autophagy and rapid development of heart failure. Genes & development *27*, 1365-1377.

Tonon, G., Wong, K.-K., Maulik, G., Brennan, C., Feng, B., Zhang, Y., Khatry, D.B., Protopopov, A., You, M.J., Aguirre, A.J.*, et al.* (2005). High-resolution genomic profiles of human lung cancer. Proceedings of the National Academy of Sciences of the United States of America *102*, 9625-9630.

Trahey, M., and McCormick, F. (1987). A cytoplasmic protein stimulates normal N-ras p21 GTPase, but does not affect oncogenic mutants. Science (New York, NY) *238*, 542-545.

Travis, W.D. (2010). Advances in neuroendocrine lung tumors. Annals of oncology : official journal of the European Society for Medical Oncology / ESMO *21 Suppl 7*, vii65-71.

Travis, W.D. (2011). Pathology of Lung Cancer. Clinics in chest medicine *32*, 669-692.

Travis, W.D., Brambilla, E., Noguchi, M., Nicholson, A.G., Geisinger, K., Yatabe, Y., Ishikawa, Y., Wistuba, I., Flieder, D.B., Franklin, W.*, et al.* (2013a). Diagnosis of lung cancer in small biopsies and cytology: implications of the 2011 International Association for the Study of Lung Cancer/American Thoracic Society/European Respiratory Society classification. Archives of pathology & laboratory medicine *137*, 668-684.

Travis, W.D., Brambilla, E., and Riely, G.J. (2013b). New pathologic classification of lung cancer: relevance for clinical practice and clinical trials. Journal of clinical oncology : official journal of the American Society of Clinical Oncology *31*, 992-1001.

Tse, C., Shoemaker, A.R., Adickes, J., Anderson, M.G., Chen, J., Jin, S., Johnson, E.F., Marsh, K.C., Mitten, M.J., Nimmer, P.*, et al.* (2008). ABT-263: a potent and orally bioavailable Bcl-2 family inhibitor. Cancer research *68*, 3421-3428.

Tsujimoto, Y., Finger, L.R., Yunis, J., Nowell, P.C., and Croce, C.M. (1984). Cloning of the chromosome breakpoint of neoplastic B cells with the t(14;18) chromosome translocation. Science (New York, NY) *226*, 1097-1099.

Tuveson, D.A., and Jacks, T. (1999). Modeling human lung cancer in mice: similarities and shortcomings. Oncogene *18*, 5318-5324.

van Delft, M.F., Wei, A.H., Mason, K.D., Vandenberg, C.J., Chen, L., Czabotar, P.E., Willis, S.N., Scott, C.L., Day, C.L., Cory, S.*, et al.* (2006). The BH3 mimetic ABT-737 targets selective Bcl-2 proteins and efficiently induces apoptosis via Bak/Bax if Mcl-1 is neutralized. Cancer cell *10*, 389-399.

Vick, B., Weber, A., Urbanik, T., Maass, T., Teufel, A., Krammer, P.H., Opferman, J.T., Schuchmann, M., Galle, P.R., and Schulze-Bergkamen, H. (2009). Knockout of myeloid cell leukemia-1 induces liver damage and increases apoptosis susceptibility of murine hepatocytes. Hepatology *49*, 627-636.

Vikstrom, I., Carotta, S., Lüthje, K., Peperzak, V., Jost, P.J., Glaser, S., Busslinger, M., Bouillet, P., Strasser, A., Nutt, S.L.*, et al.* (2010). Mcl-1 Is Essential for Germinal Center Formation and B Cell Memory. Science (New York, NY) *330*, 1095-1099.

Vogler, M., Weber, K., Dinsdale, D., Schmitz, I., Schulze-Osthoff, K., Dyer, M.J.S., and Cohen, G.M. (2009). Different forms of cell death induced by putative BCL2 inhibitors. Cell death and differentiation *16*, 1030-1039.

Wakamatsu, N., Devereux, T.R., Hong, H.H., and Sills, R.C. (2007). Overview of the molecular carcinogenesis of mouse lung tumor models of human lung cancer. Toxicologic pathology *35*, 75-80.

Wang, B., Ni, Z., Dai, X., Qin, L., Li, X., Xu, L., Lian, J., and He, F. (2014a). The Bcl-2/xL inhibitor ABT-263 increases the stability of Mcl-1 mRNA and protein in hepatocellular carcinoma cells. Molecular cancer *13*, 98.

Wang, B., Xie, M., Li, R., Owonikoko, T.K., Ramalingam, S.S., Khuri, F.R., Curran, W.J., Wang, Y., and Deng, X. (2014b). Role of Ku70 in deubiquitination of Mcl-1 and suppression of apoptosis. Cell death and differentiation *21*, 1160-1169.

Wang, D., and Lippard, S.J. (2005). Cellular processing of platinum anticancer drugs. Nat Rev Drug Discov *4*, 307-320.

Wang, F., Flanagan, J., Su, N., Wang, L.C., Bui, S., Nielson, A., Wu, X., Vo, H.T., Ma, X.J., and Luo, Y. (2012). RNAscope: a novel in situ RNA analysis platform for formalin-fixed, paraffin-embedded tissues. The Journal of molecular diagnostics : JMD *14*, 22-29.

Wang, J.M., Chao, J.R., Chen, W., Kuo, M.L., Yen, J.J., and Yang-Yen, H.F. (1999). The antiapoptotic gene mcl-1 is up-regulated by the phosphatidylinositol 3-kinase/Akt signaling pathway through a transcription factor complex containing CREB. Molecular and cellular biology *19*, 6195-6206.

Wang, K., Gross, A., Waksman, G., and Korsmeyer, S.J. (1998). Mutagenesis of the BH3 domain of BAX identifies residues critical for dimerization and killing. Molecular and cellular biology *18*, 6083-6089.

Wang, S.E., Narasanna, A., Perez-Torres, M., Xiang, B., Wu, F.Y., Yang, S., Carpenter, G., Gazdar, A.F., Muthuswamy, S.K., and Arteaga, C.L. (2006). HER2 kinase domain mutation results in constitutive phosphorylation and activation of HER2 and EGFR and resistance to EGFR tyrosine kinase inhibitors. Cancer cell *10*, 25-38.

Wang, X., Bathina, M., Lynch, J., Koss, B., Calabrese, C., Frase, S., Schuetz, J.D., Rehg, J.E., and Opferman, J.T. (2013). Deletion of MCL-1 causes lethal cardiac failure and mitochondrial dysfunction. Genes & development *27*, 1351-1364.

Wang, Y., Zhang, Z., Yan, Y., Lemon, W.J., LaRegina, M., Morrison, C., Lubet, R., and You, M. (2004). A chemically induced model for squamous cell carcinoma of the lung in mice: histopathology and strain susceptibility. Cancer research *64*, 1647-1654.

Warr, M.R., Acoca, S., Liu, Z., Germain, M., Watson, M., Blanchette, M., Wing, S.S., and Shore, G.C. (2005). BH3-ligand regulates access of MCL-1 to its E3 ligase. FEBS letters *579*, 5603-5608.

Watanabe, H., Ma, Q., Peng, S., Adelmant, G., Swain, D., Song, W., Fox, C., Francis, J.M., Pedamallu, C.S., DeLuca, D.S.*, et al.* (2014). SOX2 and p63 colocalize at genetic loci in squamous cell carcinomas. The Journal of clinical investigation *124*, 1636-1645.

Wei, G., Twomey, D., Lamb, J., Schlis, K., Agarwal, J., Stam, R.W., Opferman, J.T., Sallan, S.E., den Boer, M.L., Pieters, R.*, et al.* (2006). Gene expression-based chemical genomics identifies rapamycin as a modulator of MCL1 and glucocorticoid resistance. Cancer cell *10*, 331-342.

Weir, B.A., Woo, M.S., Getz, G., Perner, S., Ding, L., Beroukhim, R., Lin, W.M., Province, M.A., Kraja, A., Johnson, L.A.*, et al.* (2007). Characterizing the cancer genome in lung adenocarcinoma. Nature *450*, 893-898.

Weng, C., Li, Y., Xu, D., Shi, Y., and Tang, H. (2005). Specific cleavage of Mcl-1 by caspase-3 in tumor necrosis factor-related apoptosis-inducing ligand (TRAIL)-induced apoptosis in Jurkat leukemia T cells. The Journal of biological chemistry *280*, 10491-10500.

Wesarg, E., Hoffarth, S., Wiewrodt, R., Kroll, M., Biesterfeld, S., Huber, C., and Schuler, M. (2007). Targeting BCL-2 family proteins to overcome drug resistance in non-small cell lung cancer. International journal of cancer Journal international du cancer *121*, 2387-2394.

Whitmarsh, A.J., Shore, P., Sharrocks, A.D., and Davis, R.J. (1995). Integration of MAP kinase signal transduction pathways at the serum response element. Science (New York, NY) *269*, 403-407.

Whitsett, T.G., Mathews, I.T., Cardone, M.H., Lena, R.J., Pierceall, W.E., Bittner, M., Sima, C., LoBello, J., Weiss, G.J., and Tran, N.L. (2014). Mcl-1 mediates TWEAK/Fn14-induced non-small cell lung cancer survival and therapeutic response. Molecular cancer research : MCR *12*, 550-559.

Willis, S.N., Chen, L., Dewson, G., Wei, A., Naik, E., Fletcher, J.I., Adams, J.M., and Huang, D.C. (2005). Proapoptotic Bak is sequestered by Mcl-1 and Bcl-xL, but not Bcl-2, until displaced by BH3-only proteins. Genes & development *19*, 1294-1305.

Willis, S.N., Fletcher, J.I., Kaufmann, T., van Delft, M.F., Chen, L., Czabotar, P.E., Ierino, H., Lee, E.F., Fairlie, W.D., Bouillet, P.*, et al.* (2007). Apoptosis Initiated When BH3 Ligands Engage Multiple Bcl-2 Homologs, Not Bax or Bak. Science (New York, NY) *315*, 856-859.

Wolthuis, R.M., Zwartkruis, F., Moen, T.C., and Bos, J.L. (1998). Ras-dependent activation of the small GTPase Ral. Current biology : CB *8*, 471-474.

Wong, D.W., Leung, E.L., So, K.K., Tam, I.Y., Sihoe, A.D., Cheng, L.C., Ho, K.K., Au, J.S., Chung, L.P., and Pik Wong, M. (2009). The EML4-ALK fusion gene is involved in various histologic types of lung cancers from nonsmokers with wild-type EGFR and KRAS. Cancer *115*, 1723-1733.

Wong, R.P., Khosravi, S., Martinka, M., and Li, G. (2008). Myeloid leukemia-1 expression in benign and malignant melanocytic lesions. Oncology reports *19*, 933-937.

Wu, L., Nam, Y.J., Kung, G., Crow, M.T., and Kitsis, R.N. (2010). Induction of the apoptosis inhibitor ARC by Ras in human cancers. The Journal of biological chemistry *285*, 19235-19245.

Wuilleme-Toumi, S., Robillard, N., Gomez, P., Moreau, P., Le Gouill, S., Avet-Loiseau, H., Harousseau, J.L., Amiot, M., and Bataille, R. (2005). Mcl-1 is overexpressed in multiple myeloma and associated with relapse and shorter survival. Leukemia *19*, 1248-1252.

Xiang, Z., Luo, H., Payton, J.E., Cain, J., Ley, T.J., Opferman, J.T., and Tomasson, M.H. (2010). Mcl1 haploinsufficiency protects mice from Myc-induced acute myeloid leukemia. The Journal of clinical investigation *120*, 2109-2118.

Yakovlev, A.G., Di Giovanni, S., Wang, G., Liu, W., Stoica, B., and Faden, A.I. (2004). BOK and NOXA are essential mediators of p53-dependent apoptosis. The Journal of biological chemistry *279*, 28367-28374.

Yamashita, J., Ogawa, M., Abe, M., and Nishida, M. (1999). Platelet-derived endothelial cell growth factor/thymidine phosphorylase concentrations differ in small cell and non-small cell lung cancer. Chest *116*, 206-211.

Yang, T., Kozopas, K.M., and Craig, R.W. (1995). The intracellular distribution and pattern of expression of Mcl-1 overlap with, but are not identical to, those of Bcl-2. The Journal of cell biology *128*, 1173-1184.

You, M., Wang, Y., Lineen, A.M., Gunning, W.T., Stoner, G.D., and Anderson, M.W. (1992). Mutagenesis of the K-ras protooncogene in mouse lung tumors induced by N-ethyl-N-nitrosourea or N-nitrosodiethylamine. Carcinogenesis *13*, 1583-1586.

You, M., Wang, Y., Nash, B., and Stoner, G.D. (1993). K-ras mutations in benzotrichloride-induced lung tumors of A/J mice. Carcinogenesis *14*, 1247-1249.

Youle, R.J., and Strasser, A. (2008). The BCL-2 protein family: opposing activities that mediate cell death. Nature reviews Molecular cell biology *9*, 47-59.

Yu, C., Bruzek, L.M., Meng, X.W., Gores, G.J., Carter, C.A., Kaufmann, S.H., and Adjei, A.A. (2005). The role of Mcl-1 downregulation in the proapoptotic activity of the multikinase inhibitor BAY 43-9006. Oncogene *24*, 6861-6869.

Yu, H., Lee, H., Herrmann, A., Buettner, R., and Jove, R. (2014). Revisiting STAT3 signalling in cancer: new and unexpected biological functions. Nature reviews Cancer *14*, 736-746.

Yu, H., Pardoll, D., and Jove, R. (2009). STATs in cancer inflammation and immunity: a leading role for STAT3. Nature reviews Cancer *9*, 798-809.

Yuasa, Y., Srivastava, S.K., Dunn, C.Y., Rhim, J.S., Reddy, E.P., and Aaronson, S.A. (1983). Acquisition of transforming properties by alternative point mutations within c-bas/has human proto-oncogene. Nature *303*, 775-779.

Zhang, H., Guttikonda, S., Roberts, L., Uziel, T., Semizarov, D., Elmore, S.W., Leverson, J.D., and Lam, L.T. (2011). Mcl-1 is critical for survival in a subgroup of non-small-cell lung cancer cell lines. Oncogene *30*, 1963-1968.

Zhang, X.-F., Settleman, J., Kyriakis, J., Takeuchi-Suzuki, E., Elledge, S.J., Marshall, M.S., Bruder, J.T., Rapp, U.R., and Avruch, J. (1993). Normal and oncogenic p21ras proteins bind to the amino-terminal regulatory domain of c-Raf-1. Nature *364*, 308-313.

Zhong, Q., Gao, W., Du, F., and Wang, X. (2005). Mule/ARF-BP1, a BH3-Only E3 Ubiquitin Ligase, Catalyzes the Polyubiquitination of Mcl-1 and Regulates Apoptosis. Cell *121*, 1085-1095.

Zhou, B.P., Liao, Y., Xia, W., Spohn, B., Lee, M.H., and Hung, M.C. (2001). Cytoplasmic localization of p21Cip1/WAF1 by Akt-induced phosphorylation in HER-2/neu-overexpressing cells. Nature cell biology *3*, 245-252.

Zinkel, S., Gross, A., and Yang, E. (2006). BCL2 family in DNA damage and cell cycle control. Cell death and differentiation *13*, 1351-1359.

Zochbauer-Muller, S., Gazdar, A.F., and Minna, J.D. (2002). Molecular pathogenesis of lung cancer. Annual review of physiology *64*, 681-708.